UNDERLYING PROCESSES OF THE JOVIAN DECAMETRIC RADIATION

By

JAMES RICHARD KENNEDY

A DISSERTATION PRESENTED TO THE GRADUATE COUNCIL OF
THE UNIVERSITY OF FLORIDA
IN PARTIAL FULFILLMENT OF THE REQUIREMENTS FOR THE
DEGREE OF DOCTOR OF PHILOSOPHY

UNIVERSITY OF FLORIDA

1976

ACKNOWLEDGEMENTS

Throughout the preparation of this manuscript, this part-- the acknowledgements-- has constantly been on my mind. It has become clear that there are so many people who have contributed to this work over the years that proper recognition of all of them is impossible in the few words here. To those I have omitted, I hope I will find some other way to express my graditude.

I owe a significant debt to Professor John Waddell, my advisor and Chairman of the Physics Department at St. Mary's College. His perception of this student's potential was far more accurate than my own and his personal courage in pursuing an unpopular course to help a failing student salvage himself cannot be forgotten. Dr. Fredric Scott, Physics Chairman at the California State University at Fresno, provided the setting and understanding for this salvation, for which I am most grateful.

Dr. Jon Dews, at Fresno, directed my Master's program. His guidance and counsel provided my basic orientation in the ways, means and practical realities of the conduct of scientific research. His direction and friendship, and those of Drs. Michael Zender and Robert Shacklett are beyond value.

The support, financial and moral, of Dr. Alex Smith has made my pursuit of graduate work at the University of

Florida possible. For this support I am both honored and thankful. I am also grateful to have Dr. Smith and Dr. George Lebo as my committee co-chairmen. Dr. Lebo has provided and encouraged the exercise of great freedom in the pursuit of this research. This has contributed considerably to the learning experience. The contributions of other members of my committee, Dr. Thomas Carr, Dr. Frank Wood, and Dr. Stephen Gottesman are greatly appreciated. I must add too that the guidance of Dr. Charles Hooper, Jr., in my early days at Florida significantly eased the transition to this new environment.

Without friends and colleagues like John Schauble, Dolores Krausche, Richard Pomphrey, Richard Flagg, Michael Desch, Michael Lynch, and Wesley Greenman this work would not be possible. The patient, and through my fault all too often, last minute assistance of Woody Richardson and Hans Shrader in the preparation of drawings and slides has been invaluable. James McClave's assistance with the statistical aspects of the study has been greatly appreciated.

I feel compelled to also acknowledge the influence of the popular factual writings of Dr. James Watson and Dr. Isaac Asimov. Their works have been a comforting reminder that, however logical the end result, much of scientific research is the confirmation or rejection of the scientist's intuitive leaps.

Many of the drawings in this study are the work of Donald Hall whose perseverance is greatly appreciated. Dorothy Long has done a fine job of typing the final draft of this dissertation. That she has done so without a complaint, considering the demands I have made upon her, is truly remarkable.

The influence and support of my mother and father cannot be measured. Most of all, I must acknowledge the help of Robert and Shannon who may see a little more of their dad now; and that of Cathy, who has made this work as much hers as mine.

TABLE OF CONTENTS

LIST OF TABLES

LIST OF FIGURES

Abstract of Dissertation Presented to the Graduate Council of the University of Florida in Partial Fulfillment of the Requirements for the Degree of Doctor of Philosophy

UNDERLYING PROCESSES OF THE JOVIAN DECAMETRIC RADIATION

By

JAMES RICHARD KENNEDY

December 1976

Chairman: Alex G. Smith
Co-Chairman: George R. Lebo
Major Department: Physics and Astronomy

The Jovian decametric radiation is known to be excited, in part, by the satellite Io. However, much of the radiation is apparently not related to Io and the provocation for this component is not understood. This study examines the non-Io component by the systematic removal of all information associated with the "favored" orbital positions of Io at 18, 22, 26, and 27 MHz.

Three specific examinations have been made. The first has considered the possibility of a correlation between the activity of the radio sources and density waves in the solar wind. A byproduct of this aspect of the study is the development of two models for solar wind velocity stream interactions. These models predict the development of large density waves, mainly past 1 AU, in the solar wind. The waves are the result of interactions (collisions) between high speed and low

speed particle streams in the solar wind.

A positive correlation between these proposed waves and the source A and source C emission is found in the two study periods, 1967-68 and 1974. During the same periods there is evidence of a negative correlation with source B.

The second part of the study has examined the activity occurrence spectra for evidence of periodicity. A 27 day period was found in the 1974 data which may be associated with the solar correlation. In the 1967-68 and 1974 apparitions a prominent peak was found at 6.35 days in both source A and C. This peak is coincident with an alias of a principal feature in the spectrum of a joint Io-Europa exciter. No other satellite effect can cause this feature.

Another spectral peak was found at 2.7 days in both apparitions in source A. This maximum is not explainable at this time.

The third examination has considered the question of randomness. The object was to determine whether it was possible that the non-Io component was the result of some, possibly intrinsic, random process. In this study two characteristics have been examined. The first was the length of the storms themselves. Employing the frequency of length distribution of the storms it is shown that storm lengths are not randomly distributed.

The other topic was the question of the likelihood that

the 6.4 day period features seen in the Chree analysis of the radio activity could be the result of random influences. This effect was shown to be non-random with a confidence exceeding 99.5%

The study concludes that below the strata of events known to be associated with Io, there are secondary and tertiary exciters which influence the non-random emission in the 18 to 27 MHz regions.

CHAPTER 1

INTRODUCTION

Jovian Decametric Radiation

Sources

The process by which the intermittent "storms" of Jovian decametric emissions are generated has been the subject of considerable study since the radiation was discovered by Burke and Franklin (1955).

An examination of pre-discovery data by Shain (1956) revealed that the radiation was not uniformly distributed with respect to the Jovian central meridian longitude (CML). He found, rather, that the signals originated from specific "sources" which were apparently fixed to Jupiter's high latitude System II longitude scheme. Thus, these source locations rotated with the planet, though further studies by many observers showed a slight drift with respect to System II. The adoption of a radio longitude scheme, System III, largely removed this small discrepancy.

If one plots the probability of activity in the vicinity of 20 MHz versus CML, the result is a histogram such as Figure 1. The features labeled A, B, and C represent the three major source regions. The nomenclature, source "A", "B", or "C" was adopted by the Florida group (Carr et al., 1961) early in their

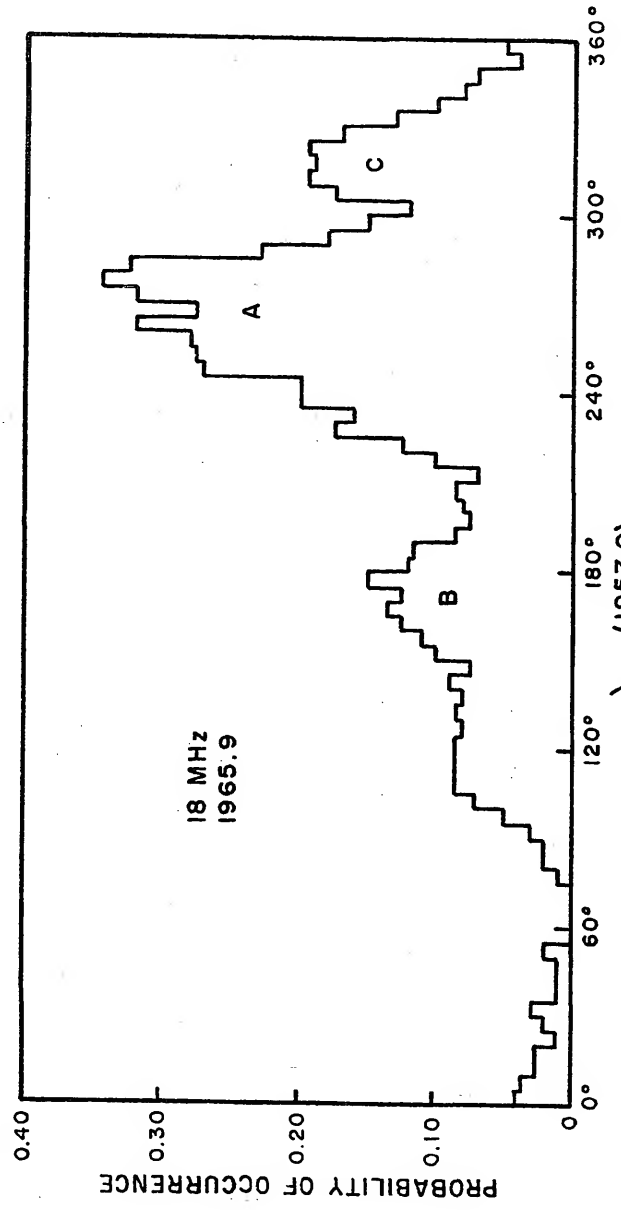

Figure 1. Histogram of occurrence probability as a function of CML. (after Register, 1968.)

studies and will be used in this presentation. However, sources A, B, and C correspond respectively to sources 2, 1, and 3 defined by Douglas (1964) and the main, early, and third sources of Dulk (1965a,b).

Io Effect

Subsequently, Bigg (1964) determined that there was a component of the decametric emission which was strongly correlated with the phase from superior geocentric conjunction of the inner most Galilean satellite, Io. More recent studies (e.g., Register, 1968; Miller et al., 1972) have shown that all three of the classical decametric sources contain both an Io related component and non-Io related component. Source A, in particular, and to a lesser extent, source C, contain significant non-Io components in the vicinity of 20 MHz. This situation, depicted by Leacock (1971) in Figure 2, seems to suggest that the position of Io enhances a pre-existing radiation process. More recently, Desch (1976) has shown that source B also has a significant non-Io component at lower flux levels.

The data presented in Figure 2 correspond to the eight-year period 1962-70, including the 1967-68 apparition which is of most interest in the present study. Thus, the definitions of the sources in terms of central meridian longitude (CML) and the "favored" Io ranges from superior geocentric conjunction (ISC) are drawn by inspection from this plot. Though there are small variations with radio frequency evident in Leacock's diagram, the values in Table 1 have been adopted for the 18 to

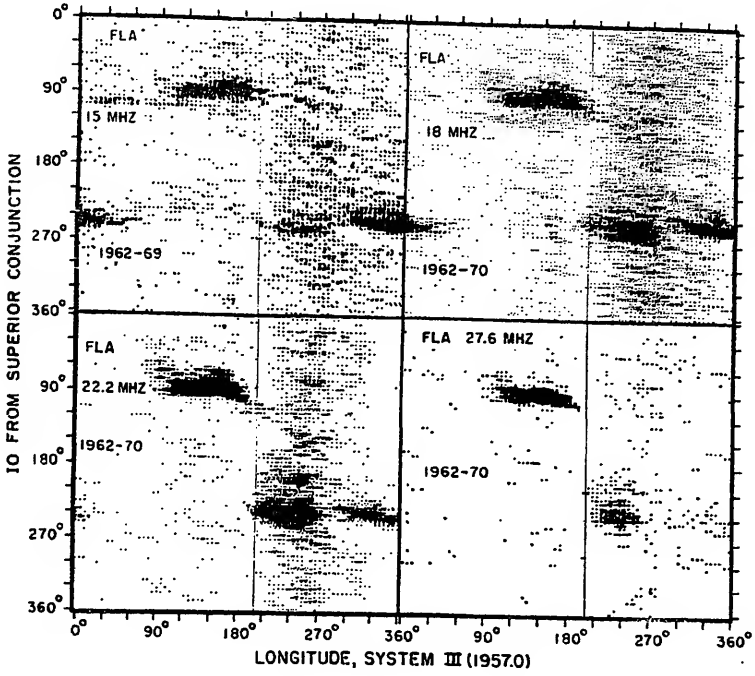

Figure 2. Maps of the occurrence of Jovian decametric events as a function of CML and ISC. (After Leacock, 1971.)

27 MHz region for the purposes of this investigation.

Table 1

18 - 27 MHz Source Definitions

Source	CML, System III 1957.0 (degrees)	ISC (degrees)
A	200 - 290	220 - 270
B	75 - 200	60 - 130
C	285 - 40	225 - 260

Research Tactics

Most of the work that has been devoted to the decametric radio emission from Jupiter can be lumped into one of two categories. The first of these categories is the study of the intrinsic properties of the emissions themselves. Among these properties are the wave polarization, energy flux, dynamic spectra, etc. The second category is the study of relationships between some property, such as the occurrence of the radiation, and other events in the outside world. Investigations of this kind ultimately take the form of some kind of cross-correlation.

This characterization of research tactics betrays the implicit assumption that the production of the intermittent radiation is (at least) a two-step process. The first step consists of having the necessary physical conditions for a

radiation mechanism to operate. For example, these might be the existence of a magnetic field and a source of electrons that might conspire to produce gyromagnetic or synchroton radiation.

The second step is the intermittent availability of an "exciter," some event which completes the chain of conditions required to set off the radiation mechanism. For example, recent work by Krausche et al. (1973), Ellis (1973), and Krausche (1975) seems to suggest that, when the Io related source B radiation is produced, it comes from electrons emitting doppler shifted gyromagnetic radiation as they move upward along the planet's magnetic flux lines. The role of the exciter in this process is played by Io. According to Goldreich and Lynden-Bell (1969), Io energizes magnetospheric electrons while driving them down to the ionosphere by acting as a unipolar electrical generator. When Io is within the favored range with respect to a source, radio emission is stimulated. Smith (1975) has recently suggested that subsequent diffusion of electrons back into the void swept out by the Io flux tube plays a role in the non-Io emission.

The Present Study

Underlying Processes

The question of the Io related emission is far from solved since, among other things, it is not clear why the localized sources themselves exist. This points out a very

fundamental problem, since a large amount of the decametric emission does not correlate with Io, but almost all of it correlates with the defined source locations.

Ignoring the question of what is special about the source longitudes, it is apparent that these longitudes are somehow associated with locations where conditions are conducive to the emission of signals receivable at the earth. If one considers only the non-Io component, a natural question is whether this component is also triggered, at least in part, by some exciter which also has origins beyond the planet itself. Alternatively, one should also ask whether there are unknown systematic influences. such as beaming effects, which affect terrestrial reception.

In view of the success of the Io relationship it is reasonable to examine the remaining three Galilean satellites. This has been done by many workers with no sure success; however, a more thorough discussion of this point is reserved for a later chapter.

At this point, a matter of semantics requires discussion. The principal thrust of this study is directed at the question of the existance of non-Ioian Jovian exciters or other reception influences. In this regard, a distinction between the term "mechanism" and "process" is made. The expression "mechanism" will be reserved to indicate the immediate source of the emission (e.g., synchrotron, Cherenkov, etc.). On the other hand, the term "process" will refer to the joint entity of exciter and radiation mechanism, though this will frequently be treated as a "black box" operation.

Randomness

The objective, then, is to examine the process itself, and, if possible, to find other exciters. In order to do this, it is important to examine the question of whether the non-Io component is a random process. If it is shown not to be random, then the existence of a systematic exciter is possible. There are statistical tools available to examine the randomness of a function and these will be employed to deal with this question.

Jupiter-Solar Correlation

Historically, this investigation began as an effort to see if the non-Io component of the various sources was related to solar wind influences. As such, considerable attention has been given to the sun, solar magnetic sectors, the solar wind and a model for solar wind velocity stream interactions.

Subsequently, it was recognized that in order to establish any such correlation one must also consider more fundamental questions, such as that of randomness. The result was a broader assault on the general problem. Even so, a preoccupation with periodic processes will become evident in what follows. This interest is motivated, in part, by the prejudice that the solar rotation may have an influence. But, the concern for periodicities is also the result of realizing that if there are periodic exciters, they would be the easiest to separate from the noise in the data due to their inherent redundancy.

Methods of Study

In approaching these problems an examination of both Jovian and solar wind data will be undertaken. The treatment of these data will consist of techniques such as autocorrelation, occurrence spectral analysis and the development of various distributions. Thus, each class of data will be viewed by itself to discover any clues that may be there to be found. Then, the two sets of data will be studied with respect to one another, principally by way of Chree (1912) analysis followed by cross correlation.

There are already a number of known or strongly suspected periodic influences on the Jovian emissions, six to be exact. These will be dealt with in the next chapter, but the point here is that the various techniques outlined above can be strongly influenced by periodic processes. Consequently, each treatment of the data must either recognize these effects in the reduced output, or be contrived in such a way that the data reduction is blind to the known effects. As will be shown, this is not a trivial problem. Indeed, modern statistics is just beginning to deal with the problem of irregular time series. Specifically, the data received at the earth are riddled with "holes" caused by the inability of a station to observe a given source continuously. Thus, the table of, let us say, daily numerical measures of activity has the potential for significant error in that it cannot reflect activity that occurred during that part of the day when the source could not be seen. Nevertheless, these problems can be managed, provided

one does not lose sight of their existence.

Choice of Apparition

Another related problem is that of whether or not the presumed, yet-to-be-discovered, exciter is truly periodic, lasting for all time, or whether it is almost periodic and exists for a time less than that of the study.

Since the examination of a possible Jupiter-solar relationship is a major part of this work, the above problem has special significance. In particular, the solar phenomenon under study is the control of the solar wind apparently exerted by the solar magnetic sectors. These sectors can be relatively stable for a time on the order of months--but not much longer. With this in mind, it has been necessary to confine the study to single Jovian apparitions.

Specifically, it was decided to restrict the study to apparitions when

1. The solar magnetic sector structure was simple and stable.
2. Good solar wind data were available.
3. Jovian decametric data were available.

The 1967-68 apparition, blessed with a stable two sector sun, was the first to meet all these criteria and hence has received the bulk of the attention. Very recently Svalgaard (1976) has published sector structure data which showed that the 1974 apparition also satisfies these criteria and this period has also been studied.

Source of Data

The Jovian decametric data employed in this research are those of the University of Florida Radio Observatory. Solar magnetic sector structure data have been provided by Wilcox (1970, 1971) and Svalgaard (1975). The solar wind data for 1967-68 were gathered by Pioneer VI and VII in solar orbit near 1 AU, essentially in the ecliptic plane, and published in Solar-Geophysical Data*. The solar wind velocity data for 1974 are from Bame et al. (1976).

*U. S. Department of Commerce, Environmental Sciences Services Administration periodical: Government Printing Office, Washington, D. C.

CHAPTER 2

OBSERVATIONAL PROBLEMS - THE STROBES

Periodic Modulation

As mentioned in the preceding chapter, there are six certain or nearly certain periodic influences on the observation of Jovian decametric radiation. These influences arise from the rotations of the earth and Jupiter, the Jovian synodic and sidereal revolutions, the earth's tropical or seasonal revolution, and finally, the revolution of Io.

Rotation of Jupiter

Since the three classical sources are of limited angular extent, their rotation with the planet presents them to the earth only once every ten hours or so. The IAU definition of the sidereal radio rotation period, the System III period, is $9^h55^m29^s.37$, though later work by Smith et al. (1965), Gulkis and Carr (1966) and by Duncan (1971) indicates that the true mean radio period is more clearly $9^h55^m29^s.70$ or some 0.33 seconds longer. However, near opposition the motion of the earth can reduce the synodic radio period to as low as $9^h54^m49^s$.

The longitudinal extent of each of the sources is on the order of 90°, and therefore the presentation of a source to the earth takes place for a period of about 2.5 hours during

each System III rotation.

Rotation of Earth

Since the earth rotates on its axis with a sidereal period of about $23^h56^m04^s$, a given station fixed on the earth near the equator can, at most, observe Jupiter for about 12 hours out of every 24. Thus, under ideal circumstances, the odds of being able to view each source during an observation period are good; still, about every other Jovian rotation goes unobserved.

It might be added at this point that, of course, due to the orbital motions of the earth and Jupiter, the rotation period of the earth with respect to Jupiter is not generally the sidereal period of the earth. It is the sidereal value only when the earth is at greatest eastern or western elongation as viewed from Jupiter. When the earth is at inferior conjunction (i.e., Jupiter is at opposition) the period is shortened by almost one minute to $23^h55^m08^s$, while, when the earth and Jupiter are at superior conjunction with respect to each other, the period is lengthened about 39 seconds to $23^h56^m43^s$.

Jovian Synodic Year

The above variation of the earth's Jovicentric rotation period, and its counterpart in the Jovian rotation period, are both related to Jupiter's synodic year. However, they are higher order effects or pertubations associated with the rotation periods. There is yet another factor which is far more potent.

Unlike many other areas of radio astronomy which use higher frequencies, work at decametric wavelengths is strongly influenced by fluctuations in terrestial ionospheric transparency. Ionization levels in the daytime F layer and sporadically in the nighttime E layer may reach levels which render the ionosphere opaque by reflecting decametric radiation, impinging on the earth, away into space. This problem is compounded by the fact that opacity, or if one wishes, reflectivity, is proportional to the secant of the zenith angle for an earth-bound observer. Consequently, as the level of ionization builds up, such an observer will generally find both natural and man-made radio sources from beyond the horizon, reflected by the ionosphere at large zenith angles and picked up by the antenna sidelobes, producing significant interference. This terrestrial interference will frequently terminate observation attempts even before smaller zenith angle opacity precludes reception of extraterrestrial signals.

It is possible to minimize the ionospheric effects either by observing at higher frequencies where the transparency is greater or by employing a narrow-beam antenna with strong sidelobe suppression. For various reasons it is generally either undesirable or not practical to take these steps, though the University of Florida's 640 dipole array at 26.3 MHz is an exception. As a result, most Jovian decametric observations are subjected to a strong diurnal effect. As Jupiter moves into the daytime sky during its synodic cycle, observation

becomes progressively more limited, usually ceasing altogether near conjunction. After conjunction the situation improves, reaching its peak at opposition. The net effect is the imposition of a modulation with a period equal to the Jovian synodic year.

Jovian Sidereal Year

Jupiter's spin axis is inclined 3°07' to the normal of the plane of its orbit. The planet's orbit, in turn, is inclined 1°18' to the ecliptic plane. These two effects combine to cause the Jovicentric declination of the earth, D_E, to vary about $\pm 4°$ over a Jovian sidereal year. The radiation centroid and abundance for Source A apparently oscillate with a period near the sidereal period of 11.86 years. This effect has been explained by Gulkis and Carr (1966) and by Donivan and Carr (1969) as the result of the source A emission being confined to a relatively narrow sheet. Thus, as Jupiter moves about its orbit the variation of D_E directs more or less of the beam towards the earth. The last peak in activity due to this effect was about 1964.3 (Carr, 1972). Presumably the following maximum will be found to have occurred around 1976.2.

Terrestrial Tropical Year

The sporadic nighttime E layer ionization mentioned above is dependent on the earth's tropical year. Sporadic E levels tend to peak during the summer months, causing not only a diminution of extraterrestial signals, but even in the presence

of locally adequate penetration, ionization clouds near the horizon often cause electrical interference--principally lightning--from beyond the horizon to skip into the side lobes of the antenna. The E layer has a minor peak in the winter months but is not too bothersome. Not only is the probability of opacity much less but the lightning problem is largely a summertime phenomenon as well.

Io Effect

The role of the satellite Io in the Jovian decametric process has been outlined in Chapter 1. Io is particularly effective in producing source B activity, at least that which can be observed from the earth.

Io revolves about Jupiter with a period of about $42^h28^m39^s$, while Jupiter rotates under it with a synodic period of $12^h57^m03^s$. There is evidence to suggest that the principal period for the Io related activity is the 13-hour period. Duncan (1965) reported an occurrence spectral peak at $12^h57^m08^s$. Further, superposed epoch analysis of activity using this period revealed a peak when Io was near Jovian longitude 200°--the plane thought to contain the Jovian magnetic pole. Duncan points out, however, that in order for emission to be beamed at the earth, CML 110° (source B) or CML 250° (source A) must also be aimed at the earth. He then suggests that, since the same relative angular separation of Io and sources A and B occurs at the 13-hour intervals, every 13 hours the source emission probability is enhanced irrespective of geocentric or heliocentric central

meridian longitude. If this were fact it would certainly have a strong effect on models for the radiation mechanism. A review of Duncan's analysis by this author does not reveal a compelling case for the reality of the 13-hour period itself, though the rest of his conclusions seem valid.

Kaiser and Alexander (1973) have done a similar study employing 17 years of data. They find almost six times as much power in the 13-hour peak as in the 42-hour period. However, in an earlier analysis Bigg (1966) concluded the opposite; that is, that the 13-hour period was merely a mathematic artifact and that the 42-hour period was dominant. Suffice it to say at this point that the Io effect can only influence the radiation received at the earth when the source is aimed at the earth and Io is near longitude 200°. This is not in dispute and the periodic motion of Io about Jupiter can be considered mathematically independent, as can also the Jovian rotation.

Other Modulations

There are a number of other sources of unwanted influences that might, in effect, contaminate the data. Periodic emissions of data, as might occur from the observing habits of regularly scheduled observers, will cause no serious problems due to the nature of the data reduction procedure. Aperiodic effects, particularly random ones, will also have little effect. An examination of the data has not revealed any substantive problems. An open mind, nevertheless, must be maintained in this regard and cross checks on the data will be made and

evaluated in what follows.

Radiation Process Model

The Observation Function

The preceding sections have been written to underscore the fact that whether or not one observes Jovian decametric radiation depends strongly on several known periodic influences. Even though some of these influences may be intrinsic to the generation of some of the emissions, as in the Io effect, they can all be treated as observational artifacts. They are known to exist and it is not wished to study them here. Rather, if they can be removed, what remains is that which is to be studied here.

Since this examination has been contrived to cover single apparitions, it is possible to ignore several of the known periodicities (specifically, those effects which have periods in excess of one apparition, or about 200 days). This eliminates synodic, tropical and sidereal year influences and leaves the rotation of Jupiter and the earth, and the revolution of Io.

It is now wished to develop a mathematical expression as a model for the observations themselves. This expression can take the form of a time series which, in its simplest form, has a value of one when the source is being observed and a value of zero when it is not. This function will be periodic, containing components corresponding to the Jovian, terrestrial and Ioian periods. If we assume that these three components

are independent we may define four functions, each having a value of one when the condition is true (e.g., the Jovian source is aimed at the earth) and a value of zero otherwise. For a given source S, these functions are

$J_S(t)$: Is the source aimed at the earth?

$E_S(t)$: Can the station "see" Jupiter?

$I_S(t)$: Is Io in the favored range?

$N_S(t)$: Is Io out of the favored range?

Of course $N_S(t)$ is just $1 - I_S(t)$. The composite function representing whether or not a specific source is being observed then is

$$O_S(t) = J_S(t)E_S(t)I_S(t) \text{ for Io related observations}$$

$$O_S(t) = J_S(t)E_S(t)N_S(t) \text{ for non-Io related observations.}$$

The composite observation function O(t) will have a value of one only when all the necessary conditions are met, that is, the source S is aimed at the earth, the earth station is aimed at Jupiter and listening, and Io is in the appropriate ISC range.

The Activity Function

Though O(t) expresses whether or not the observer has the opportunity to observe radiation, it in no way guarantees that such emissions will be seen. For example, during the 1967-68 apparition source A was active at 18 MHz only 7.7% of the time during non-Io observations and 32% of the time during Io observations using a relatively low sensitivity Yagi

array. A more complete view of activity statistics is discussed at the end of this chapter, including a comparison of activity indices of low sensitivity systems versus high sensitivity systems. The principal point here is that there is an activity function, analogous to the observation function, which expresses whether or not emissions are detected. Actually, there are two activity functions, one of this is global, that is, an intrinsic function which is defined as having a value of one whenever a given source emits, with Io in the appropriate range, regardless of whether the source is aimed at the earth or whether the earth station can see the source, and a value of zero otherwise. The other activity function represents merely the observed activity, that which occurred when $O_S(t)$ was equal to one.

If one represents the global or intrinsic activity function as $A_S(t)$ and the observed activity function as $A'_S(t)$, they are related by

$$A'_S(t) = A_S(t)O_S(t)$$

which for non-Io activity is

$$A'_S(t) = A_S(t)J_S(t)E_S(t)N_S(t).$$

While the intrinsic function A(t) above represents the entire activity produced by the underlying processes, the earth-bound observer is permitted only a tantalizing view of this process as if it were illuminated by a strobe lamp driven by a voltage

containing the constituent frequencies of O(t).

In principle, then, given adequate data one might hope to find the intrinsic function $A_S(t)$ by the simple expediency

$$A_S(t) = \frac{A'_S(t)}{O(t)} .$$

Effect on Jovian Data

The Raw Time Series

The previous section has indicated the direction of this program: the development of procedures that might permit the separation of the "true" activity from the artifact modulated activity. Such procedures, however, are constrained to dealing with the actual raw data.

While the concept of $A_S(t)$ expressed above is simple enough, the fact is that the various observational functions are not known analytically. It is true that in principle they can be, but for practical purposes it is far more important to deal with the actual functions as they really evolved. As such, they are dependent on many transient influences: the occurrence of thunderstorms, the inability of an observer to stand his watch, the presence of hunters with walkie-talkies, and other earth-bound stations on nearby frequencies providing interference, etc.

The observed activity time series will be developed from what the Florida group calls an "intermediate deck." This is a catalog of Jovian decametric radio observations which reports

the CML at the beginning and end of each observation, and at the beginning and end of any observed activity, the corresponding position of Io (ISC) and so forth. All these angular measures are generally reported in blocks or "zones" of 5°. Thus, 0°-5° CML corresponds to zone 1, while zone 72 represents 355°-360° CML.

Since the intermediate deck reports observational data independently of activity data, it will also be possible to develop the corresponding raw observation time series. The observation series is somewhat model dependent. Nevertheless, as previously stated, the probability of observation is assumed to be constantly one or constantly zero. This is a simplification, since the distribution of activity within a given source, such as is shown in Figure 1, suggests that $J_S(t)$ is more nearly gaussian. In all probability, the incidence of reception at an earth-bound observatory is highest at transit and lowest near the horizon, with a corresponding effect on E(t). The precise shape of all of the component functions is not known, however, and the rectangular approximation seems a good compromise at this point. At worst, it somewhat exaggerates the weight of events that occur near the limits of one of the component functions.

At this point, we have two raw time series whose function values are either zero or one. The problem then is to try to compensate the activity function for the observational effects.

Compensation Procedure

It has been stated earlier that, in principle, the underlying activity function, A_S, could be known from

$$A_S(t) = \frac{A'_S(t)}{O(t)}.$$

However, as $O(t)$ is often zero, the mathematical expression is undefined over much of its range. Physically, this means that one cannot say whether or not there is an underlying activity when the source was not observed. On the other hand, $A_S(t)$ does have some real values. Whenever $O(t)$ is one, the expression yields meaningful numbers.

Due to the desire to explore specifically the possibility of solar correlation and the fact that solar wind data were generally confined to one sample per day, the decision was made to adjust the available values of $A_S(t)$ to one value per day. Thus, the intrinsic activity function was chosen to be estimated by

$$A_S(t) = \frac{\Sigma_i A'_S(t)_i}{\Sigma_i O(t)_i} \qquad O(t)_i \neq 0,$$

where $A'_S(t)_i$ and $O(t)_i$ are expressed in 5° zones. The activity function, then, is nothing more than a daily activity index expressed as the ratio of the number of source zones seen storming to the number of source zones observed each day.

A table of values for $A_S(t)$ will have a real value for most days, since each source is usually observed, at least in part, every day. Nevertheless, as often as one day in four for a source may be skipped.

Influence of the Compensation

The question naturally arises, then, as to what effect these covert and overt indeterminacies will have on any attempt to use $A_S(t)$ to study properties of the presumed underlying phenomena. Since the time series will become the input to autocorrelation and power spectrum routines, it was indeed disappointing to discover that the bulk of current statistical theory was predicated on the existence of evenly spaced, uninterrupted time series.

In the present case, the situation is further complicated by the fact that the "samples" in the time series are themselves composed of samples. That is, the daily values of A(t) are calculated from a sample of the total activity for that day. The minimum valid sample size for a given observation is one 5° zone, while the maximum sample size may exceed 20 zones.

The number of zones sampled on a given day, as expected, will be shown to be a somewhat complicated periodic function of time. As a result, the sample size from which the daily values of A(t) are derived is variable. This means, among other things, that the weight of each daily number is not constant. Thus, from time to time, when there are only a few samples, a value of A(t) will appear which is inordinately

high or low, and yet will be considered on a even par with other values drawn from larger samples more likely to approach the population mean.

A subsequent chapter contains a discussion of the various statistical properties of the data, and it will be shown that about 90% of the non-zero values for O(t) contained 5 or more zones, while only 7% of the observed storms lasted longer than five zones. Consequently, the errors introduced by varying sample size are not expected to be serious.

Having calculated a table of the daily values of A(t), some of which are indeterminate, the question then arises as to what effect these indeterminacies will have on, say, the power spectrum of the time series. Jones (1962) has studied this problem for data with "regularly missed" observations. In his work he assumed that data were collected at equally spaced intervals, but that periodically observations had to be skipped for whatever reason.

In making the spectral analysis he used the common technique of first calculating the autocorrelation function and then taking its Fourier transform. However, in the autocorrelation he included only pair products where both terms existed and simply excluded those which did not contain both terms. He then showed that, using this technique, the error in estimating the spectral density was not greatly increased. Figure 3 shows his plot of the upper bound of the increase in covariance for a repeated sequence of α observations followed

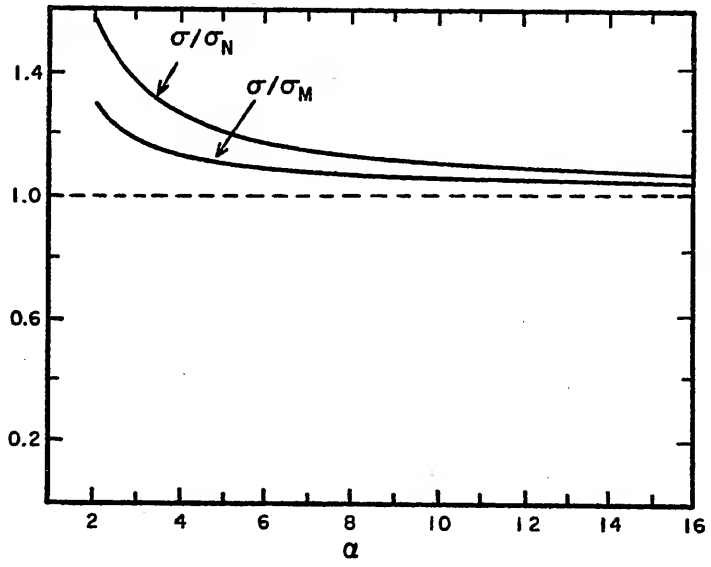

Figure 3. Effect of missing data on power spectrum estimates. σ is the upper limit for the standard deviation of the spectrum of a time series missing one point every α points. σ_N is the standard deviation for N actual and missed points, while σ_M is the standard deviation for M actual points. (After Jones, 1962.)

by one skipped observation. It shows, for example, that if every fourth observation is missed the standard deviation of the spectral density will increase by at most 25%.

Jovian Data Reduction

Zone Filters

The Jovian data reduction process in this study begins by acting on the Florida intermediate deck, in either card or magnetic tape form with a computer program designated as Jupzone (see Appendix). This routine consists of a series of filters which, first, selects only intermediate deck records which are within the desired apparition. Second, it rejects any of those records which do not represent the observations of the chosen Jovian source. Third, it sorts the accepted records into four categories:

1. Io related activity,
2. Io related observations,
3. Non-Io related activity,
4. Non-Io related observations.

Finally, the program reduces the records in each of these categories to a single entry per day--the total number of 5° zones in that category for that day.

The output from the Jupzone program consists of the (abbreviated) Julian date and a list of the four zone counts for each day, for each specified source, during the given apparition. This information is produced in card form and

serves as the input to a variety of other analysis routines which will be described later. Table 2 shows a printed example of a segment of this output.

The Reduced Time Series

It should be clear that the time series generated by Jupzone can easily be used to produce the function $A_S(t)$ for both the non-Io and Io related components. While much of the ultimate data analysis does deal directly with $A_S(t)$, some routines require the separate listing of activity and observation. Consequently, the series are left in the separated form at this level, enabling subsequent programs to choose whether or not to calculate $A_S(t)$. For example, by leaving the series separate it was possible to suppress the effect of sample size biasing in reporting the activity index for an entire apparition, $\overline{A_S(t)}$, in the following section. In this process, separate sums of the daily zone counts were made over the entire apparition and then their ratio was taken, rather than taking the average of the daily ratios.

Gross Statistics

Radio Frequencies

During the 1967-68 apparition the reception frequencies employed in this study were 18, 22, and 27 MHz. While the University of Florida operates receiving systems outside this range, the source definitions in the 18 to 27 MHz region are essentially identical. At the same time, data are more

Table 2

Example of Filtered Jupiter Data

JUPZONE

SOURCE LIES FROM ZONE 25 TO 40. IO ZONES ARE FROM 12 TO 26.
FREQUENCY 18 MHZ. ZONES ARE FIVE DEGREES OF CML WIDE.

JULIAN DATE	IO RELATED ZONES ACTIVE	IO RELATED ZONES TOTAL	NON-IO ZONES ACTIVE	NON-IO ZONES TOTAL
39773	0	0	0	13
39774	0	0	0	0
39775	0	5	0	0
39776	0	0	0	0
39777	0	0	0	0
39778	0	0	0	12
39779	0	0	0	0
39780	0	0	0	10
39781	0	0	0	0
39782	0	0	0	3
39783	0	0	0	7
39784	0	0	0	0
39785	0	0	0	16
39786	0	0	0	0
39787	0	0	0	10
39788	0	0	0	2
39789	0	0	0	0
39790	0	0	0	12
39791	0	0	0	0
39792	0	0	0	15
39793	0	0	0	0
39794	0	0	0	1
39795	0	0	0	8
39796	0	0	0	0
39797	0	0	0	16
39798	0	0	0	0
39799	0	0	0	10
39800	0	4	0	0
39801	0	0	0	0
39802	0	0	0	15
39803	0	0	0	0
39804	0	0	0	8
39805	0	0	0	0
39806	0	0	0	7
39807	0	6	0	0
39808	0	0	0	0
39809	0	8	0	8
39810	0	0	0	0
39811	0	0	0	12
39812	0	0	0	0

consistently available in this range than at lower frequencies where the various ionospheric effects become increasingly more difficult.

For the study of the 1974 apparition the same choices in frequency were made. However, data were also available from the 640 dipole array at 26.3 MHz. This filled aperture array has been described extensively by Desch (1976) and offers a sensitivity some three orders of magnitude greater than conventional Yagi antennas.

Activity Indices

Table 3 reports the values of the activity function, $A_S(t)$, where the summation is over the entire apparition rather than on a once-a-day basis. The Table shows that in 1967-68 and in 1974 with the standard low sensitivity systems, the values of the Io related activity indices are within an order of magnitude for all sources at a given frequency. It is also evident that, for these systems, there is a general inverse relationship between frequency and observed activity.

It is interesting to note that the non-Io component is far more dependent on which source is observed than is the Io related component. For the low sensitivity systems, the non-Io activity indices for source B are 2 to 3 times less than sources A and C at 18 and 22 MHz.

With respect to the comparison of 1967-68 and 1974 it is pointed out that in 1974 non-Io activity was observed about twice as often as it was during 1967-68. This is entirely consistent with the D_E hypothesis since the earlier apparition

Table 3

Overall Activity Indices Expressed as Percentages

Io Related - 1967-68				Non-Io Related - 1967-68			
Frequency (MHz)	A	B	C	Frequency (MHz)	A	B	C
18	32.0	33.1	31.3	18	7.7	1.8	5.5
22	26.2	23.8	12.9	22	3.3	0.7	3.9
27	7.4	10.2	4.4	27	0.4	0.7	4.2
Io Related - 1974				Non-Io Related - 1974			
18	29.7	32.0	22.6	18	14.1	2.7	14.7
22	26.7	29.3	13.0	22	12.5	1.1	6.5
27	14.7	16.9	10.1	27	1.7	1.0	4.5
26*	30.2	68.6	41.3	26*	29.8	31.2	12.4

*High Sensitivity System

occurred near the minimum of the presumed effect while the 1974 apparition was more nearly at the expected 1976 maximum.

Perhaps the most dramatic effect shown in Table 2 is the impact of the high sensitivity system at 26.3 MHz with respect to the established low sensitivity patterns. The "big array" shows that Jupiter is a far more prolific emitter than the conventional receiving systems have indicated. Not only is the non-Io related component more frequently active, but the non-Io related activity is anywhere from 3 to 30 times more prominent.

CHAPTER 3

SOLAR WIND

Steady Flow Models

Early Clues

Perhaps the earliest recognized clues to the existence of a wind of particles blowing out from the sun were correlations between certain geomagnetic events and solar phenomena. By the early 1930's, two such classes of correlated magnetic disturbances were identified. Chapman and his collaborators (Chapman, 1963) established the connection between solar flares and the sudden commencement (SC) type of geomagnetic storm. They noted that many large solar flares were followed some 12 to 36 hours later by a SC. Since it was clear that the assumed exciter was either electromagnetic or particulate, the time delay was due either to some kind of hysteresis effect in the geomagnetic reaction to an exciter propagating at the speed of light, or it was due to the transit time of a particulate exciter moving at 1000 to 3000 km/s. The hypothesis which evolved held that a cloud of ionized particulate ejecta from the flare compressed the geomagnetic field sharply when the two collided producing the rapid onset of the observed increase in the horizontal component of the field. The development of a ring current due to the subsequent

trapping of some of the ejecta accounted for the depression in the field which followed in a day or so.

Taken by itself, the flare-SC relationship did not indicate whether the wind was a continuous process or just a transient one associated only with flares. However, Bartels (1932) reached the conclusion that there was a long-term process in his study of "M-region events". These events represented a second class of geomagnetic storms which, rather than being transient, frequently recurred with a period of about 27 days. These storms showed no particular association with active regions of the sun, but Bartels correctly identified their period as being due to persistant streams of particles emitted at low latitudes on the rotating sun.

Another clue turned up years later in the study of cometary tails. It was noted that in tails containing large concentrations of heavy ions such as N_2^+ and CO_2^+ (rather than dust) radiation pressure was inadequate to push the tails away from the sum. Nevertheless, the "heavy" tails pointed away from the sun just as did the lighter dust tails. Biermann (1951) suggested that the "heavy" tails were being pushed away by collisions between the ions in the tail and particles continuously flowing out from sun with velocities of 500 to 1500 km/s.

Hydrodynamic Models

Biermann's work motivated Parker (1958) to study the theoretical feasibility of such an outflow. He recognized

that for any reasonable temperature in the corona the thermal velocity of hydrogen ions was no more than about one-half the 500 km/s solar escape velocity at that level. It was not believed that even the high-end tail of the velocity distribution could account for the number of particles thought to be escaping. Parker approached the problem in two ways. His first tack was to examine whether or not hydrostatic equilibrium was possible. In doing so he assumed the sun was a spherically symmetric gravitating body whose surface--the outer corona--was at a given temperature. He further assumed that above this surface there were no sources or sinks of heat, that mass was conserved, that all flow was strictly radial and that there was no magnetic field. He then invoked the barometric equation of hydrostatic equilibrium:

$$\Delta p(r) + g(r) = 0$$

where p is the thermal pressure, g is the force due to gravity and r is the radial distance. By solving this relationship for p(r) he was able to show that the pressure at infinity was <u>not</u> zero, in fact, it was several orders of magnitude higher than estimates of the pressure of the interstellar medium. Hence, he concluded that there must be an effusion of plasma--a solar wind.

Having proved the failure of static equilibrium, his second step was to modify the barometric equation by adding a term to account for bulk motion, giving

$$\nabla p(r) + g(r) = -\nabla K(r)$$

where K is the bulk kinetic energy. He proceeded to solve this equation for the solar wind bulk velocity u(r). Remarkably he found that his hydrodynamic model predicted that the velocity was a monotonically increasing function of radial distance. In other words, despite the solar graviational field, the wind continued to accelerate as depicted in Figure 4. Parker goes on to show that mathematically this unexpected result stems from the fact that the expansion occurs in three dimensions rather than one. If the model had assumed an infinite flat sun, the wind velocity would decrease monotonically with distance.

When Parker's paper was published there were no direct measurements of the solar wind. The earliest direct measurements would not occur until the following year, 1959, when the Russian probe Luna 1 was flown. There were other, essentially contemporary, theories such as those of Chapman (1954) and Chamberlain (1960) which, proceeding from different assumptions, held that there was little or no wind, though interplanetary space was filled with matter more or less in hydrostatic equilibrium. However, once the direct measurements were obtained it was clear that Parker's assumptions were more

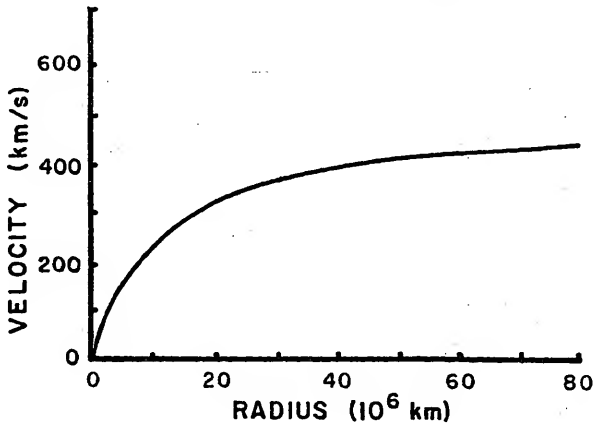

Figure 4. Solar wind bulk velocity u(r). (After Parker, 1958.)

nearly correct. With the launch of Mariner 2 for Venus in 1962, extended measurements became available (Neugebauer and Snyder, 1966) and the number of models proliferated rapidly.

The basic requirements to devise a model are a set of conservation equations for mass, momentum, and energy together with appropriate boundary conditions. Both the form of the equations and the boundary conditions are influenced by the assumption of some kind of heating mechanism which acts on the wind somewhere between 2 and 20 solar radii. This process is the primary energizer for the wind.

The nature of this heating mechanism was, and still is, poorly understood. It is also unfortunate that the number of terms that might conceivably be included in the conservation equations is large. For example, the energy equation might have significant terms representing gravity, bulk velocity, thermal pressure, magnetic pressure, thermal conduction, thermal radiation, viscosity, magnetohydrodynamic radiation and damping, plasma oscillation radiation, state changes, species interactions and so forth. A great deal of the model building that has been done has involved modifying the heating mechanism assumption by selecting which of the terms to retain in the conservation equations and which to delete as insignificant. Parker, for example, used only gravity, thermal pressure and bulk kinetic energy terms in his energy equation; Noble and Scarf (1963) added terms for thermal conduction and viscosity. Whang and Chang (1965) deleted

viscosity and tried convection of kinetic energy; Hartle and Sturrock (1968) deleted convection and argued that the plasma, being fully ionized and essentially collisionless, can be regarded as a two fluid gas--protons and electrons--and thus each species can have a different temperature. They made the appropriate change in the equations and produced another model. Subsequently, Yeh (1970) developed a three fluid model by adding alpha particles, while Cuperman and Metzler (1975) considered a collisional three fluid model with provision for turbulence heating.

It is surprising that so many models have been developed which ignore the influence of the magnetic field. One would think that the field would be a powerful agent in the lower corona where the primary heating of the wind plasma occurs. Furthermore, even far from the sun heat conduction in a fully ionized plasma would only take place parallel to the field. It is even more surprising that the field-free models actually predict the various wind parameters fairly accurately, though they consistently underestimate the average bulk velocity at 1 AU by 20 to 30%. The results of a number of steady flow models are presented in Table 4, together with various experimental findings. In this table the value reported for Parker (1958) corresponds to a coronal temperature of 8×10^5 K° at 14 solar radii.

In reviewing the various models it is difficult to understand why most modelers appeared content with bulk velocities in the 300-330 km/s range. Snyder et al. (1963),

Table 4

Comparison of Theoretical and Experimental
Solar Wind Parameters at 1 AU

Model (B=0)	u (km/s)	n (cm^{-3})	T ($10^5 K°$)	B (γ)
Parker (1958)	350			
Noble & Scarf (1963)	352	7	2.8	
Whang & Chang (1965)	260	8	1.6	
Hartle & Sturrock (1968)	250	15	3.5*	
Cuperman & Metzler (1975)	318	10	1.5*	
Model ($B \neq 0$)				
Urch (1969)	371	8	4.39	3.7
Wolff et al. (1971)	303	9	2.0*	8
Whang (1971)	302	5	1.5	5.8
Whang (1972)	331	6	1.5*	6.3
Observation				
Snyder et al. (1963)	504			
Wilcox & Ness (1965)	315	9		5
Hundhausen (1970)	325	4	1.4*	
Gosling et al. (1971)	426			

*Electron temperature

the review by Ness (1968) and Gosling et al. (1971), all clearly show that the mean value over a solar rotation was greater than 400 km/s. Most modelers emphasized that their models were for the quiet sun, but 1962 was near the minimum of Cycle 20 and the values reported by Mariner 2 averaged 504 km/s. The 300 km/s figure is more nearly the lowest observed value published after 1963.

MHD Models

Formal inclusion of the magnetic field in a steady flow model seems to have been done first by Weber and Davis (1967). The one fluid inviscid conduction model of Urch (1969) was the first to resolve the bulk velocity discrepancy, but it overestimated the proton temperature and underestimated the azimuthal velocity, both by an order of magnitude. Wolff et al. (1971) produced a viscous two-fluid conduction MHD model with the same basic discrepancies as Urch.

In an effort to resolve the velocity problem in his earlier field-free model (Whang and Chang, 1965) with its assumed strictly radial flow, Whang (1971) proposed an MHD model which included a process by which magnetic field energy was continuously converted into kinetic energy as a by-product of the expansion process. His calculations indicated that this process would increase the velocity at 1 AU by 17%. He subsequently extended this work to a two fluid model (Whang, 1972). However, Barnes (1974) showed that in MHD models the assumption of strictly radial flow is no longer valid. Near the sun the intense magnetic field attempts to

impose corotation on the plasma. The resultant azimuthal acceleration imparts an azimuthal velocity component which can no longer be ignored. The net result was that Whang's radial velocity increase was reduced to about 1% at 1 AU.

Recently Nerney and Suess (1975) presented a model which assumed symmetry about the sun's spin axis only. Their model shows a weak meridional magnetic pressure gradient. The resulting force pushes plasma out of the equatorial plane and toward the poles. This transport process imposes a -2.6 km/s meridional velocity component on the solar wind near 1 AU. They suggest that as much as 20% of the equatorial plasma may be displaced from the solar equatorial plane at 5 AU.

Comments

The underestimation of the bulk velocity of the solar wind remains a feature of most models. Consequently, the observed bulk kinetic energy is on the order of 60% greater than that for which the models can account. Since 95% or more of the total energy flux is due to bulk kinetic energy, a major source of the wind's energy is still not appreciated.

A universal feature of the models considered is the call for a monotonically increasing bulk velocity with radial distance. Taken at face value this would imply that one should expect the solar wind to be moving faster at Jupiter than at the earth. This increase varies from 3 to 29% depending on the model. It also represents an extrapolation of models which have been "tuned" to fit known conditions in the corona

and at 1 AU.

Measurements made by Mariner 2 failed to find any decrease in wind velocity as it moved in toward Venus (Snyder et al., 1963). Likewise, the expected increase in velocity was not seen in comparative measurements made by Pioneers X and XI in the vicinity of 4.5 AU and 1.5 AU respectively (Collard and Wolfe, 1974). However, since the models have steady flow as a basic assumption and the actual flow is quite variable, the Mariner and Pioneer measurements may not be directly comparable to velocities in the steady flow models. At the very least it seems that there should be some kind of weighting in the averaging process to enhance the importance of the velocity on days when the particle density is high and diminish the importance of the velocity on days when the particle density is low.

The Observed Wind

Rather than being uniform and symmetrical, the solar wind is found to have large scale structure affecting all of its measured parameters. At times this structure is very regular and predictable, while on other occasions it appears chaotic.

Bartels' Streams

After a preliminary review of the first 4.5 months of Mariner 2's solar wind data, Snyder et al. (1963) reported

that the solar wind velocity was deeply modulated, containing four or five major peaks every 27 days. Furthermore, the velocity peaks strongly correlated with peaks in the geomagnetic index K_p. Figure 5 shows a segment of their data.

The inescapable conclusion was that Bartels' picture of the recurrent "M-region" geomagnetic disturbances being due to the existence of long-lived high-flux streams of solar particles was indeed correct. It would turn out, in fact, that geomagnetic conditions were so well correlated with the solar wind that they could be used to extrapolate back to as early as 1932 to produce estimates of the daily orientation of the interplanetary magnetic field (IMF) as has been done by Svalgaard (1976).

Interplanetary Magnetic Sectors

In late 1963 the IMP satellite was launched into a very eccentric orbit which carried it into the interplanetary medium. From its sensors Wilcox and Ness (1965) were able to determine that the magnetic field intensity, particle density and particle flux were also strongly correlated with the high velocity streams. During the three-month period of the satellite's observations they found that there were four high-velocity streams in each 27 day solar rotation. As the sun rotated three of these streams were seen at intervals of about 7.7 days and the fourth stream 3.9 days later. The width of the three wider streams was about 4 days followed by 3 to 4 days of slow wind speed.

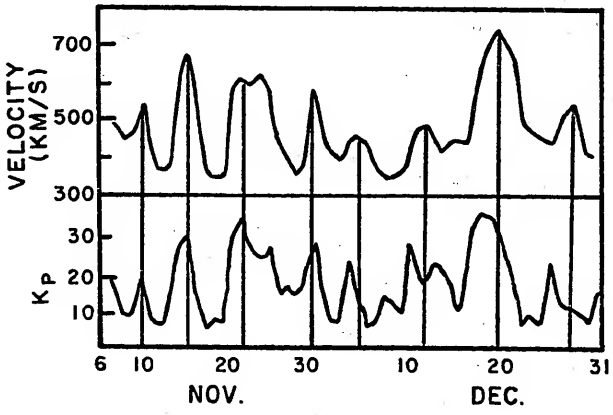

Figure 5. Solar wind bulk velocity from Mariner 2 and geomagnetic index ΣK_p. (After Snyder et al., 1963.)

The observations of the magnetic field showed that during the entire period from one fast stream to the next, the field direction was either directed inward or outward from the sun. However, just before the next fast stream, the magnetic field direction reversed itself. Consequently, the plasma was organized into four regions or "magnetic sectors" of alternately inward and outward directed magnetic field. The boundary between two successive sectors is very abrupt. The field reversal at the boundary was seen to occur in less than 5 minutes. Figure 6 shows this four sector situation as it was observed a year later by IMP 2 (Wilcox and Colburn, 1969).

Extended observations have shown that the two sector and four sector configurations are those most frequently seen (Svalgaard, 1976). When these occur the pattern usually remains stable for several months to a year. At other times the pattern may be very confused, having as many as twelve sectors of relatively short life leading to rapidly changing configurations.

The question of solar cycle effects on sectors has been examined extensively by Wilcox and Colburn (1969, 1970), Intriligator (1974), Vasyliunas (1975) and others with mixed results. Most recently Bame et al. (1976) have concluded that high amplitude streams with high peak velocities and broad angular extent are more probable in years of low or declining sunspot numbers.

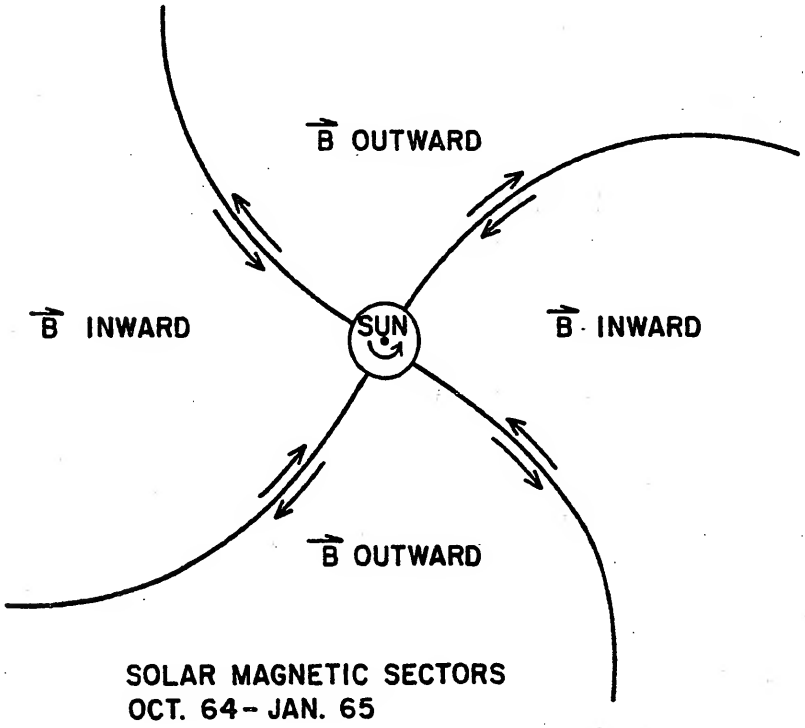

Figure 6. Solar magnetic sectors 1964-65.

The sharpness of the sector boundary has been interpreted to mean that the magnetic fields within a sector are actually open lines rather than part of a closed loop structure. The field itself is regarded as being an extension of closed loop features in the lower corona. As field lines from these lower structures extend into the 2 to 20 solar radii region they are swept away by the wind as it is rapidly accelerated outward. Newkirk (1971) has identified a class of linear north-south loop patterns in computer extrapolations of the photospheric fields into the corona. These features, dubbed "coronal arcades" for their similarity in appearance to covered walkways, are thought to be the origin of the sector boundaries (Newkirk, 1972).

The regions from which the high speed streams are emitted may be "coronal holes" characterized by abnormally low densities and temperature (Krieger et al., 1973). In these regions the diverging magnetic field is believed to play the role of a de Laval nozzle in accelerating the wind to abnormally high speed (Adams and Sturrock, 1975).

Velocity Stream Interactions

Snowplow Effect

During periods of stable sector structure an observer in interplanetary space near 1 AU sees a periodic fluctuation in the solar wind velocity. This variation will have a frequency of twice the number of sectors since each sector has a high

speed and a slow speed component. Figures 7 and 8 show that the day of the sector boundary passage is at or near a velocity minimum, followed 1 to 3 days later by a maximum--the beginning of the high speed stream--which is sustained for a few days then diminishes to a minimum at the next boundary passage.

As the high and low speed components propagate through space the fast stream from the beginning of one sector gradually overtakes the slow stream from the end of the preceeding sector. Each stream consists of fully ionized plasma in a magnetic field and consequently one stream may not pass through another, though Papadopoulos (1973) has shown that interpenetration of two streams may occur up to about one ion gyroradius. Eventually there is a "collision" between the two streams which compresses both streams adiabatically, raising the temperature, magnetic field and particle density (Burlaga et al., 1971). The plots in Figure 7 show the density buildup in the trough just before the velocity wave. This process was aptly likened to the buildup of snow before the blade of a snowplow by Sonett in a comment on a paper by Davis (1972).

The collision process is inelastic as it seems the material from both streams becomes part of a joint entity--the building density wave--share momentum, and continue at a speed intermediate to those of the original streams with the sector boundary trapped in the wave. In time the original velocity waves will be damped out by these interactions leaving instead a series of density waves moving at the average wind

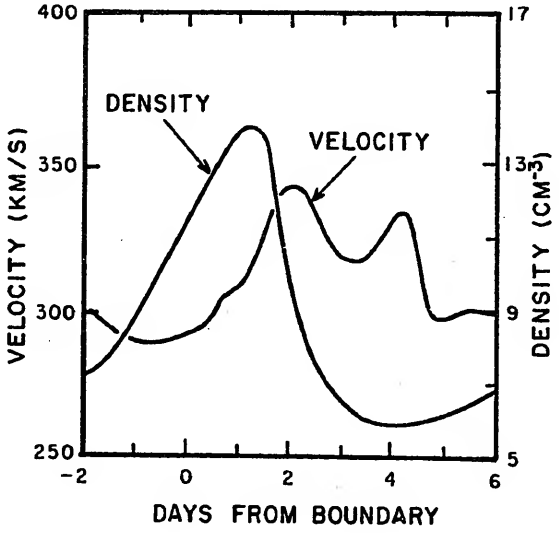

Figure 7. Solar wind velocity and particle density versus days from magnetic sector boundary. (After Wilcox and Ness, 1965.)

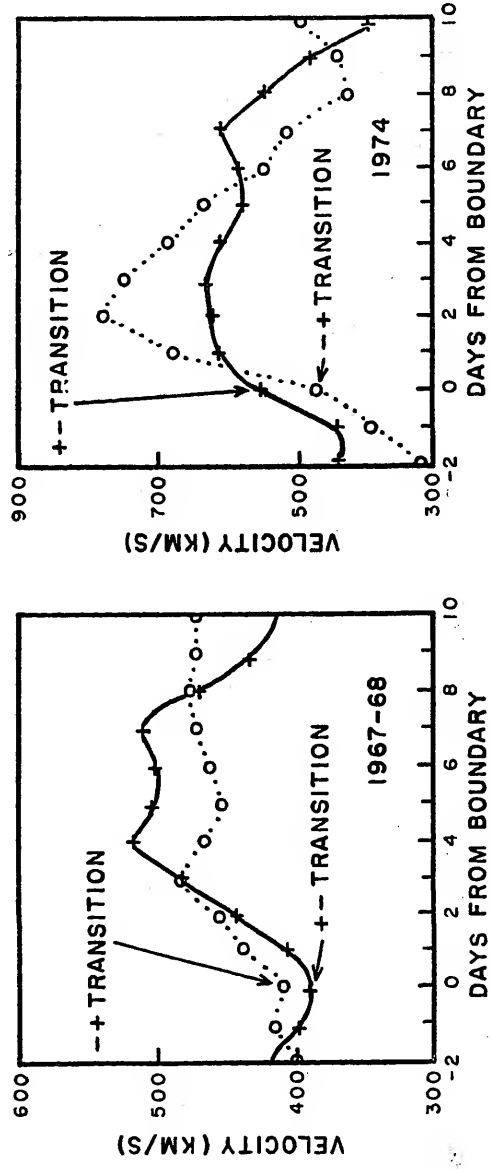

Figure 8. Solar wind velocity versus days from magnetic sector boundaries.

velocity. At this point the magnetic fields will become perpendicular to the radial flow of the density waves. Siscoe and Finley (1970) have applied velocity perturbations to a non-spherically symmetric steady flow wind model with essentially this result, while the comparative study of the Pioneer X and XI data by Collard and Wolfe (1974) shows the strong damping effect of the velocity waves near 4.5 AU in 1973.

There is another effect of the stream interaction process which may be a factor in stimulating Jovian emissions--shock waves. The bulk wind velocity is superalfvenic and supermagnetosonic. In the region between the earth and Jupiter where much of the stream interaction occurs, the fast magnetosonic wave velocity is in the 30 to 70 km/s range. It will be seen shortly that the velocity difference between colliding streams is often greater than the MHD wave velocity. As a result a by-product of such a collision is the production of two fast mode shocks, one moving outward and other other moving inward relative to the collision but carried outward by the bulk wind flow. Experimental evidence of this effect is seen in geomagnetic disturbances referred to as sudden impulse (SI) pairs (see for instance Razdan et al., 1965; Dessler and Fejer, 1973; and Beard, 1965).

Stream Interaction Models

Since one of the objectives of this research is to compare the arrival of the density wave peaks at Jupiter with

observed Jovian decametric emissions, a model describing the process of the formation of the density waves is required. Velocity wave data at 1 AU will be used as input to such a model to predict the density waves' arrival at Jupiter. In order to simplify this task as much as possible the two apparitions to be studied were chosen to be periods with stable two sector suns as shown in Figure 9. The benefit of this choice is two-fold. First, it reduces the number of waves considered to a minimum--two per solar revolution. Second, it reduces the amount of interaction to a minimum since the fast and slow streams start out as widely separated as possible. Figure 8 shows the velocity wave structure at 1 AU during these periods.

In devising a suitable model for the stream interaction it must be remembered that only large scale effects are of interest. The microscopic details of the interaction appear to be very complex and they will be ignored as much as possible in favor of predicting the macroscopic development of the density wave. Intuitively, the smaller the amount of interaction that takes place before the wave-Jupiter encounter the less important the microscopic details are.

Input Data

Before proceeding with the development of the models a discussion of the treatment of the experimental data is in order. The reduction procedure for the October 1967 - May 1968 apparition and that of the April 1974 - December 1974 apparitions

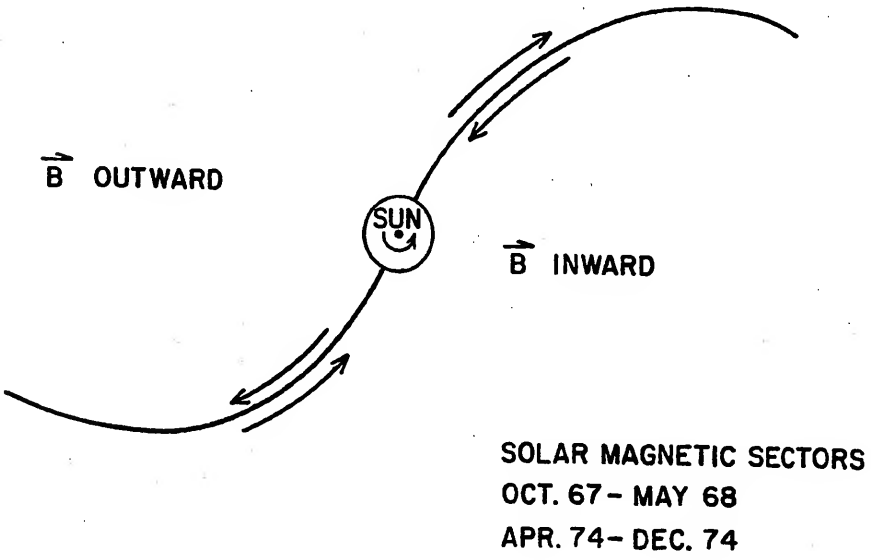

Figure 9. Solar magnetic sectors 1967-68 and 1974.

differed in some respects. The ultimate goal, however, was the same.

Figure 10 shows the relative positions of the earth, sun, and Jupiter for some arbitrary time before opposition. Since the velocity of the streams is radial, the data of interest are the velocities as a function of time at 1 AU on the line connecting the sun with Jupiter. Since in general no observations are continuously made at that point, it is necessary to either interpolate or extrapolate what data are available to that point.

Despite the radial motion of the stream, the "garden hose" effect causes the position of the point of intersection of the stream on the 1 AU orbital circle to rotate with the sun. Consequently, any projection of measurements made off the sun-Jupiter radial to the radial involves not only a projection in space but in time as well. The intersection point moves in the posigrade sense about 13° per day. Consequently, if a measurement is made at a point 13° behind the radial line, that value becomes an estimator of the velocity on the radial the following day. If interpolation between two satellites which straddle the sun-Jupiter radial is employed, one must assume that any changes that occur are sufficiently gradual that no inflections lie between the two observations. If extrapolation from a single point is used, one simply assumes that the velocity is stable over the period of time involved.

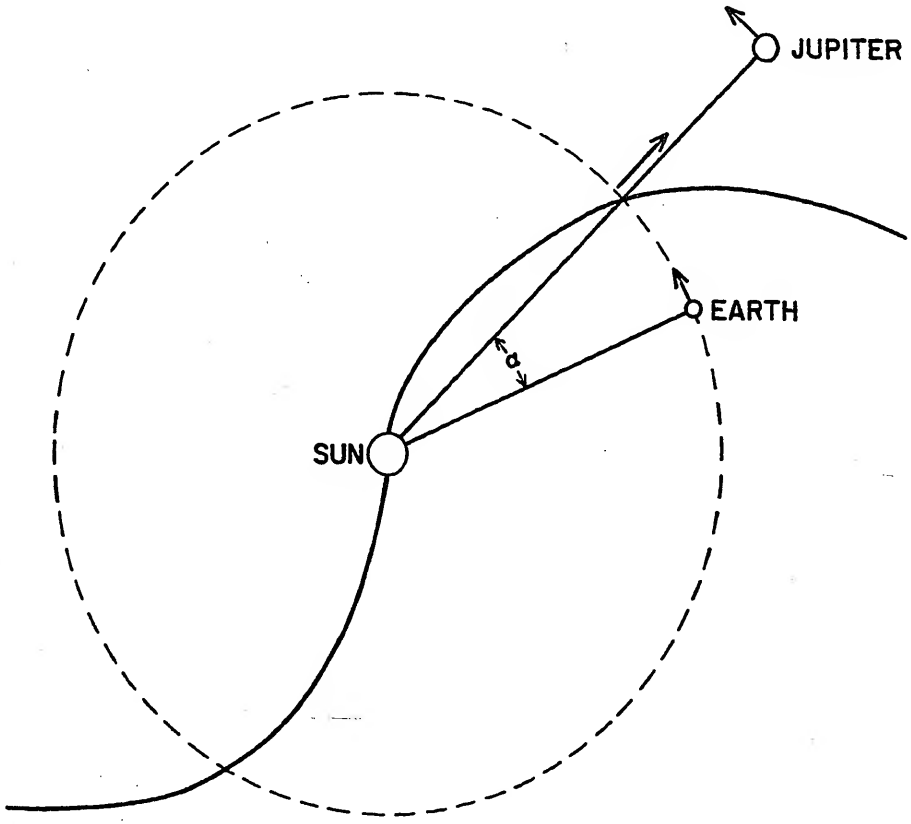

Figure 10. Sun, earth and Jupiter geometry.

Gosling and Bame (1972) have shown that if one makes a prudent choice of apparition the stream structure one full rotation away--27 days--may autocorrelate with the current structure r $\geq$0.7. It must be added that such a high correlation is the exception rather than the rule and thus the operative phase is "prudent choice." The validity of assumptions of stability is strengthened if the 27-day autocorrelation coefficient is reasonably high and one interpolates or extrapolates over periods significantly less than 27 days.

The solar wind data are in the format of a single average value per day. It is also necessary to point out that since the Jovicentric solar sector rotation period is the period of real interest in comparing solar and Jovian events, the solar rotation periods referred to in the balance of this study will be the solar magnetic sectors' Jovicentric synodic rotation period. This period is nominally 25.7 terrestrial solar days.

1967-68 apparition. The velocity information during this time was that from Pioneers VI and VII. These satellites were in solar orbit very near 1 AU. They were separated by about 155° in the ecliptic plane such that they straddled the sun-Jupiter radial throughout the apparition. Thus, one satellite or the other was never more than 5 rotation days from the radial. The table of values for the velocity on the radial was obtained by a linear interpolation in space of the

respective estimators for each day at the radial line. This is to say, the value of the velocity at each satellite was projected in time to the radial. The value chosen for the velocity on the radial for a given day was the average of the corresponding measurements from each satellite linearly weighted in favor of the nearer satellite. The autocorrelation of the 1967-68 period is shown in Figure 11 to have a value of 0.44. This is regarded as quite satisfactory for the "interpolation."

1974 apparition. The solar wind velocity data for this period of time were provided by the IMP 7 and 8 satellites which were in highly eccentric earth orbits. Unfortunately, this situation was not as satisfactory as the 1967-68 period since interpolation was not possible. The only alternative was to extrapolate the single daily average to the sun-Jupiter radial line. Figure 12 shows the autocorrelation function for the 1974 period. The peak in the function after one solar rotation is 0.81. However, the 1974 data picture may be overly optimistic. At this writing the only available velocity data for the 1974 are for the 81-day period from June 25 to September 14. These data show remarkable repeatability in the velocity structure. However, this is an inadequate length of time to permit proper cross-correlation with Jovian data. Svalgaard (1976), on the other hand, has shown that the magnetic sector structure was quite stable throughout most of the year. In order to satisfy the requirements of the cross-correlation algorithm the June-September data have been

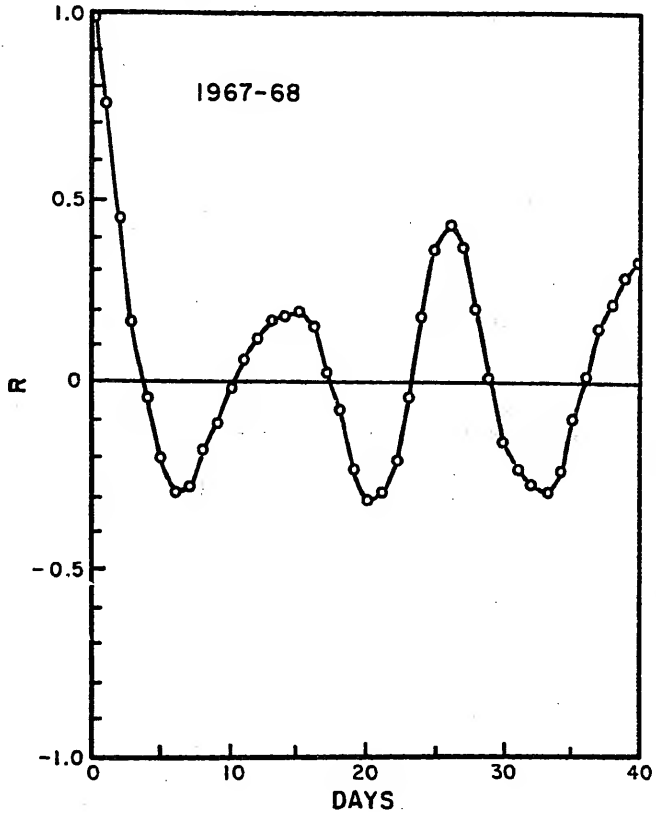

Figure 11. Solar wind velocity autocorrelation function, 1 AU 1967-68.

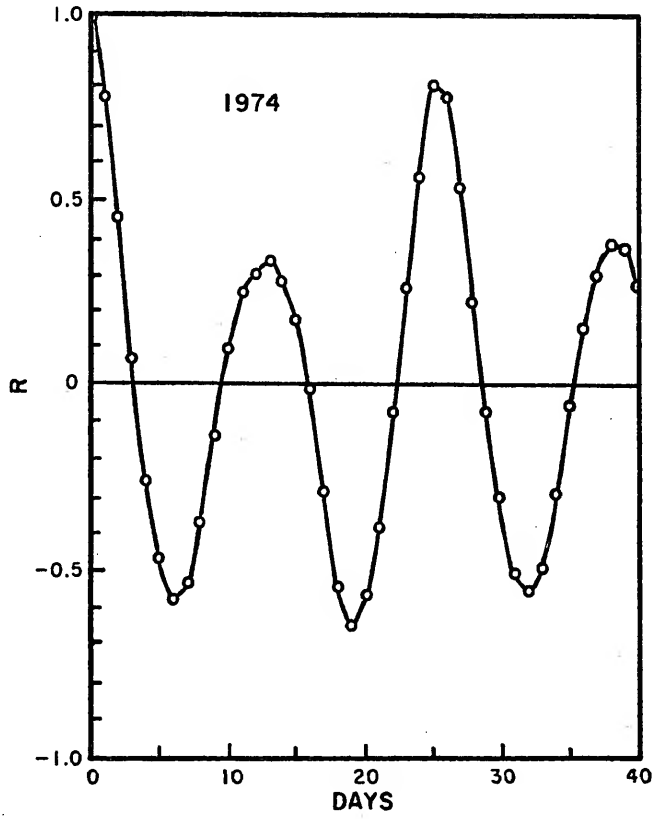

Figure 12. Solar wind velocity autocorrelation function, 1 AU 1974.

used to simulate the 81-day periods immediately preceding and following the true June-September period. No doubt this procedure has introduced some errors which may be eliminated when more complete solar wind data become available.

Magnetic-Field-Free Model

The simplest model for the stream interaction is to assume there is no interaction. In the absence of a magnetic field the solar wind is simply a collisionless plasma. Consequently, no interaction between streams occurs. Nevertheless, this model predicts the buildup of a large scale (length >0.2 AU) density wave as the fast stream approaches the slow stream leaving a rarefaction behind. This development of a density wave from a velocity wave is analogous to the "bunching" process in a klystron.

The field-free model is applicable in situations where the initial velocity spread between adjacent streams and their initial separation in space are such that fast streams do not often have the opportunity to pass completely through slow streams before reaching Jupiter. Since the model permits no stream interaction, at some point in space all of the fast streams will have passed through the slow streams and the density wave will decay. In nature, this decay probably does not occur; consequently, a basic test of the applicability of the field-free model will be to ascertain whether the model, given the input velocities for a given apparition, predicts such a decay before the encounter with Jupiter (i.e., before

about 5.2 AU). If the decay does not occur, the model can be used. The precise manner of performing this test will be detailed shortly.

A FORTRAN program designated "Snoplow" (see Appendix) was developed to generate the modeled values for wind density and flux as a function of time and space. Starting with the table of solar wind velocities at 1 AU on the sun-Jupiter radial, this program extrapolates these values back in time and space to the sun. Then the model releases groups of particles from the sun with constant arbitrary density at six-hour intervals. The four groups for a given day are assigned the wind velocity extrapolated from the earth for that day. The progress of each group is tracked for forty days to insure that even the slowest reaches Jupiter before they are discarded.

Once a day the groups are examined to determine the density and flux in space at increments of 0.2 AU. Since part of this program's objective is to permit a view of the wave building process, the decrease in density caused by the expansion of the wind (i.e., the $1/r^2$ dependence) is deliberately omitted in this calculation. As a result, the "density" and "flux" calculated are really the product of the true density or flux, the square of the radial distance, and some scale factor. Clearly, for any given radial distance this product is directly proportional to the true density at that point. Consequently, the term "density" will frequently be used to denote the product.

The net result of Snoplow is two two-dimensional arrays, one representing the density, and the other the flux, as

functions of time and space out to 6 AU. Figure 13 is an example of such an array. From this one can select a row corresponding to a given day and see the density or flux as a function of space, or one can select a column corresponding to a radial distance and see the density or flux as a function of time.

Growth test. In order to test the applicability of the field-free model, a simple auxiliary program examines the density array. At each increment of radial distance the program calculates the average and standard deviation of the density across the apparition. The program then plots the standard deviation, expressed in units of the average density, for each increment in radial distance. This function, then, is merely the normalized RMS wave amplitude as a function of distance. If a density wave building process is occurring, the amplitude will monotonically increase with distance. Conversely, if a decay is occurring the amplitude will monotonically decrease with distance. The derivative of the amplitude function may also be used as an index of growth.

Simple-Field Model

A second model has been developed to handle the case where the growth test contraindicates the field-free model. This model implicitly assumes the presence of the interplanetary magnetic field, but does not attempt to account for the fine detail of the stream interaction. The model invokes three assumptions:

Figure 13. Solar wind model density map. The values of the points in the map are those of R2x(Particle Density) in arbitrary units. The mean per point is 4.0.

1. Groups of particles cannot pass through one another ($B \neq 0$),
2. The stream collisions are completely inelastic,
3. Momentum is conserved.

These assumptions have been incorporated as a user option in the program Snoplow outlined in the previous section.

Since Snoplow treats each four hour group of particles as independent entities rather than as members of a particular stream, the assumptions are applied at the group level. Consequently, this model will permit the wave to build up as an infinitely thin sheet of mass. This is physically unrealistic because both plasma and magnetic pressure will limit the compression of the density front. The effect is offset somewhat by the coarse scale of the radial distance used in the density and flux arrays. This insures that the density wave will never appear smaller than 0.2 AU.

There is another, probably related, effect that the model does not account for. If one refers back to Figure 7, Wilcox and Ness show that the peak of the density wave front actually precedes the peak of the velocity front by about one day at 1 AU. The forward one-half amplitude point of the density front precedes the corresponding point on the velocity front by two days. However, the model will place the density front at the collision point--the leading edge of the velocity wave. There are no data available on the phase relationship between velocity and density fronts at 5.2 AU. However, if the 1 AU characteristic persists out to Jupiter, the model will consistently

overestimate the arrival date of the density fronts at Jupiter by as much as 2 days.

Model Selection

The first step in the selection of the appropriate model was to invoke the field-free model for both apparitions. The growth test routine was then run to plot the density wave growth for each apparition.

Figure 14 shows the amplitude plot for 1967-68. It indicates that the RMS density wave amplitude at 1 AU was 0.47, which is quite consistent with values seen at the earth. The plot also shows that the principal evolution of the density fronts took place beyond 1 AU and that the growth arrested at about 3.4 AU. There is a plateau which is essentially constant through 5.8 AU and then the decay process apparently begins in earnest. It was decided that, since there was little decay at 5.4 AU (the location of Jupiter in 1967-68), the field-free model was an acceptable choice for this apparition.

The field-free amplitude plot for the 1974 apparition is shown in Figure 15. In contrast to 1967-68, it shows a much higher growth rate with the amplitude peaking at 2.2 AU followed by an immediate decay. This characteristic clearly shows that the field-free model is not satisfactory for the 1974 period.

The accelerated growth of the 1974 density waves, as compared to the 1967-68 waves, stems directly from the more

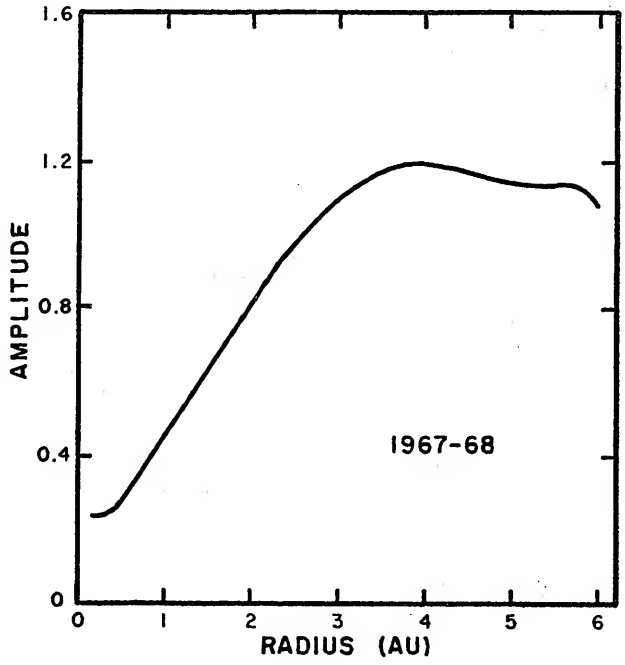

Figure 14. Field-free model RMS density wave amplitude, 1967-68.

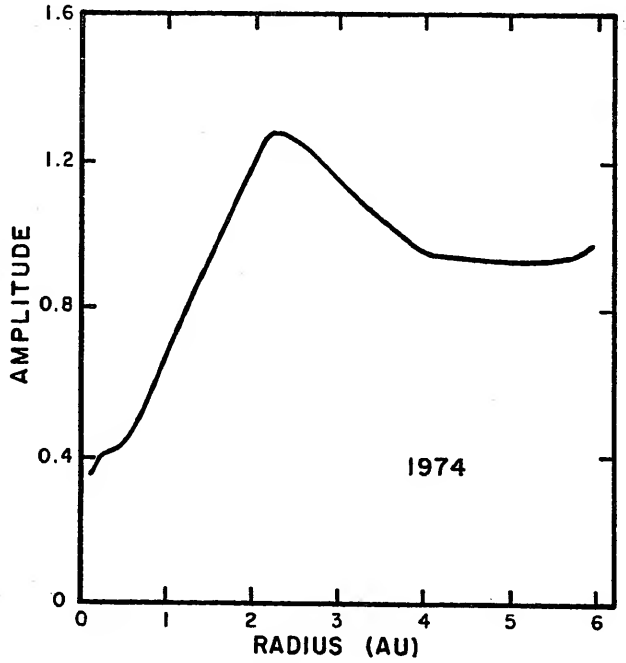

Figure 15. Field-free model RMS density wave amplitude, 1974. The inflection at 2.2 AU shows that the model fails beyond that point.

profound peak-to-peak amplitude of the 1974 velocity wave. Referring back to Figure 8 it is clear that value of the peak-to-peak velocity averages from cycle to cycle was 130 km/s in 1967-68, but the value in 1974 was 450 km/s. Consequently, the fast streams overtook the slow ones much faster in 1974.

The simple-field model was then applied to the 1974 data and a new amplitude plot obtained. The latter is displayed in Figure 16. The 1 AU value, 0.77, is higher than that usually observed but not substantially different from the 1 AU field-free value. The rapid growth evident in the field-free model is also evident here in the simple-field model. The 1 AU amplitude value is probably reasonable in that light, though 1974 observational data are not yet available.

The growth process is seen to diminish as it approaches the Jovian orbit, suggesting that the interaction process is nearing completion. This is an expected result for this model. Once a fast stream has completely accumulated the preceding slow stream, the only further interaction which can take place will be between the density fronts themselves. Since they are widely separated and moving at about the same speed, such collisions would be very infrequent.

In comparing the two models out to 2.2 AU before the field-free model breaks down, the two both provide similar amplitude values. As expected, even in this region, the simple-field model shows a somewhat higher growth rate. The accumulated amplitude exceeds that of the field-free model by 34% at 2.2 AU. Nevertheless, it is comforting to see that

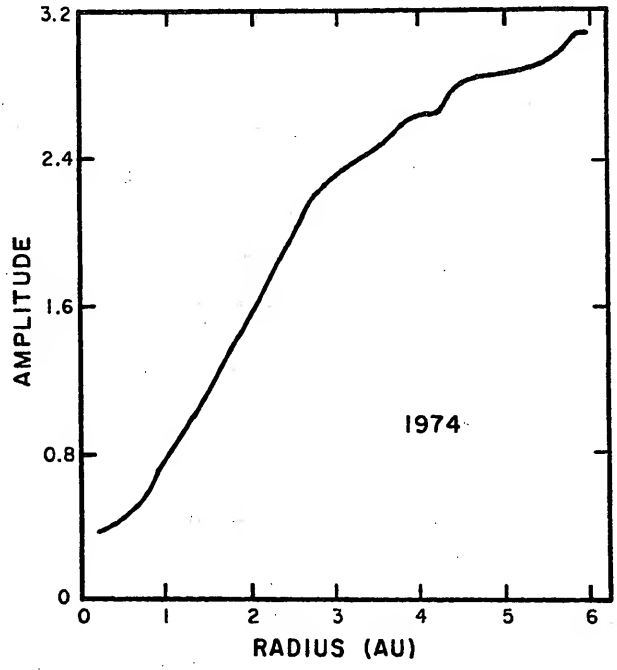

Figure 16. Simple-field model RMS density wave amplitude, 1974.

where they are both valid, these two basically very different models do not perform differently in any essential way. It is clear though that, of the two, the simple-field model would have to be used for the 1974 data.

CHAPTER 4

SOLAR-JUPITER CORRELATION

Previous Investigations

The matter of the relationship of solar and geomagnetic events was discussed at some length in the preceding chapter. By the time Burke and Franklin published their discovery of the Jovian decametric emission in 1955, the solar-terrestrial correlations were already well recognized, even though their precise nature was not. Since solar events--particularly solar flares--were seen to produce such dramatic effects as visible and radio aurora, auroral absorptions (PCAs) and profound geomagnetic disturbances, it was reasonable for early students of the Jovian radiation to consider the possibility of solar-Jovian relationships. This natural flow of thought no doubt was intensified by the timing of the discovery just prior to the International Geophysical Year, the peak of solar Cycle 19, and Parker's theoretical insights on the nature of the solar wind.

Several processes were proposed to explain the emissions such as Jovian lightning, plasma oscillations excited by shocks caused by Jovian volcanoes, and atmospheric chemical activity. In 1958, Carr proposed that the emissions were triggered by energetic particles of solar origin trapped by

the Jovian magnetosphere. At about the same time Kraus (1958) noticed two intense Jovian storms following two large solar flares and made the same suggestion. The possibility of such a connection was actively pursued by a number of investigators.

What early observers did not know was that there was a very powerful and periodic exciter, Io, which was responsible for much of the activity they were seeing. The influence of the Io effect was clearly evident in these early observations. Carr et al. (1958) reported that they had found a very definite 8-day period in their observed activity. (The 8-day period--7.71 days actually--is nothing but the alias of the second harmonic of the Io revolution period with the 24-hour sampling period imposed by the rotation of the earth.) They then suggested that the period was due to tidal action induced by one of Jupiter's satellites. Unfortunately this possibility was not explored more exhaustively at that time. The discovery of the Io effect would wait for Bigg in 1964.

The presence of the Io modulation would cloud efforts to detect solar correlations. There was yet another pitfall. Until Snyder et al. (1963) published their Mariner 2 observations, the velocity range and the stream structure of the solar wind were not known. Consequently, there was great uncertainty as to the appropriate delay time between, say, an M-region geomagnetic storm and an expected Jovian event. The only events where the timing might be inferred were solar flares followed by SCs. In this case the velocity of the wind disturbance was measurable, at least between the

sun and the earth. Since these early investigations took place near the peak of Cycle 19, flares were in relative abundance.

Pursuing the search for a solar correlation Carr et al. (1960) presented evidence to suggest that there was an enhancement of Jovian activity 8 days after geomagnetic disturbances. Warwick (1960) examined solar radio continuum events and reported increased activity, particularly 1 to 2 days after the cessation of the continuum. More evidence for an 8-day delay after geomagnetic events was introduced by Carr et al. (1961).

On the other hand, Six (1962) examined the 8-day delay and found no clear correlation. Lebo (1964) studied the delay from flares and geomagnetic storms but extended the maximum length of delay considered from 15 to 35 days. This was an important step because the just published Mariner 2 data indicated that the average solar wind velocity was in the 500 km/s range and the instantaneous values were often smaller. Thus, the average delay between the earth and Jupiter was 15 days. In doing so he found indications of peaks in Jovian activity with delays in 8 to 9 days and 15 to 21 days. Lebo also suggested that future studies be expanded to cover M-region events as well.

Armed with recognition of the Io effect Sastry (1968) examined the question anew. He recognized correctly the complexities imposed by the "artificial" periodicities in

the Jovian data on efforts to find time dependent effects, such as time-of-flight delays. However, he did not attempt to remove or compensate for the effects. Sastry reexamined Jovian radio activity from 1958 through 1963 and concluded that the probability of emission is higher after geomagnetic activity than before. He cautioned that the correlation might be an artifact produced by the periodicities.

A paper by Conseil et al. (1971) shows a tantalizing but invalid relationship between the sign of the derivative of the solar wind velocity and the definition of "Io-related" activity. They have considered Jovian activity and solar wind velocity measurements of Pioneers VI and VII in orbit at 1 AU during 1967-68--the same period as one of the two examined in this study. Unfortunately, they explicitly required that, "propagation effects [in the solar wind] are not very important." It must be clear that the extent of these interactions is all-important. However, the effect they observed may, in fact, be real, but for the wrong reason.

During the 1967-68 apparition, it has been argued here that the difference between the velocities of high and low speed streams was such that the field-free or non-interaction model adequately describes the evolution of the density wave out to Jupiter. Conseil's assumption of the unimportance of the interaction constitutes the invocation of the field-free model. Their error was in failing to consider the density wave.

Using the satellites' wind velocity data, Conseil and his colleagues developed a table of solar wind velocities versus dates at Jupiter. They then examined the Jovian decametric data for correlations with the velocity table. What they reported was that the "favored" range of Io phase (ISC) for source A and source C storms shifted toward lower angles on days when the wind velocity was increasing and toward higher angles when the velocity was decreasing. This effect is shown graphically in Figure 17.

However, it seems very unlikely that the velocity derivative at 1 AU would be maintained at Jupiter. The derivative of the velocity is necessarily far more sensitive to stream interactions than is the velocity itself. But, it is known that a positive velocity derivative at 1 AU corresponds to the leading edge of the fast stream which, in turn, is coincident with the peak of the density wave. In a similar manner, a negative velocity derivative corresponds to the trough of the density wave. As a result, one may interpret their result as actually being a correlation between the "favored" range of Io and the density wave, not the velocity wave as they propose.

Kovalenko (1971) examined the relationship between Jovian emissions and interplanetary shocks caused by flares and stream collisions. Using the "Forbush decreases" in cosmic-ray intensity as an indicator of a shock passage at the earth, he used an extrapolation procedure identical to

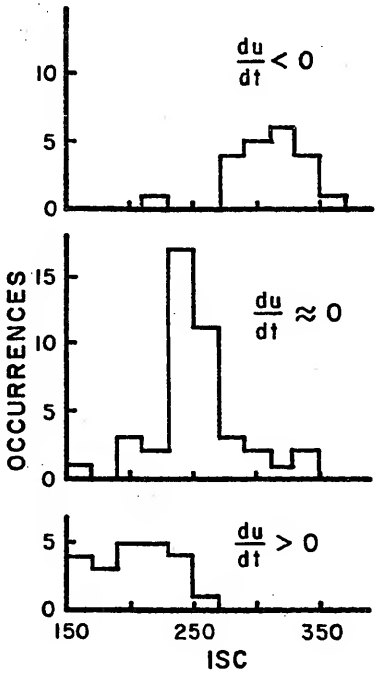

Figure 17. Decametric storms versus ISC for sources A and C, 1967-68. (After Conseil et al., 1971.)

the one described in the preceding chapter to place the shock on the sun-Jupiter radial. He concludes that for the period 1961 to 1964 there was a one-to-one correspondence between geomagnetic events and Jovian activity.

The principal shortcoming of Kovalenko's work stems from the fact that he had no solar wind velocity data. As a consequence he was forced to infer the velocity at 1 AU using an algorithm which related the wind velocity to the magnitude of the shock and its accompanying geomagnetic storm. He also failed to make any separation of Io and non-Io related events. Consequently, the 7.7 day Io cycle may well have produced the "27-day" cycle he reports (4 x 7.7 = 28.3). Had the cycle been due to a solar influence the period would have been the Jovicentric synodic period, 25.7 days.

In 1972 in a precursor of the present study, the author presented an apparent correlation between the non-Io related component of source A and the projected passage of sector boundaries at Jupiter in the 1964-65 apparition (Kennedy, et al., 1973). In that work the occurrence of sector boundaries at the earth, projected to the sun-Jupiter radial, and Jovian radio data were each subjected to a superposed epoch analysis using the Jovicentric 25.7 day period as the base period. These two plots were then shifted relative to each other to see if there was a time shift corresponding to the time-of-flight delay in the sector boundary arrival at Jupiter. The best match between the two plots occurred at a shift of 13.5 days. This delay indicates an average solar wind velocity of

514 km/s during the period of the study (the average for the entire year 1964 was given by Gosling et al. (1971) as 465 km/s). Figure 18 shows this comparison.

This approach was regarded as simplistic in that it demanded that the sector boundary propagate at the average wind velocity. At the time it seemed likely that the velocity of the sector would be modified by the stream interactions--which had not been accounted for. In retrospect, however, the procedure may have been better than it appeared. The sector boundary does become trapped in the density wave which is traveling at an intermediate velocity due to the stream collision process. Furthermore, as Collard and Wolfe (1974) have shown, the peak-to-peak velocity dampens and converges on the average velocity as the stream moves outward. During 1964-65 the sun had four sectors, which means the distance between fast and slow streams was half that of a two sector sun. Though velocity data are not available, it is safe to assume that the amount of interaction damping was much higher at 1 AU due to the four sectors than during the two-sector periods of the present study. The result would be to further insure that the density wave at the earth was already at or near the average wind velocity.

Barrow (1972) has examined Jovian data from 1961 to 1968. He noted that due to the earth-sun-Jupiter geometry the time-of-flight delay is a function of the position of the earth relative to Jupiter. For example, after opposition particles on the sun-Jupiter radial are already past 1 AU by the time the solar rotation presents that stream to the earth.

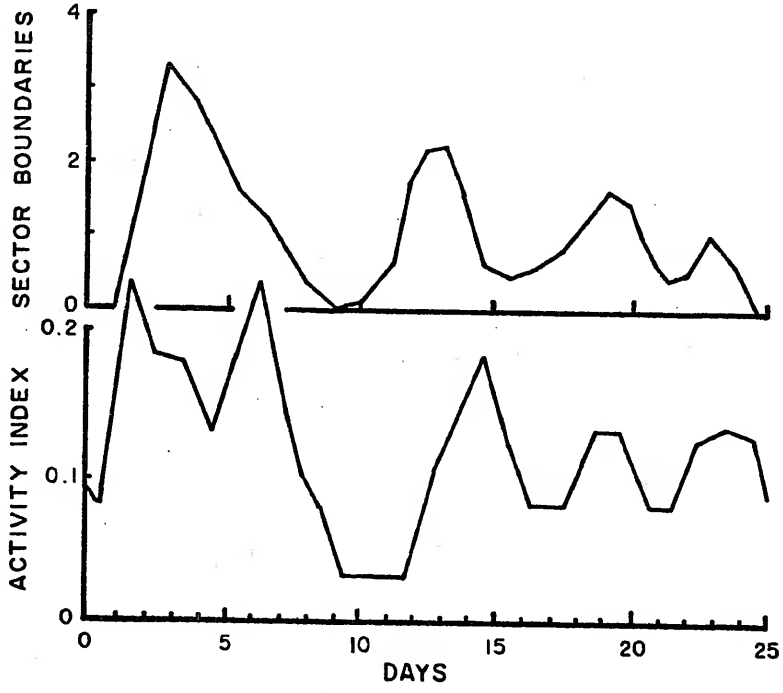

Figure 18. Superposed epoch analyses of sector boundaries at 1 AU and Jovian activity in 1964. The boundary plot is delayed 13.5 days with respect to the activity plot. (After Kennedy et al., 1973.)

Unfortunately, there is an error in Barrow's work. His Figure 2 is incorrect. The plot should have been made from $\emptyset = -180°$ to $\emptyset = 180°$, not from 0° to 360°. This error led him to the statement, " . . . immediately before opposition . . . values may be such that Jupiter can be active before the particles reach the earth." This is obviously incorrect since, before opposition the particles always arrive at the earth first. This is compounded by the fact that he does not differentiate between Io and non-Io related events. Since he has selected which Jovian storms to study in a way that emphasizes major storms, much of the data he used is Io related. Barrow reports a positive correlation but his errors cast doubt on the validity of the result.

Vladimirsky and Levitsky (1976) have recently reported a correlation between Jovian activity and solar proton flares. They maintain that the predominantly more dense and slower wind found in the solar equatorial plane by Hundhausen et al. (1971) forms a quiet zone which shields Jupiter when its heliocentric latitude is between 2° North and 2° South. They report that when Jupiter is outside that range the incidence of Jovian activity 1 day after a proton event is more than twice the average incidence.

Solar proton events are caused by a stream of very high speed particles blown away from the sun by a very energetic flare. The velocity of these streams is typically 10^4 to 5×10^4 km/s. Such a stream is different from the main body of flare ejecta which moves slower by a factor of 10. The latter are

responsible for SCs while the proton events result in PCAs.

The sector rotation period suggests that the high speed streams are emitted at solar latitudes of about 20° North and South rather than from the equator. This is regarded as the most likely explanation of Hundhausen's finding of higher density and lower speeds in the equatorial plane. Vladimirsky and Levitsky believe that this thin band acts as an imperfect barrier for particles that try to cross the equatorial plane. These assertions certainly seem plausible, as does the proton-event-Jovian relationship.

Summary. The correlations obtained by Conseil et al., Kennedy et al., and Vladimirsky and Levitsky may be real. The positive results of solar-Jupiter correlation studies reported by other workers must be considered less than convincing, if only because of the uncertain influence of the Io related events. Sastry's concern that the periodic Io effect might mimic a periodic solar relationship is well founded. Most of the early studies also failed to take the earth-sun-Jupiter geometry into account. Consequently, timing errors of several days are induced in the projected arrival of M-region events, though flare correlations would not be affected by this problem.

Analysis

Chree Analysis and Correlation

Preceding chapters have described how the Jovian decametric data were filtered and segregated to provide a separate

listing of each source at each frequency for both the Io and non-Io component. Likewise it was shown how solar wind velocity data for 1 AU were used to generate a table of model particle flux densities at Jupiter. Motivated by the belief that the supposed solar influence was not a strong effect, it was decided to use a special case of Chree analysis to minimize noise in the data. The data were superposed on themselves with a period of about 25.7 days, the Jovicentric synodic solar rotation period, and collected in 25 channels each representing one day.

In order to account for daily sample size variations the superposition was done separately for the observation and activity data. In this fashion the zone counts for observations for each channel were summed over the long apparition while the same process was going on separately with the activity zone counts. When the summations were complete, the ratio of the counts for each pair of activity and associated observation channels represented the apparition-long activity index for that channel.

The table of solar wind flux values was superposed upon itself, summed and then averaged to give the solar wind information in the same form as the Jovian data. The two Chree analysis tables were subjected to a Hanning smoothing procedure (see Chapter 5) and then shifted with respect to each other in one day (channel) increments with the cross-correlation coefficient being determined at each shift. A shift of zero days corresponds to the projected dates of arrival of the density waves at Jupiter. The whole process of Chree analysis

and cross-correlation is accomplished by a computer program designated "Jupsol V" (See Appendix). Figure 19 shows an example of the Chree analysis and cross-correlation functions.

The subject of the development of confidence limits for the Chree analysis tables is reserved for a later chapter. The confidence intervals for the cross-correlation procedure are obtained using the standard "t test" (see Hartnet, 1970). If two functions are both randomly distributed, then the function

$$t = \frac{r\sqrt{n-2}}{\sqrt{1-r^2}},$$

where r is their correlation coefficient and n is the number of points in each function, has a Student t distribution with n - 2 degrees of freedom. This function will permit testing a null hypothesis that the functions are not correlated. The correlation coefficient limits for various confidence intervals for the 25 point cross-correlation used in the present study are given in Table 5.

Table 5

Confidence Intervals

Level	Interval
90%	$-0.337 \leq r \leq 0.337$
95%	$-0.396 \leq r \leq 0.396$
99%	$-0.505 \leq r \leq 0.505$

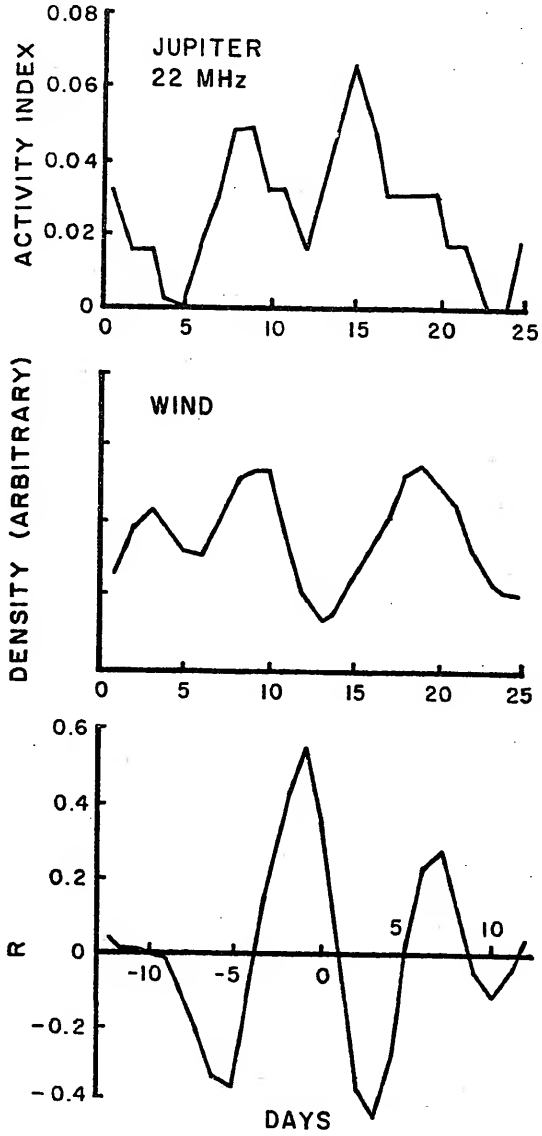

Figure 19. Superposed epoch analyses of Jovian activity and solar wind density are shown in the upper two plots. The lowest plot is the plot of the cross-correlation function, R, of the activity and density functions.

The Apparitions

As has been mentioned the two Jovian apparitions to be studied here are those of 1967-68 and 1974. Table 6 has been prepared to compare and contrast the various conditions surrounding these measurement periods. It is noted that in many ways the two apparitions are antisymmetric. The dates of opposition are about 6 months apart, the radial distances, D_E and sunspot cycle conditions are all near opposite extremes. One point of similarity deserves note. The heliocentric latitude of Jupiter was well with the 4° quiet zone suggested by Vladimirisky and Levitsky.

Table 6

Apparitional Statistics

Parameter	1967-68	1974
Opposition	23 February	6 September
Radial Distance	5.38 AU	4.98 AU
Synodic Sector Period	25.75d	25.58d
Heliocentric Latitide	1°	-1°
D_E Effect on Activity	Near Minimum	Near Maximum
Sunspot Cycle	Near Maximum	Near Minimum

The Cross-Correlations

The cross-correlation functions obtained for the 1967-68 non-Io component of source A, B, and C are presented in Figures 20, 21, and 22 respectively. These show strong positive correlations at or near zero days relative shift for sources A and C at all frequencies except for source A at 18 MHz. The plots also show a statistically significant anticorrelation for source B at 18 MHz. The various coefficients and the corresponding time shift relative to the predicted wave-Jupiter encounter are summarized in Table 7. It should be noted that day zero corresponds to the encounter day, negative days are before encounter and positive days are after encounter.

The cross-correlation plots for the 1974 apparition are shown in Figures 23 through 26. They show a similar picture. Source A has positive peaks at 26 and 27 MHz, Source B anti-correlates at 18, 22, and 27 MHz, while source C has positive correlation peaks at 18, 22, and 27 MHz. These values are summarized in Table 7.

An interesting feature of the 1974 plots is the fact that the features of interest fall not in the -1 to 0 day range but they occur between -4 and -2 days.

Conclusions

During both apparitions there is a tendency for the extrema to precede the predicted encounter day. However, it has been noted that the crests of the density waves actually observed at 1 AU do in fact precede the stream collision point

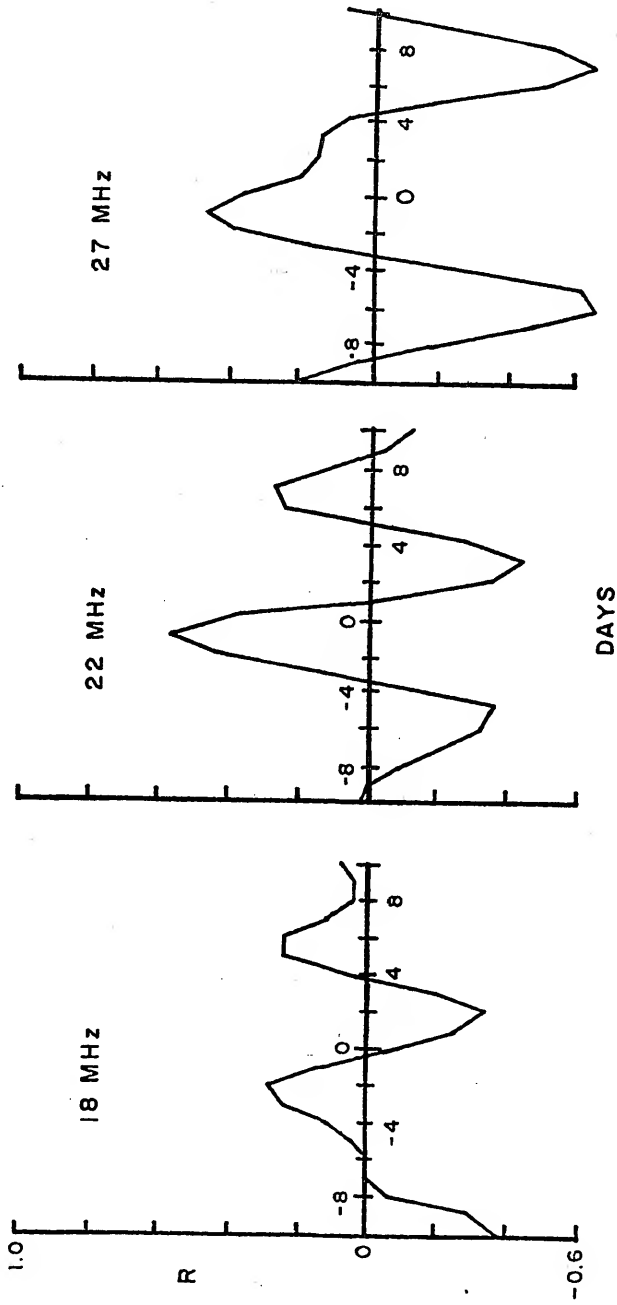

Figure 20. Cross-correlation functions of solar wind flux and Jovian activity, source A, 1967-68. R is the cross-correlation coefficient, Source definitions are found in Table 1 on page 5.

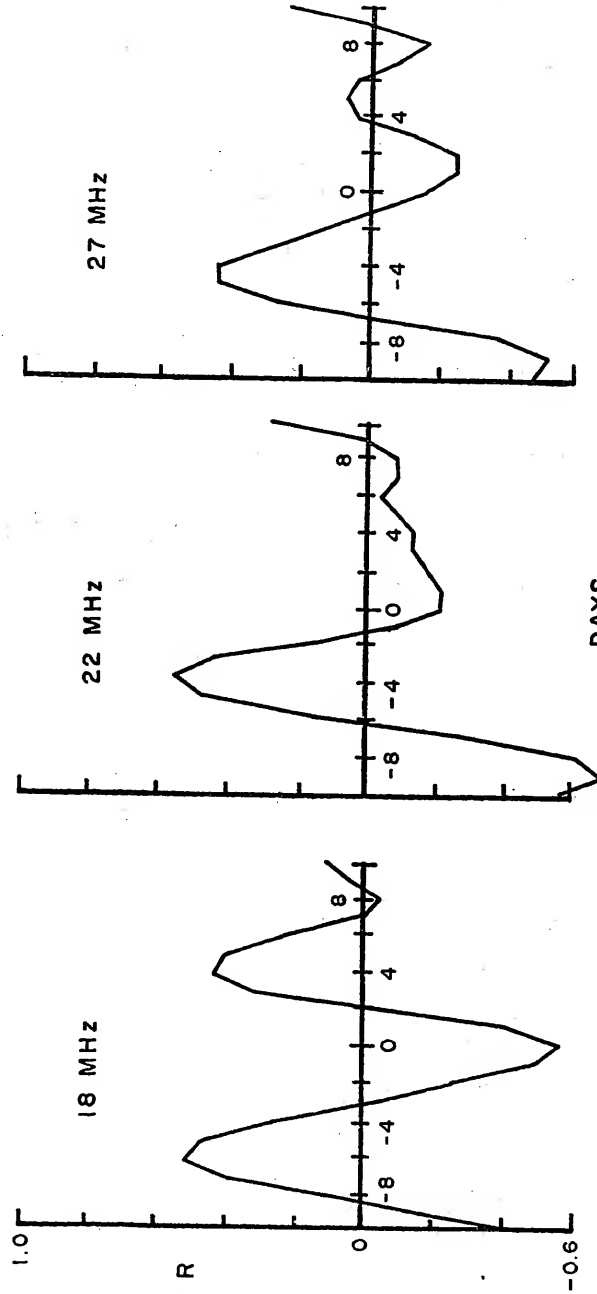

Figure 21. Cross-correlation functions of solar wind flux and Jovian activity, source B, 1967-68.

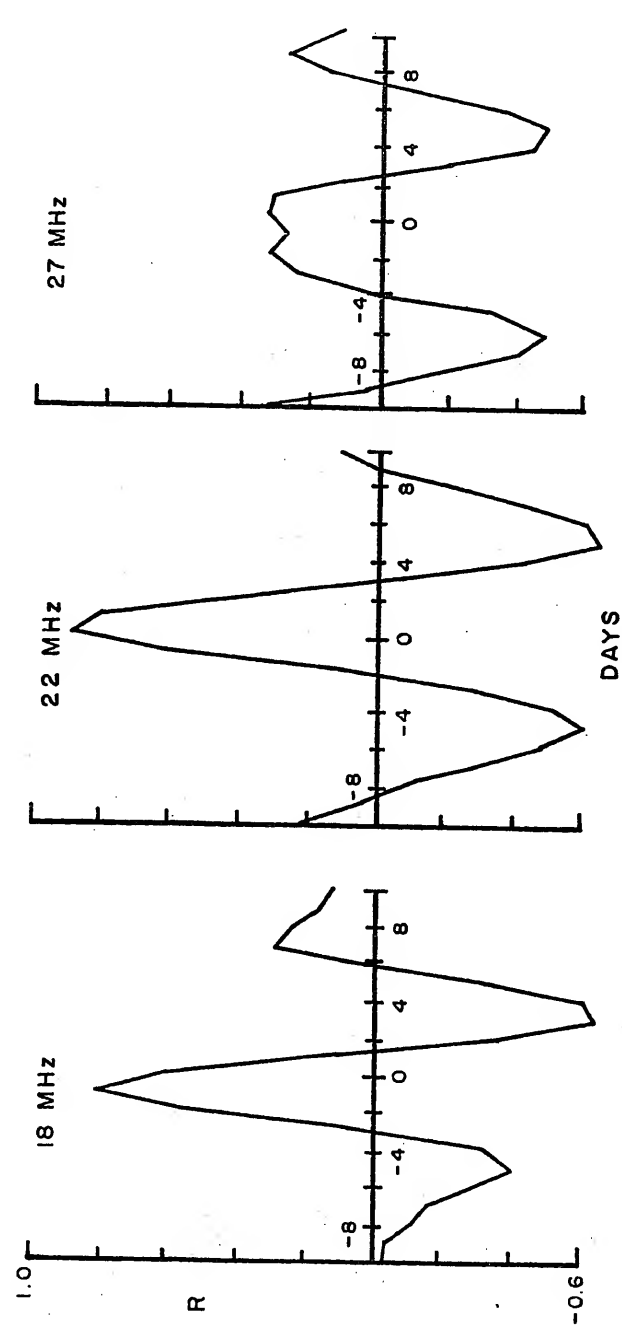

Figure 22. Cross-correlation functions of solar wind flux and Jovian activity, source C, 1967-68.

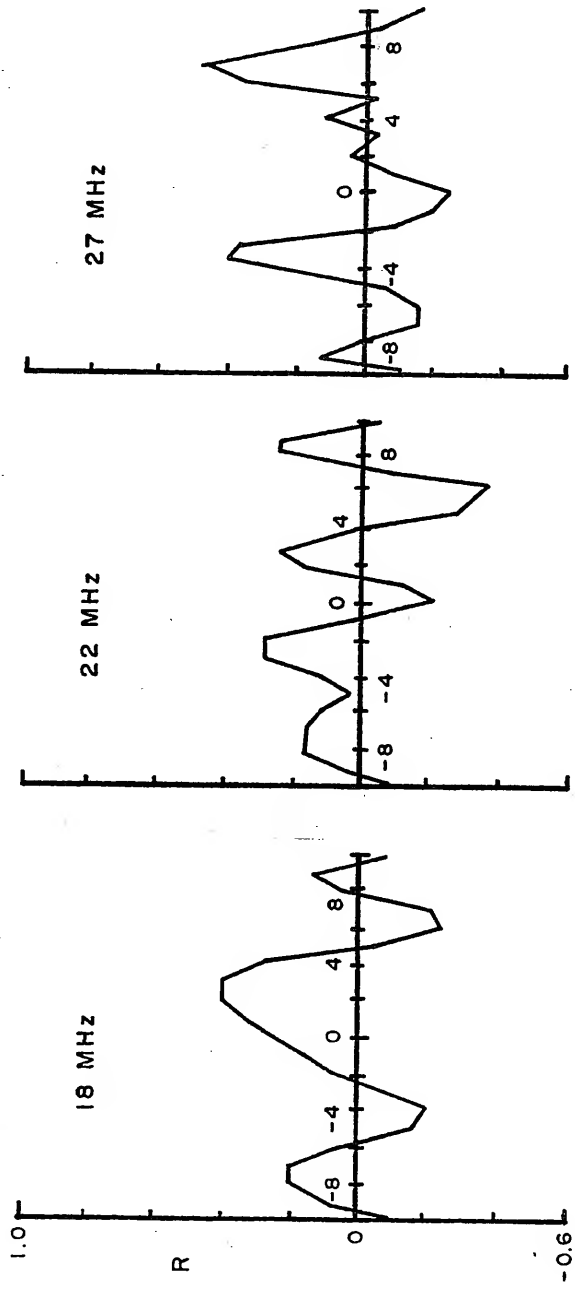

Figure 23. Cross-correlation functions of solar wind flux and Jovian activity, source A, 1974.

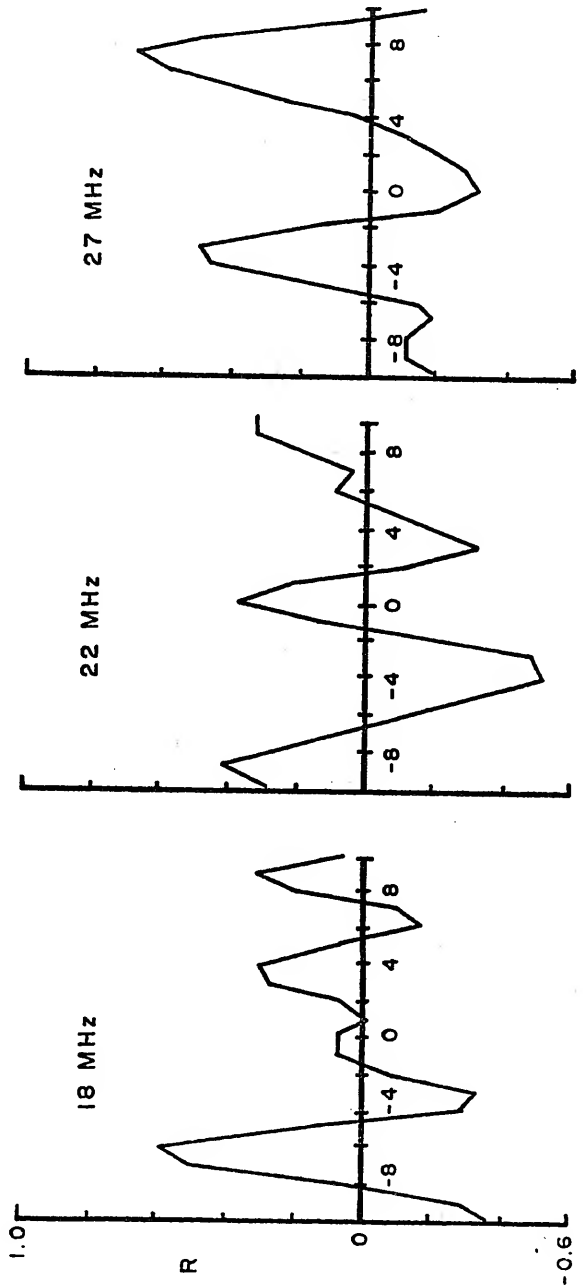

Figure 24. Cross-correlation functions of solar wind flux and Jovian activity, source B, 1974.

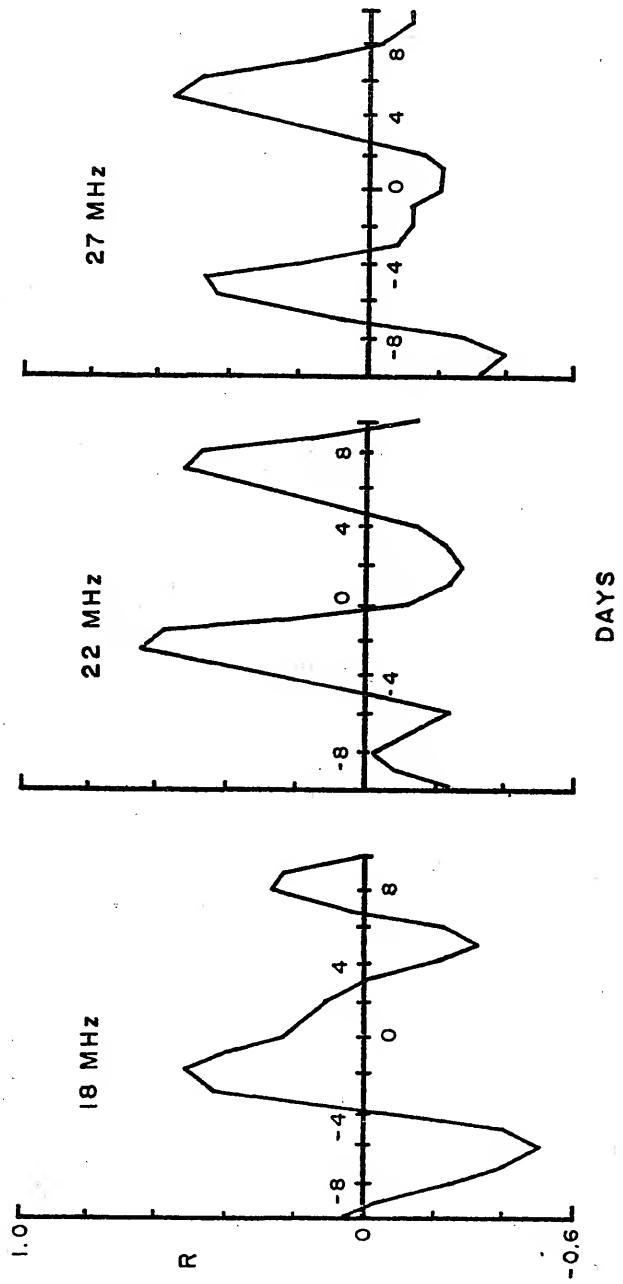

Figure 25. Cross-correlation functions of solar wind flux and Jovian activity, source C, 1974.

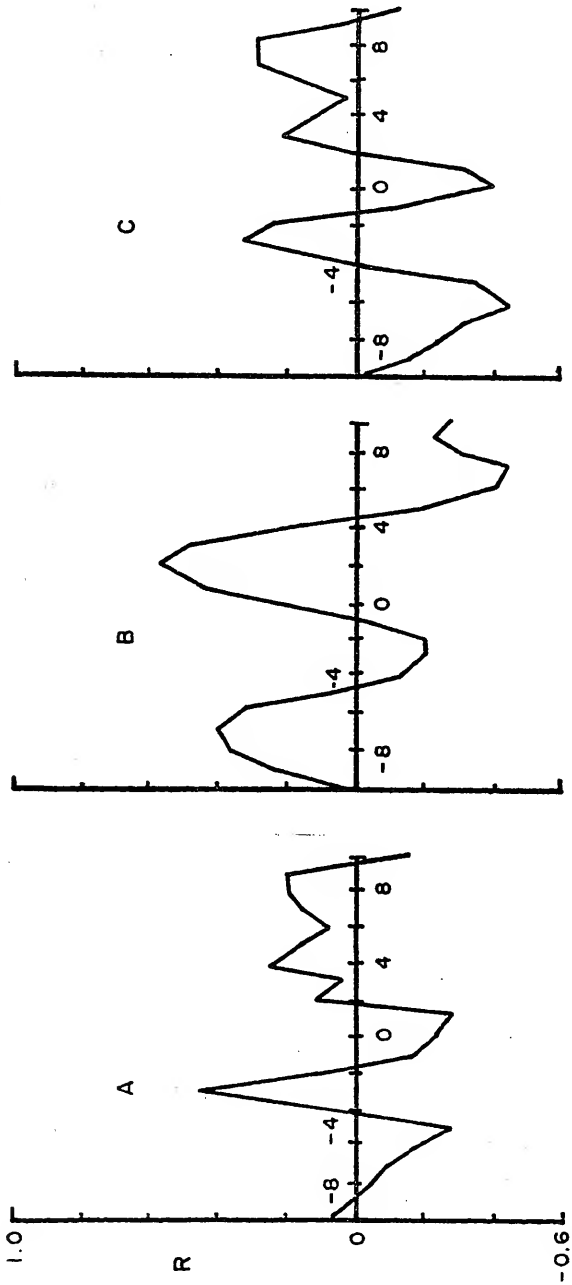

Figure 26. Cross-correlation functions of Jovian activity and solar wind flux at 26.3 MHz, 1974.

Table 7

Correlation Extrema Near Encounter

Frequency (MHz)	Source A	Source B	Source C
1967-68 Apparition			
18	-	-0.57* @ 0d	0.79 @ -1d
22	0.56 @ -1d	-	0.87 @ 0d
27	0.47 @ -1d	-	0.32 @ 0d
1974 Apparition			
18	-	-0.32* @ -3.5d	0.54 @ -2d
22	-	-0.51 @ -3.5d	0.65 @ -2.7d
26	0.42 @ -3d	-	0.32 @ -2.7d
27	0.40 @ 3.5d	-0.48* @ -3.5d	-

*Dominated by a single event.

by about one day and the half-amplitude point on the leading edge of the wave precedes the crest by still another day.

Neither of the two models took this fact into account, though it was expected that the problem would be more evident in the simple-field model due to the very thin wave fronts which it develops. By contrast, the field-free model permits some diffusion in the 3.8 - 5.4 AU region. The result is that the wave front is more diffuse and the leading edge of the front is predominantly composed of the unimpeded high speed groups which reach Jupiter before their trapped counterparts in the simple-field model. Consequently, one would expect to see the real density wave interact with Jupiter before the day predicted by either model. Moreover, one would expect to see the simple-field model predict later arrivals than the field-free model. Qualitatively this seems to be the case with the results in Table 7.

Another factor which may account for the early arrival of the wave is the acceleration of the solar wind with radial distance predicted by many quiet wind models. This acceleration was not observed by Mariner 2, nor was it seen by Pioneers X and XI. However, this writer questions whether simple time averages which are blind to the density variations is properly descriptive of the mass transport process.

Finally, it has been suggested that the triggering agent may not be the density wave itself but the shock fronts produced by the supermagnetosonic collision between the two streams. This front would propagate forward in the moving

wind stream at the fast-mode velocity and thus arrive at Jupiter ahead of the density wave itself. For example, a shock which left the wave at 1 AU in a wind having an average bulk speed of 470 km/s would reach Jupiter about 2 days before the wave.

The ultimate question as to whether or not the correlations represent a physical reality is reserved to the final chapter. There are other items of evidence yet to be presented.

CHAPTER 5

SPECTRAL ANALYSIS

Previous Investigations

In general, most spectral analysis studies of the Jovian decametric emission have been directed toward one of two goals: the measurement of the Jovian rotation period or the measurement of frequencies associated with the Io effect. The first of these studies was conducted by Shain (1956) who plotted the probability of emission versus the CML. While this study in a sense was not really a frequency analysis, it did indeed reveal the presence of the periodic source structure. Similar studies have been done since and improved the precision of this result. Using essentially the same technique Bigg (1964) plotted the probability of emission versus ISC to discover the Io effect. Using a rather different method Duncan (1965) presented strong evidence confirming Bigg's discovery. Duncan's procedure involved choosing a period and performing a superposed epoch analysis of all available data. He then defined the function

$$Z = \left[M \sum_{1}^{M} \left(\frac{N_i}{N} \right)^2 \right] - 1$$

where M is the number of channels used in the analysis, N is the total number of total events in the study and N_i is the number of events per channel. Closer inspection will show that this equation is nothing more than the equation for the variance, σ^2, of the distribution of events per channel, normalized so that the average event per channel is equal to one. In other words, his function Z is the square of the RMS value of the waves that would be seen in the Chree analysis. Except for the square root, this is exactly the same procedure used in Chapter 3 to measure the growth of density waves in the various solar wind models. Having calculated Z, Duncan would then add a small increment to the period used in the first Chree analysis and do a second Chree analysis and calculate Z again. By many iterations of this procedure he was able to obtain a function of the "waviness" versus period. As the period of Chree analysis approached the period of some component in the data, Z would climb until it reached a peak when the period was equal to the period in the data. Thus, his function Z(t) represented a power spectrum analysis. Duncan has used this method in subsequent papers (1966, 1967, and 1971) to study both the Io effect and the System III rotation period.

The method has one serious drawback, however. It provides no means of distinguishing between the fundamental, harmonics or sub-harmonics. If, for instance, the period at the moment was identically equal to the fundamental of a period in the data there would be one full cycle of that wave in the

Chree analysis plot. If, on the other hand, the period were equal to twice that of the one in the data, there would be two full cycles of that wave in the plot. The calculation of Z, however, would give the same value in both cases.

Bigg (1969) has used Duncan's method to "discover" two previously undetected Jovian satellites. Douglas and Bozyan (1970) have shown that both of these periods were actually due to beats between harmonics of the terrestrial, Jovian, and Ioian periods, not to "new satellites."

Kaiser and Alexander (1972 and 1973) used a somewhat different technique to perform their spectral analysis. In an effort to overcome the difficulties imposed by the unequally spaced observations they employed a two step process. They would first pick a period and then do a crude first order least squares fit of a Fourier series to their data. The coefficients of the series provided a rough estimate of the power in the time series at that period. They would adjust the period to maximize the power in its vicinity and then do a much higher order fit on the series and examine its spectrum. By repeating this procedure and varying the period under consideration they were able to develop a plot of power versus period. In their 1973 paper, one of the subjects they addressed was the question of a period in the Jovian data that might indicate solar control. Using 17 years of data they examined the spectrum in the region near 25.5 days for evidence of a peak. Their result was negative and they concluded, that, therefore, there was no evidence of solar control.

Their conclusions, however, are not supported for two reasons. First, as already discussed, the principal period of a solar influence would be expected to be no longer than about 13 days, not 25. Secondly any such effect would have been washed out in their study because they employed 17 years of data, whereas the solar sector structure is stable for periods on the order of several months, but no more.

Analysis

Autocorrelations and Fourier Transforms

It has been long known that a time series is related to its frequency power spectrum by a Fourier transform process. There are two general approaches which may be employed owing to an interesting property of the relationship. If S(t) is a time series, F(S) is its Fourier transform, F*(S) is the transform's complex conjugate, C(S) is the autocorrelation function of the time series and P(f) is its power spectrum, then

$$P(f) = \alpha F^*(S)F(S)$$

and

$$P(f) = \beta F[C(S)]$$

where α and β are constants. This is to say that one may obtain the power spectrum of a time series by either obtaining the square of the modulus of the Fourier transform of the series or by obtaining the Fourier transform of the autocorrelation function of the time series. (The reader is referred to Blackman and Tukey (1958) and Bracewell (1965) for a detailed discussion of these properties.) The procedures are entirely equivalent and the

"transform squared" technique is often the choice of workers today. However, for reasons that will become apparent the "transformed-autocorrelation" procedure is used in this study.

The application of both the transform and the autocorrelation has limitations when dealing with real data. Since any shift other than zero necessarily neglects points at opposite ends of the time series and its image, the maximum shift is limited by the finite length of the time series. The longest period one might study with the autocorrelation function is on the order of the maximum shift employed. Ideally, this maximum shift should be small compared to the length of the series. Shifts greater than 20% must be regarded carefully. If one wishes to look for longer periods, the best method is direct examination of the series.

The Fourier transform suffers from similar problems. It is affected by the finite length of the data because the transform theoretically has integration limits at positive and negative infinity. Practically speaking the transform thinks it is operating on a product of two functions when it deals with finite data length. These two functions are an infinitely long data function and a "window" function which has a value of 1 only where the actual data exist and a value of 0 everywhere else (this particular window is often referred to as a "boxcar" function).

The effect of the window function is that the resulting spectrum is the convolution of the data spectrum and the window spectrum. The simplest window one might choose is the

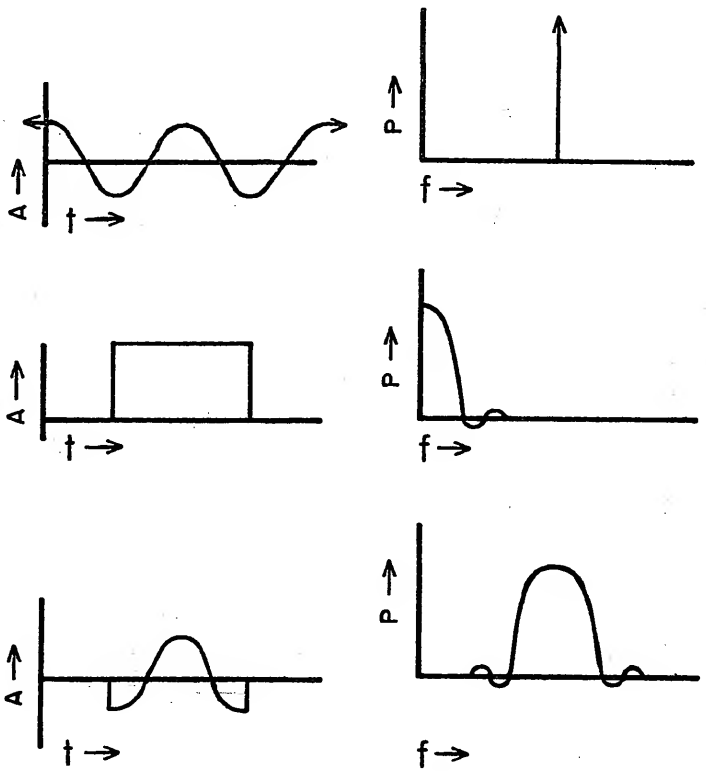

Figure 27. Time series and spectrograms showing the effect of finite boxcar window. The uppermost plots represent an infinitely long cosine wave time series and its spectrum. The center plots are of a boxcar time series and its spectrum. The lowest plots are those of the combination of the cosine and boxcar time series and the resultant spectrum.

boxcar function mentioned above. The transform of this function is of the form

$$F = \alpha \frac{\sin X}{X} .$$

Consequently, if the data spectrum consisted of infinitesimally thin (monochromatic) lines, the effect of the window is to widen the spectral line by making each line have the sinX/X shape shown in Figure 27.

The most striking feature of Figure 27 is that in addition to widening the line it also has some negative fringes! Both of these problems can be controlled somewhat by choosing a more subtle window. When the transformed autocorrelation approach is used, one can attack the window problem either in the time domain by weighting the original time series by something other than the boxcar function, or in the intermediate (1/time) domain of the autocorrelation function, or in the frequency domain after the Fourier transform. By any route, one is effectively introducing a smoothing procedure which acts on the finally derived spectrum.

There are a number of window functions in common use. Perhaps the two most frequently used functions are the Hanning and Hamming functions. The forms of these functions vary according to which step in the time series-spectrum process they are introduced. If they are introduced as the last step (after taking a boxcar windowed transform) the two procedures merely provide a 3-point weighted smoothing of the spectral function. This smoothing corresponds to

$$P_i' = 0.25\ P_{i-1} + 0.50\ P_i + 0.25\ P_{i+1} \qquad \text{Hanning}$$

$$P_i' = 0.23\ P_{i-1} + 0.54\ P_i + 0.23\ P_{i+1} \qquad \text{Hamming}$$

where P_i is the i^{th} value of the boxcar windowed power spectrum. Figure 28 compares the spectra of several windows.

The Hanning procedure is used extensively in the present study. One of the salient features of Figure 28 is that with a Hanning window, the half-power width of the windowed transform is two channels. Thus, the value of each point in the power spectrum is coupled somewhat to each adjacent channel as the equation above indicates and thus there are (N-1)/2 independent points in the analysis. One might also say that there are N Hanning dependent points.

The data impose a second restriction on the transform in that they are not continuous but consist of discrete samples. Clearly then, if the samples are evenly spaced, the data contain a strong periodic component--the sampling frequency. This component is just an artifact of the data collection regime and should not be allowed to show up in the spectral analysis. The standard approach to this problem is to limit the highest frequency analyzed to one-half the sampling frequency.

Another interesting feature of the analysis is the effect the process has on the precision of the results. The autocorrelation function in this study has values for each one-day shift. That is to say, the function consists of evenly spaced values at one day intervals in the time domain.

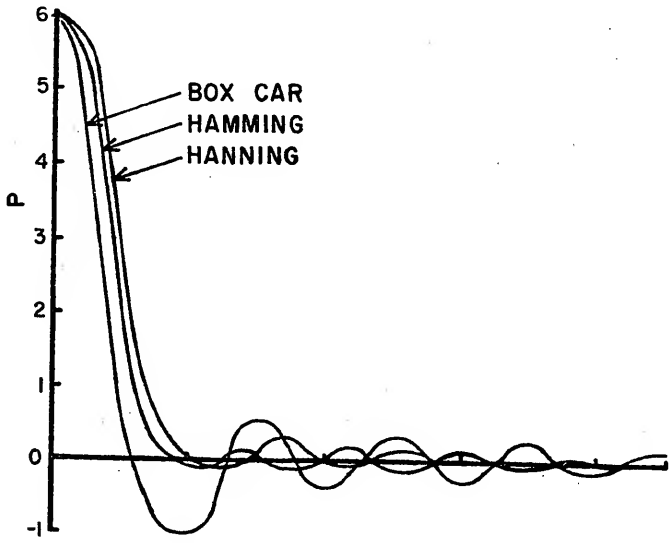

Figure 28. A comparison of the line width and fringes with boxcar, Hanning and Hamming windows. The Hamming window produces a narrower main lobe peak than the Hanning window but its sidelobes, though initially weaker, damp out much slower than the Hanning sidelobes.

The application of the Fourier transform yields evenly spaced values in the frequency domain. As a result, the "period bandwidth" associated with the final spectrum is directly proportional to the period.

This effect is not unreasonable considering that the nature of the transform is to take events in the time domain and create the frequency domain image of those events. In the process the evenly spaced points in the time domain map into evenly spaced points in the frequency domain. Thus, the higher the frequency the higher the precision in the measurement of period associated with that frequency. The spacing of the periods in Table 8 on page 110 illustrates the feature.

Basically, the question here is one of recognizing the independence of values. One can compute the value of the power density for any frequency within the limits already discussed, but one should only be interested in points that are marginally coupled to each other, no more and certainly no less. The failure to recognize this requirement led Holmes (1966) into a serious error in his study of Jovian periods. He followed the same basic procedure as that employed in this study--the autocorrelation-transform approach. However, he chose to separate his calculations at equally spaced intervals in time (period). As a result his "spectra" contained strongly coupled or dependent points in the longer period region and omitted a significant number of independent points in the short period region.

In the present study the maximum autocorrelation shift was 54 days. Using the Fourier transform with a Hanning window this will lead to 55 Hanning dependent points in the frequency spectrum. The relationship of the frequencies and periods is shown in Table 8.

Aliases

While it is desirable to avoid problems associated with the sampling frequency this cannot be fully achieved unless--in addition to restricting the analysis to frequencies less than one-half the sampling frequency--the input data have previously been filtered to remove all frequencies above the cutoff frequency in the analysis. Even though such information is outside the range considered in the analysis, the frequency of the beat or heterodyne between high frequency information and some harmonic of the sampling period will fall into the analysis range. These false features in the spectrum are known as "aliases."

Unfortunately, the filtering of the Jovian data is impossible. Both the rotation of Jupiter and the revolution of Io occur at frequencies above the 0.5 cycles per day (c/d) analysis cutoff. Consequently, any effort to filter will cause all of the data to be rejected! As a result aliases will occur at a frequency f_a whenever

$$f_a = |kf_s - f| < \frac{1}{2} f_s \qquad k = 1, 2, 3, \ldots$$

where f_s is the sampling frequency and f is the "out-of-range" frequency. In the case of the present study this relation becomes

$$f_a = |k - f| < 0.5 \qquad k = 1, 2, 3, \ldots$$

For example, the System III synodic rotation frequency is 2.417 c/d. Consequently, we may calculate the alias of the fundamental System III frequency

$$f_a = |2 - 2.417| = 0.42 \text{ c/d}$$

which corresponds to a period of

$$p_a = 2.40\text{d}$$

By the same process, the alias of the second harmonic of the System III period is found to be

$$f_z = |5 - 4.834| = 0.166 \text{ c/d}$$

$$p_a = 6.02 \text{ d}$$

The form of the observation function O(t) was discussed in Chapter 2. There it was noted that this function was regarded as the product of three periodic rectangular functions. In the context of this discussion the earth function E(t) represents the sampling function while the Jovian and Ioian functions J(t), I(t), and N(t) represent the input data. Therefore, the frequency spectrum of the products J(t)I(t) and J(t)N(t) will consist of the fundamental and harmonic frequencies of each component in the product plus the sums

Table 8

Spectral Analysis Frequencies and Periods

Frequency Index (1/108 c/d)	Period (d)	Frequency Index (1/108 c/d)	Period (d)
0	∞	28	3.86
1	108.0	29	3.72
2	54.0	30	3.60
3	36.0	31	3.48
4	27.0	32	3.38
5	21.6	33	3.27
6	18.0	34	3.18
7	15.4	35	3.09
8	13.5	36	3.00
9	12.0	37	2.92
10	10.8	38	2.84
11	9.8	39	2.77
12	9.0	40	2.70
13	8.31	41	2.63
14	7.71	42	2.57
15	7.20	43	2.51
16	6.75	44	2.45
17	6.35	45	2.40
18	6.00	46	2.35
19	5.68	47	2.30
20	5.40	48	2.25
21	5.14	49	2.20
22	4.91	50	2.16
23	4.70	51	2.12
24	4.50	52	2.08
25	4.32	53	2.04
26	4.15	54	2.00
27	4.00		

Table 9

Calculated Aliases for J(t)I(t)

Origin	Frequency (c/d)	Period (d)	Frequency Index (1/108 c/d)
J	0.417	2.40	45
2J	0.166	6.02	18
I	0.435	2.30	47
2I	0.129	7.77	14
J-I	0.144	6.94	15-16
J+I	0.016	62.50	2
J-2I	0.285	3.51	30-31
J+2I	0.457	2.19	49
I-2J	0.263	3.80	28
I+2J	0.393	2.55	42

and differences of those frequencies. Table 9 shows the expected frequencies of the fundamental, and first harmonic combinations of these products. Note that the component frequencies of both products are the same by the definition of N(t).

The graph in Figure 29 displays the actual spectrum of the observation functions for source B at 18 MHz during 1967-68. It will be noted that peaks at virtually all of the first and second order frequencies in Table 9 are in fact found in the actual functions.

Timing precision. The question of periods naturally requires a statement about the precision of their measurement. In the data reduction process no effort has been made to keep track of the exact time an event occurred. Consequently, the fundamental unit of time in this study is one day. As a practical matter the uncertainty of the time of a storm is ± 6 hours from local midnight. Since data from the entire 200-250 day apparition are used to arrive at the various periods the precision is on the order of

$$\varepsilon = \pm \frac{0.25}{200} = \pm 0.125\%$$

In comparing the System III spectral peaks with theoretical values a disturbing discrepancy arose. The theoretical alias frequencies had been calculated based on an estimate of the average terrestrial and Jovian synodic period during the apparition. In making the estimate the assumption was that the fluctuation of the synodic period

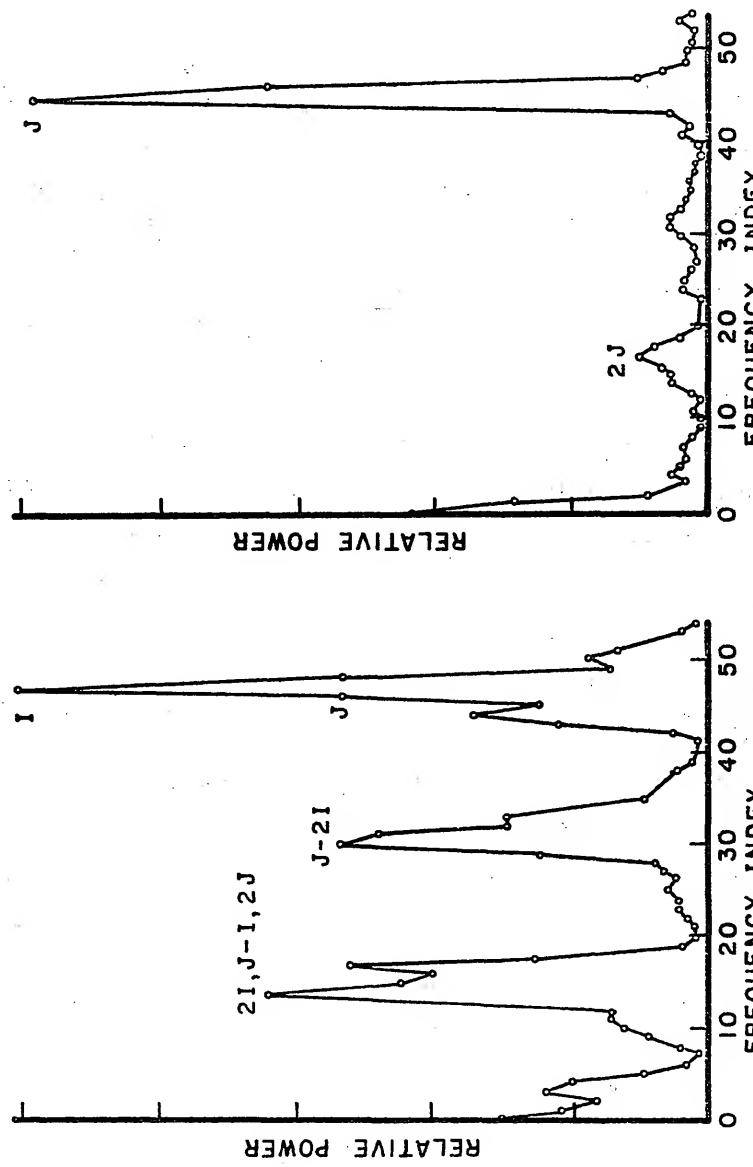

Figure 29. Spectra of Io and non-Io observation functions for Source A, 1967-68.

due to orbital motion was approximately sinusoidal. The average value was taken to be the RMS value over the apparition. These values are

$$p_E = 23^h55^m24^s \pm 1^m48^s$$

$$p_J = 9^h55^m01^s \pm 48^s$$

The problem was that the fundamental alias of the Jovian rotation frequency is predicted by these periods corresponds to a period of 2.45d, but the observed peak was clearly at 2.40d in the spectral analysis. Further the 2.45d figure is significantly out of the precision tolerance.

It was recognized that if the peak were to be at 2.40d then one of the periods above was wrong. It became apparent that one reason for the discrepancy is the fact that in the effort to avoid daylight, the time of the center of observing sessions is systematically skewed. At the beginning of an apparition observations are made for a short time in the early morning hours. As the apparition progresses the observations and their centroid occur earlier and earlier. The net effect is that the synodic period of the observatory is lengthened with an accumulated difference of about one hour a month. If one assumes that the terrestrial period is wrong the "correct" value can be computed back from the 2.40d period in the data. Doing so yields

$$p_e = 23^h57^m57^s$$

The error due to the "station lag" is 1^m58^s. There was a second error of 19^s due to an incorrect provision for Jupiter's orbital motion which was also discovered, leaving a total correction of 2^m17^s. This added to the originally calculated theoretical value gives

$$p_e = 23^h57^m41^s \pm 1^m48^s$$

This figure is in excellent agreement with the experimental value. As a result, the experimental value is used in all calculations such as those showing the expected alias frequencies in Table 9.

Amplitude confidence. The establishment of confidence intervals for the amplitude of spectral density measurements is a difficult task. If the data are that of a random Gaussian distribution, the sampling distribution is approximately a χ^2_n distribution of order

$$n = 2N/M$$

where N is the number of points in the sample and M is the maximum shift or lag in the autocorrelation (Blackman and Tukey, 1958). Current statistical theory has not yet resolved the problem of the time series which contains significant non-random components. This

problem is exacerbated by the relative shortness of the time series (200-250) points.

If the time series did have a random Gaussian distribution, the confidence interval about the average power density $\bar{P}$ is given by

$$\frac{n\bar{P}}{\chi^2_{n,\alpha/2}} \leq P \leq \frac{n\bar{P}}{\chi^2_{n,1-\alpha/2}} .$$

Since the number of degrees of freedom n depends directly on the number of points in the series, the width of the interval is strongly dependent on that factor. For example, the 95% confidence interval for 216 points and a 54-day maximum shift is given by

$$n = 2 \times \frac{216}{54} = 8$$

$$0.46\ \bar{P} \leq P \leq 3.67\ \bar{P} \qquad 95\%\ \text{confidence}.$$

Thus with 216 points, the interval is very wide, spanning a range of 8:1. On the other hand, if the sample contained 2160 points

$$n = 2 \times \frac{2160}{54} = 80$$

$$0.75\ \bar{P} \leq P \leq 1.40\ \bar{P}$$

which results in a range of 2:1.

In extreme cases with non-random functions, such as those whose spectra are shown in Figure 29, common sense dictates that the line features reflect the non-random component. Thus one can recognize the "floor" between peaks

as representing the random component. When this occurs, one can apply the confidence interval relationship to the floor values only. However, it is not obvious where to apply this relationship when confronted with a spectrum like that in Figure 30 or Figure 32. This is indeed unfortunate because such situations are precisely those for which the intervals are most necessary.

An extremely conservative approach would be to apply the confidence interval relationship using the overall average--including possible non-random peaks. This procedure will always overestimate the width of the interval with non-random data.

A more liberal approach would be to define local minima as representing floor points. Thus one would consider the average of the random component to be the average of the minima.

The Galileo Club

At first sight, one of the problems that spectral analysis might hope to address is that of the existence of additional satellite exciters. Unfortunately, this will prove a difficult task. Almathea and the Galilean satellites are the only ones which are within the Jovian magnetosphere more or less continuously. It seems reasonable, therefore, to restrict attention to this group. Almathea is the innermost moon and is quite small (250 km in diameter). The four Galilean satellites, Io, Europa, Ganymede and Callisto are

all quite a bit larger, ranging from 3000 to 5000 km in diameter.

The Galilean satellites form a harmonically locked orbital system. Apparently after eons of perturbations they have assumed orbital periods which are related by rational numbers. Table 10 demonstrates this relationship.

Table 10

Orbital Periods of the Galilean Satellites

Satellite	Period (h)	Ratio with Preceding Period
Io	42.47	-
Europa	85.23	2:1
Ganymede	171.71	2:1
Callisto	400.53	7:3

As might be expected, this situation causes a number of redundancies in the various periods in the power spectrum. Fortunately, the frequencies of all but Io and Almathea are lower than the 0.5 c/d cutoff frequency so aliases will be less of a problem. Experience has shown the third order alias effects are negligibly small and thus they will be ignored. Table 11 shows the expected frequencies for the various satellites. In scanning the table the redundancies become apparent. Io, Europa, and Ganymede all have predicted periods in the range of frequency index 14 to 16, while

Europa and Ganymede have components in the 30 to 32 range.

The plots in Figures 30, 31, and 32 depict the frequency spectra of the daily activity index $A_s(t)$ as defined in Chapter 2 for 1967-68. In principle, this function is free of the observation spectra previously displayed in Figure 29. In these plots the Io effect has deliberately not been removed in order to demonstrate the effect of a periodic exciter on the data. Source B has long been recognized as the prototype for Io related activity. These plots show clearly that this is the case. The Io features in the vicinity of indices 14-16, 30-31 and 47 are the dominant features in the source B spectrum. All but the strong peak at index 17 can be attributed to the Ioian, Jovian, and joint interactions outlined in Table 9. The same pattern is also evident in the source A plot, though the unexplained index feature is absent. Most of these periods are absent in the source C plot. The strongest peak in the C spectrum corresponds to the principal System III alias at 2.40 days. This period has supposedly been removed from the data by the compensation procedure which defines $A_S(t)$. This point will be addressed shortly.

A Matter of Priorities

Tables 9 and 11 illustrate that the number of true and alias frequencies which might show up in the occurrence spectrum is large. Nevertheless, it is clear that there is a descending order of importance as the various interactions become more complex. In this regard it is worthwhile to

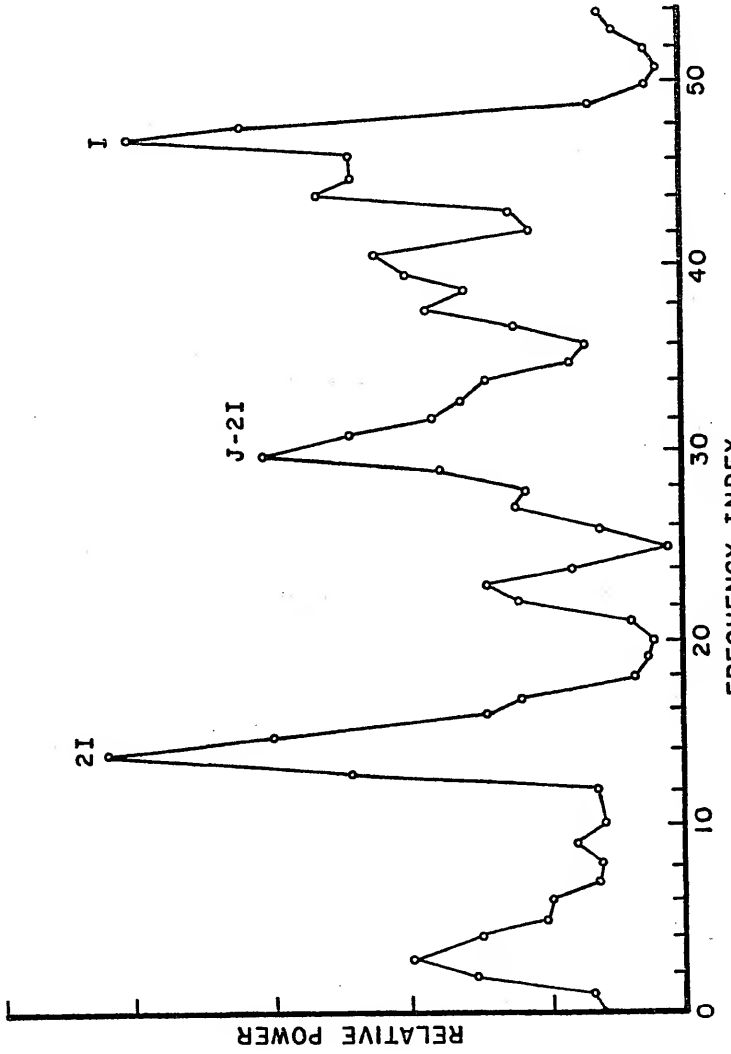

Figure 30. Activity spectrum of source A, 1967-68, Io included.

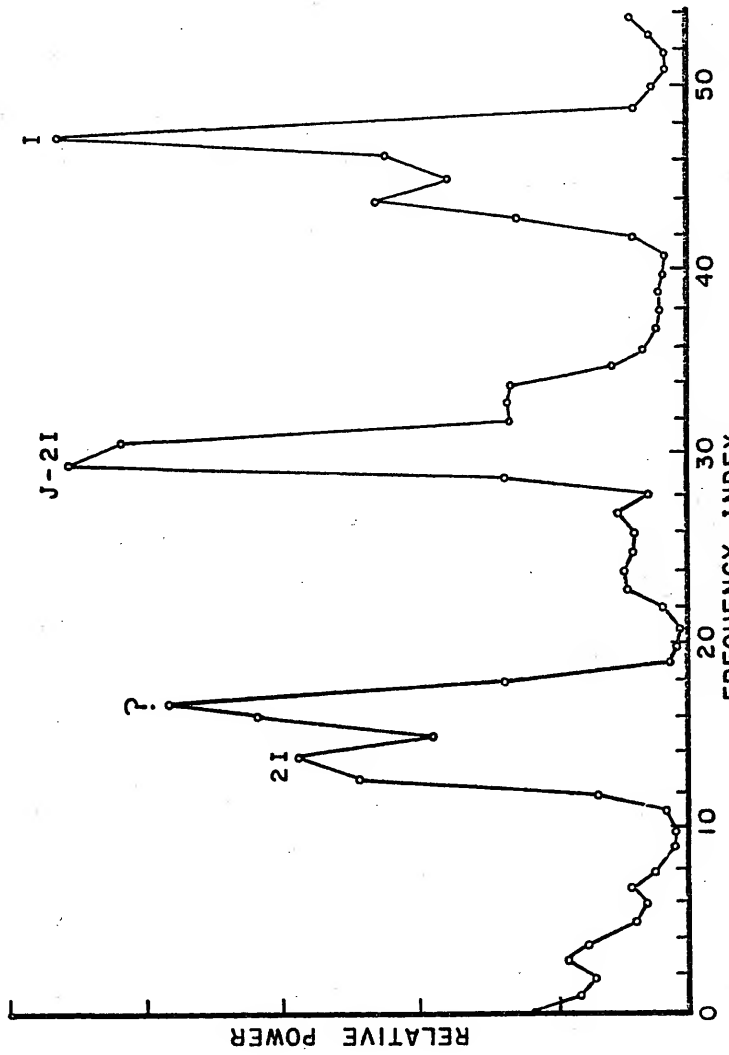

Figure 31. Activity spectrum of source B, 1967-68, Io included.

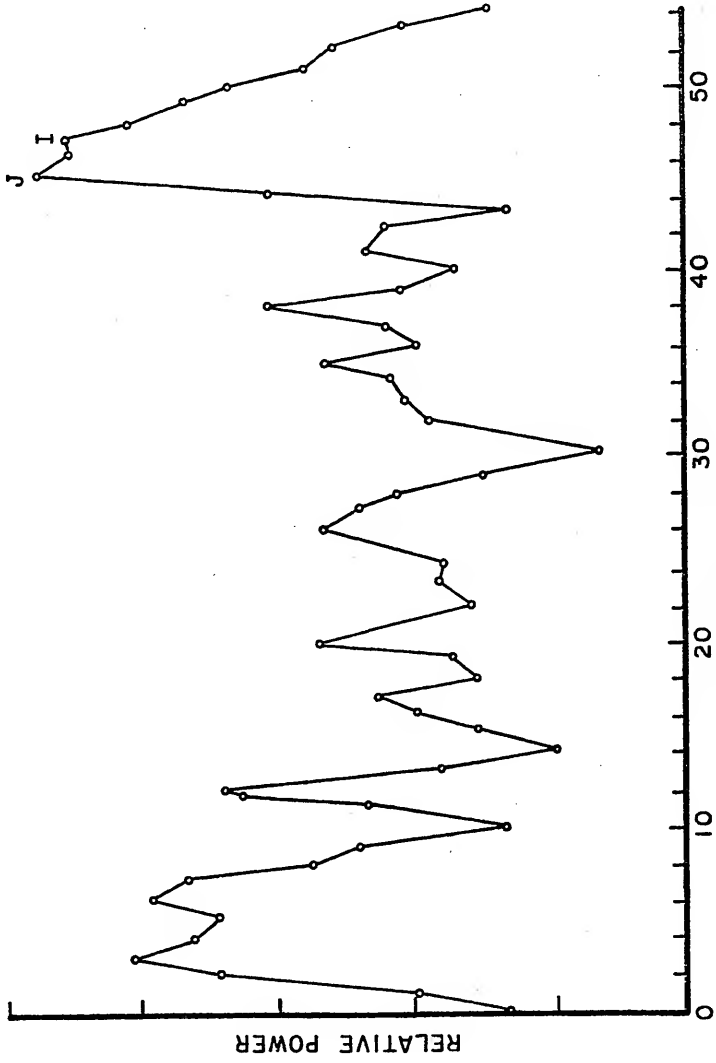

Figure 32. Activity spectrum of source C, 1967-68, Io included.

Table 11

Sidereal Frequencies of the Five Innermost Satellites

Satellite	Origin	Frequency (c/d)	Period (d)	Frequency Index (1/108 c/d)
Almathea	A	0.020	50.92	3
	2A	0.040	25.00	4
	A-J	0.082	12.19	9
	A+J	0.090	11.09	9
Io	I	0.435	2.30	47
	2I	0.129	7.77	14
	I-J	0.144	6.94	15-16
	I+J	0.016	62.5	2
Europa	E	0.281	3.57	30-31
	2E	0.438	2.29	47
	E-J	0.139	7.20	15
	E+J	0.299	3.35	32
Ganymede	G	0.140	7.17	15
	2G	0.279	3.58	30
	G-J	0.280	3.57	30
	G+J	0.440	2.27	48
Callisto	C	0.060	16.71	7
	2C	0.120	8.36	13
	C-J	0.360	2.78	39
	C+J	0.480	2.08	52

formally recognize this hierarchy.

All fundamental frequencies will be classified as being of "first order." Frequencies arising due to the cross-product interaction (sum or difference) between two fundamentals, including a self-interaction, are classed as "second order." Those frequencies which occur due to a three-fold fundamental interaction, including self-interactions, will be termed as "third order" effects.

A priori one would expect first order effects to dominate the spectra of a source. These influences are precisely what the compensation procedure leading to $A_S(t)$ was intended to remove, at least for Jupiter and Io. If this goal has been achieved then the remaining periods would be of second, third and higher orders, or they would be first order effects of influences not yet considered.

To this point in the discussion third order effects have been neglected as insignificant. However, if the first order effects can be removed, then the higher order influences obviously descend one order and thus become more important. In the examination of the spectra which follows the hierarchy of interactions will be used to overcome the problems associated with such things as redundant frequencies due to the harmonically locked Galileo Club. This will be done by the invocation of three "golden" rules.

1. The fundamental frequencies and their harmonics of all orders for E(t), I(t), and N(t) will not be seen, nor will their aliases, due to the $A_S(t)$ procedure.

2. A cross-product (joint interaction) frequency or its alias will only be seen if at least one of its constituents has not been removed by the $A_S(t)$ procedure.

3. A higher order frequency or its alias will not be seen if lower order frequencies or their aliases composed of the same constituents or their subharmonics are not seen.

Figures 33 through 39 show the occurrence spectrograms of the non-Io component of each of the sources at 18, 22, and 27 MHz for 1967-68 and 18, 22, 26.3, and 27 MHz for 1974. The small amount of data available in some of these source-frequency combinations has rendered their particular plots useless, specifically, all of the source B plots and the 1967 source A at 27 MHz plot. The average source observation time represented on these plots was about 1400 zones over the apparition and yet, due to the small activity probability, fewer than 25 zones were observed storming. Thus, activity was limited to only a few events. The effect of this condition is visible in most of these plots.

The 26 MHz plots are also viewed with suspicion. While the activity probability was much higher, the large array was operational for only about 620 zones of observations--less than half the time logged by the low sensitivity systems; thus there are many gaps in the time series where there are no data. Consequently, the bulk of attention will be directed to the source A and source C low sensitivity systems.

The spectrograms have been plotted against an arbitrary power scale of from 0 to 5 units. If one adopts the view that the minima in the function represent the floor or background

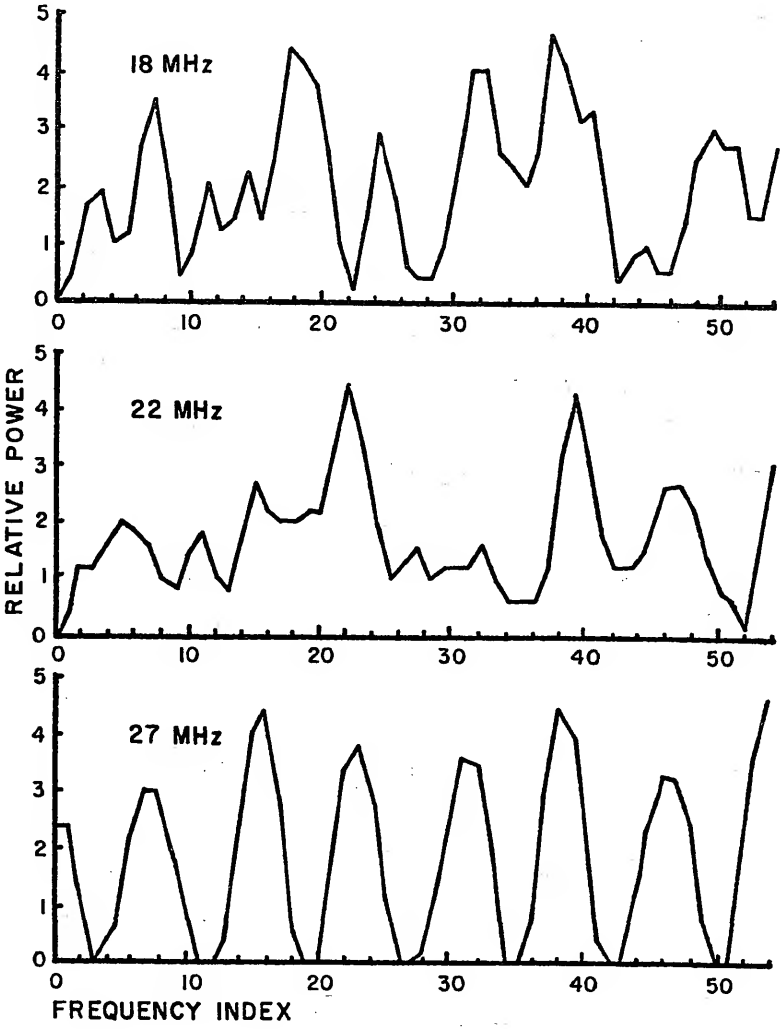

Figure 33. Source A, 1967-68 activity spectra. The 27 MHz spectrum is data limited. Its apparent periodic nature is an artifact produced by the autocorrelation of two events.

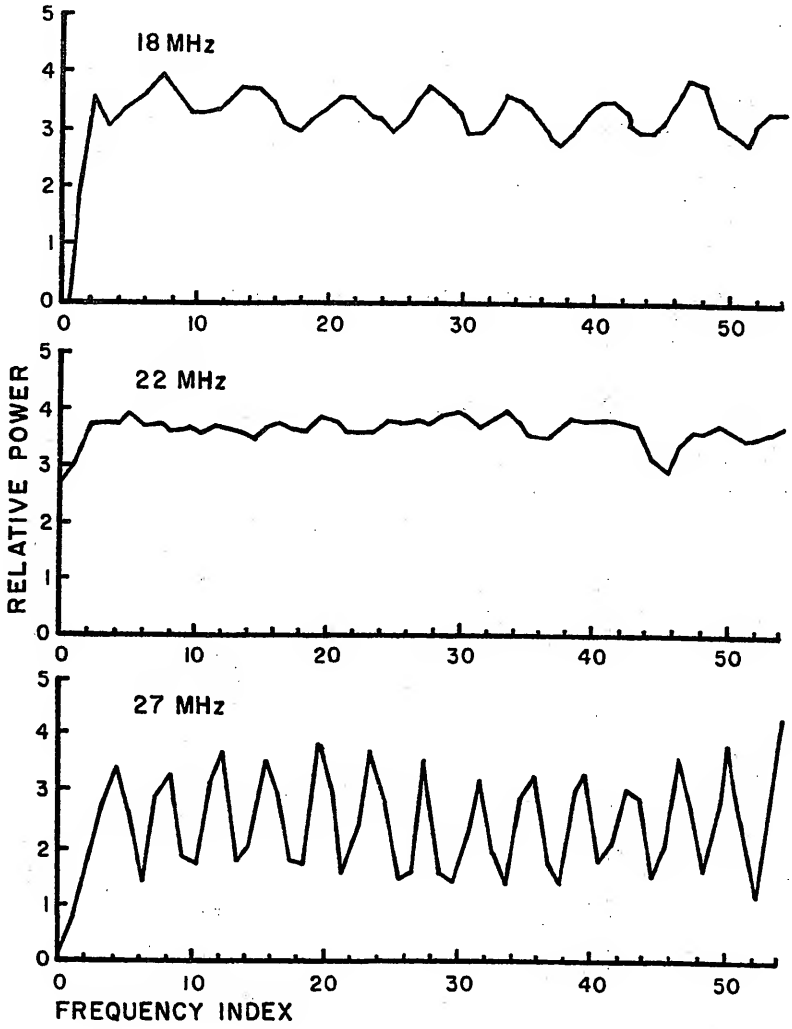

Figure 34. Source B, 1967-68 activity spectra. All frequencies are data limited.

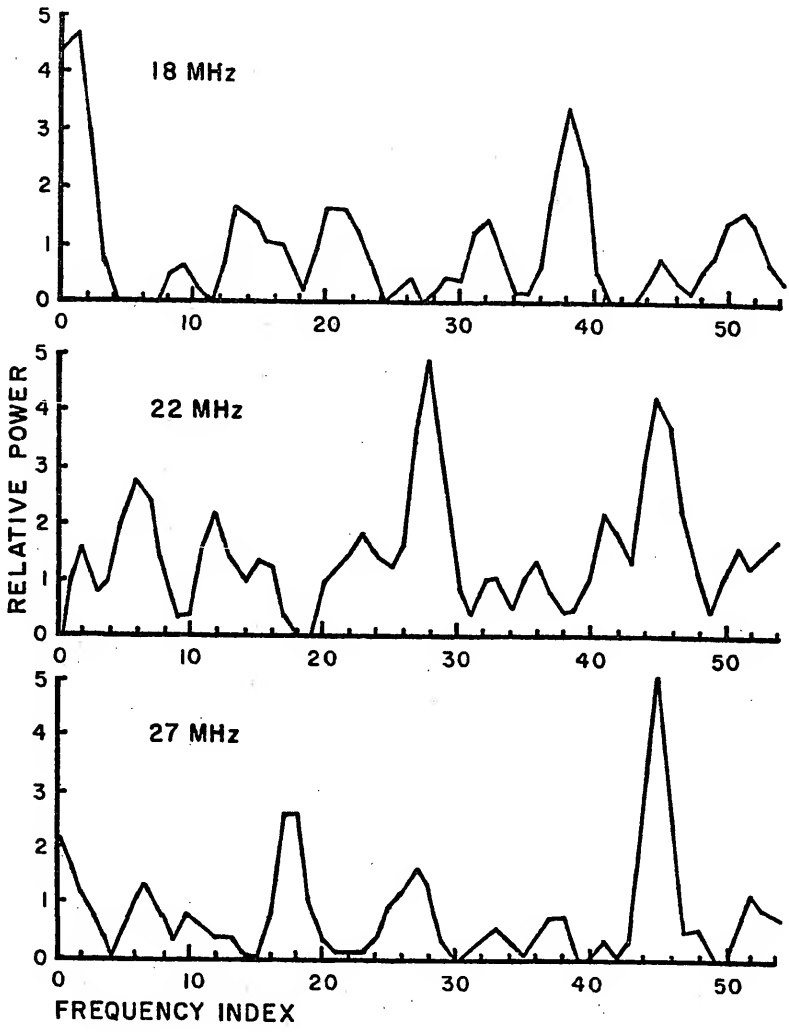

Figure 35. Source C, 1967-68 activity spectra. The 22 and 27 MHz plots are contaminated by System III; see text.

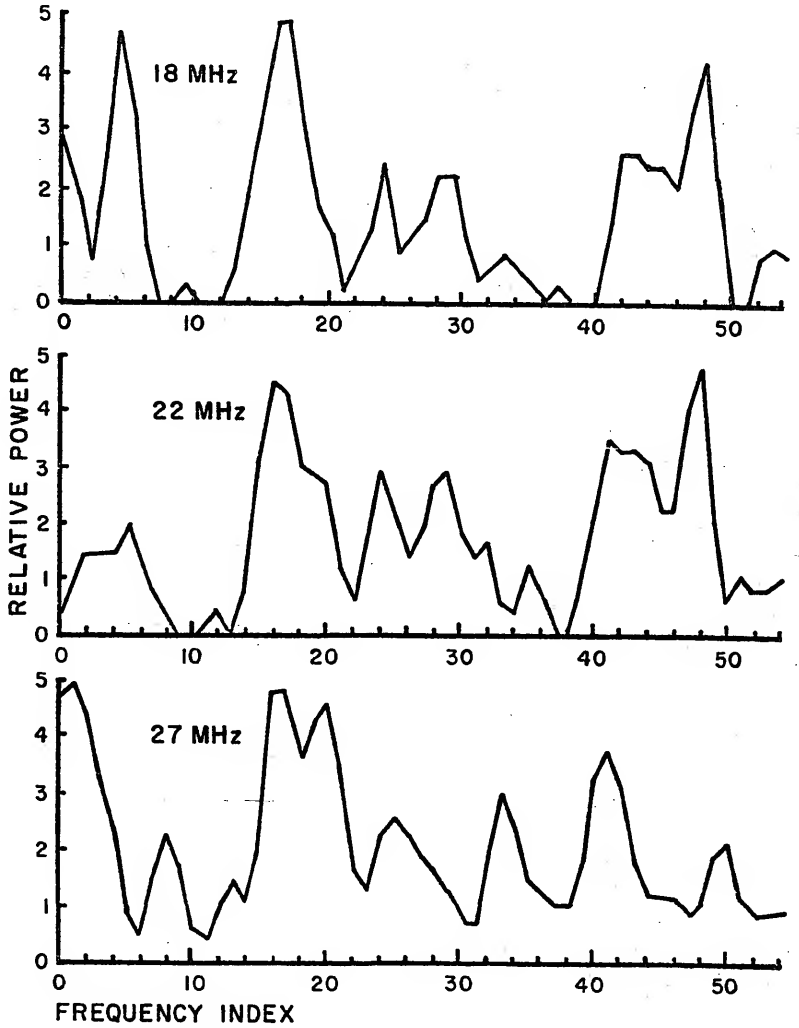

Figure 36. Source A, 1974 activity spectra.

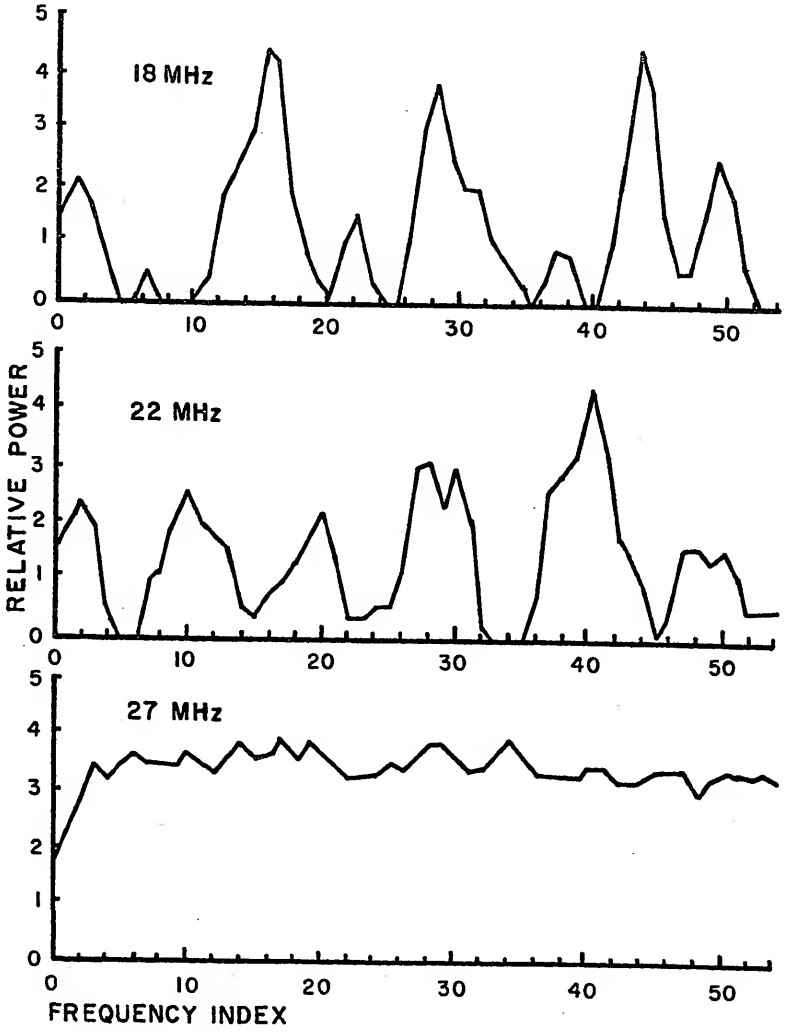

Figure 37. Source B, 1974 activity spectra. All frequencies are data limited.

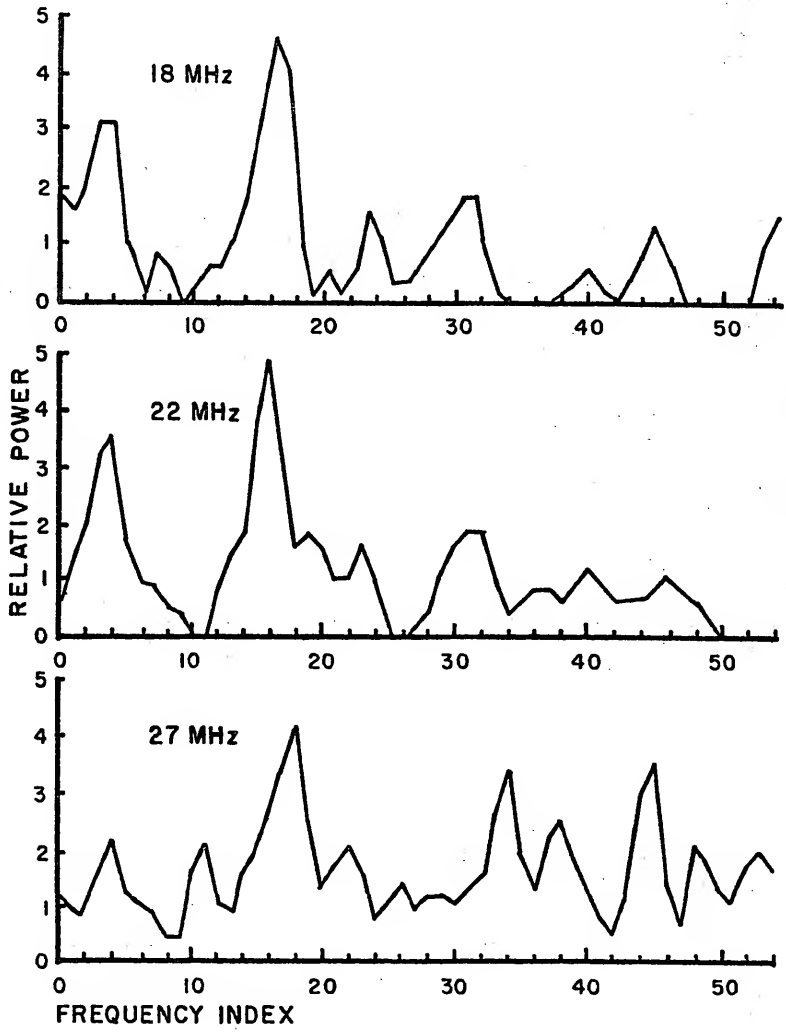

Figure 38. Source C, 1974 activity spectra. The 27 MHz spectrum is contaminated by System III.

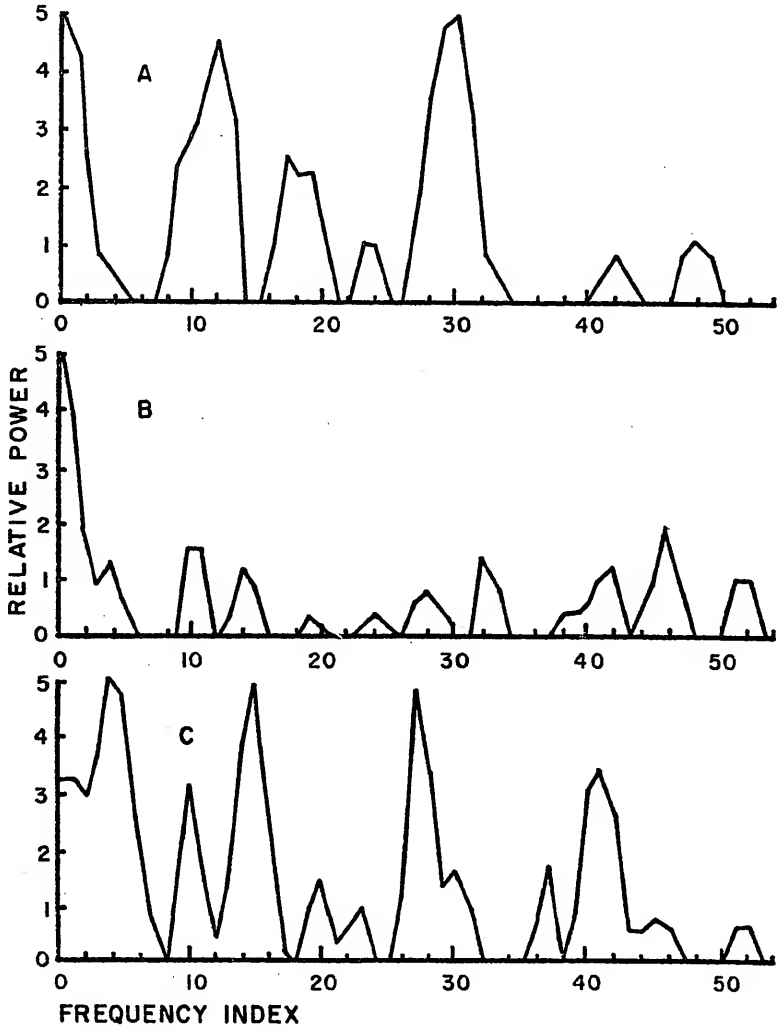

Figure 39. 26.3 MHz activity spectra 1974. All sources are data limited.

of random noise, then the background level is 1 or less in the source A and source C plots. Thus, the 90% confidence interval is

$$0.52 \leq P \leq 2.93.$$

Contamination

It turns out that the first golden rule can be violated by at least one odd circumstance. Examination of the source C spectrograms reveals statistically significant maxima at index 45 (2.4 days) in 1967-68 at 22 and 27 MHz and in 1974 at 27 MHz. Low level vestiges of this feature are found in all the remaining source C plots.

Inasmuch as index 45 is the alias of the System III rotation fundamental frequency, its discovery in the spectrogram caused considerable concern over the validity of the removal of Jovian and Ioian periods by the $A_S(t)$ procedure. The success of the procedure with source A allayed the fear but did not explain the presence of the spectral line.

Examination of the input data to the autocorrelation-spectrum routine ("Jupcor III", see Appendix) revealed the cause of the problem. Despite the fact that the non-Io component of source C has a relatively small emission probability in terms of the percentage of observed time spent storming, it storms quite frequently. For the source frequency combinations showing the intense line, about 6 days out of 10 produced a storm, perhaps better a "spurt", since

each was only one zone long! As a result, the time series consisted largely of $1/O_s(t)$ which naturally has the same period as $O_s(t)$.

The explanation for the state of the data is uncertain. The phenomenon occurs only in source C and it becomes more prominent with increasing frequency. It occurred in both 1967-68 and 1974. It is tempting to conclude that the source is active frequently but only the peak of a storm is powerful enough to be detected by low sensitivity (yagi) antenna systems. If this is the case, the storms themselves must, nevertheless, be short because comparing the 1974 26 MHz high sensitivity activity index to the 27 MHz low sensitivity index (Table 3) shows an increase in the activity index by a factor of only 2.76. However, the 26 MHz spectrogram has only the slightest hint of the frequency index 45 spectral line.

In any case the situation is some kind of data limiting problem and must be regarded as an artifact. Thus, caution must be used in the interpretation of any other features in the spectrograms of source C 22 and 27 MHz in 1967-68 and 27 MHz in 1974.

Solar Control

It was recognized early in this work that the auto-correlation and power spectral functions view periods in data from different perspectives. A clear example of this is seen by comparing Figures 40 and 41. In Figure 40 both the auto-correlation and power spectral functions describe a fairly

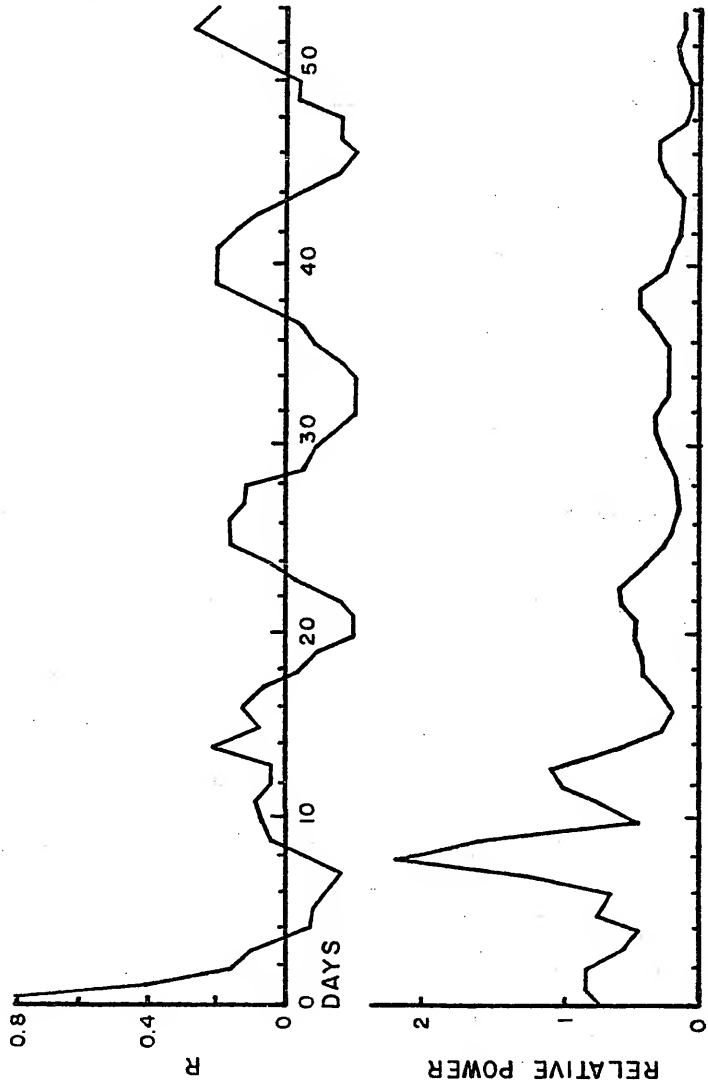

Figure 40. Solar wind autocorrelation and power spectrum 1967-68.

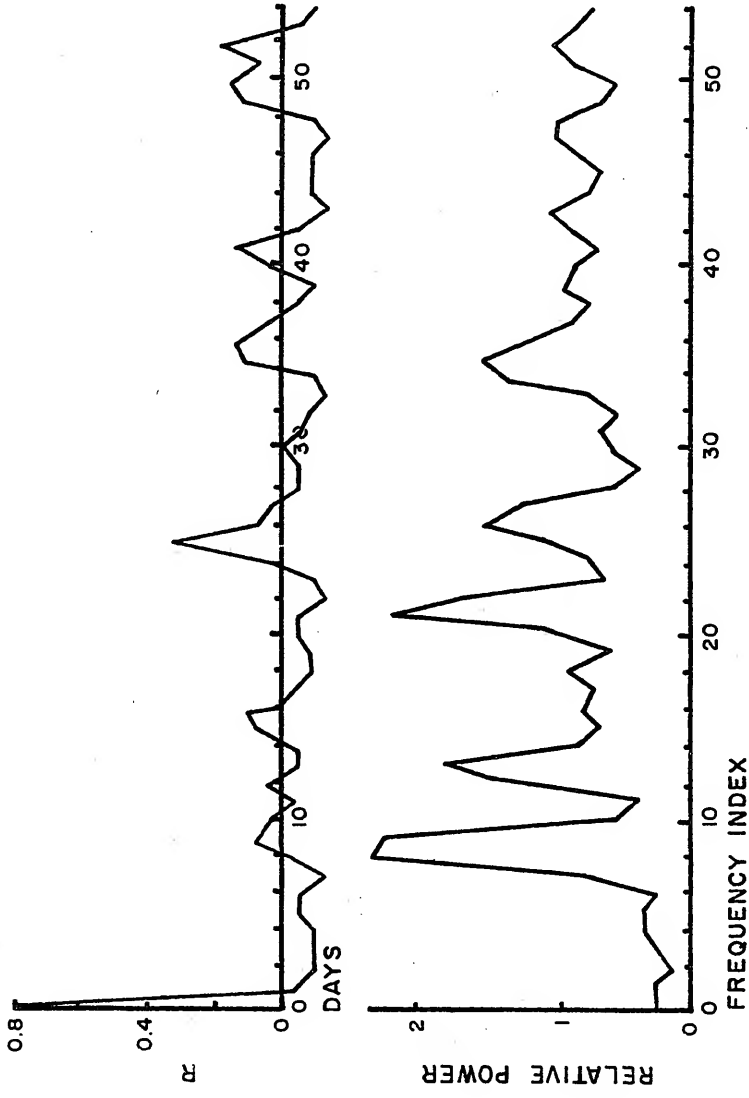

Figure 41. Solar wind autocorrelation and power spectrum, 1974.

monochromatic 13-day period in the solar wind particle flux density as predicted by the field-free model for 1967-68. On the other hand, the autocorrelation function of the 1974 simple-field flux density shown in Figure 41 has its largest peak at 25 days, while the spectral function shows the principal power peak near 13 days.

The difference between the 1974 autocorrelogram and the spectrogram is not a contradiction. The velocities of the two high speed streams in 1974 were noticeably different. Due to this asymmetry (refer back to Figure 8) the best auto-correlation occurred at 25 days even though the principal period was 13 days. Nevertheless, the spectrogram shows very little power at 25 days. The transformed-autocorrelation technique for obtaining power spectra was used in order to have the advantage of both viewpoints.

No assumptions have been made about the nature of the density wave or shock front interaction with the Jovian magnetosphere nor about the workings of the radiation mechanism(s). As a result it is not known whether the asymmetry in initial wind velocities is reflected in the observed Jovian radiation. It is possible, for instance, that some threshold process might "accept" one wave and emit while "rejecting" the other and remaining silent. Alternatively, one wave might bend the beam of radiation away from the earth while the other might direct the beam at the earth. Therefore, the possibility of a 25- or 26-day period in the Jovian emission when the velocity is highly asymmetric should not be ignored.

In the 1967-68 Jupiter spectrograms none of the plots show statistically significant levels at either 13.5 or 27 days (the nearest points to 13 and 26 days), though several show higher than average power at 13 days. The 1974 functions are somewhat different. The cross-correlations in Chapter 4 showed that source A correlated with the wind at 26 and 27 MHz. The spectra for both these source-frequency combinations have high power levels at 13 days though they are not outside the confidence interval. The source C cross-correlations for 1974 had positive peaks on 18, 22, and 26 MHz. In all three cases, the spectrograms show statistically significant maxima at 27 days. Furthermore, at 27 MHz where there was no cross-correlation, the 27-day maximum is present but much weaker.

Satellite Control

Excluding the 3 peaks caused by System III contamination, there are 24 features of statistical significance in the 11 source-frequency combinations which are being examined at this point--sources A and C at 18 and 22 MHz in 1967-68 and 18, 22, and 27 MHz in 1974. In order to visualize these features a histogram, Figure 42, has been constructed showing the distribution of spectral index numbers which exceed 90% confidence for all source A functions, all source C functions, and the sum of the A and C functions. The source A diagram shows two prominent features, one at about indices 17 and 18 and the other at about index 40. The source C histogram shows only the index 17 peak. The composite diagram shows three

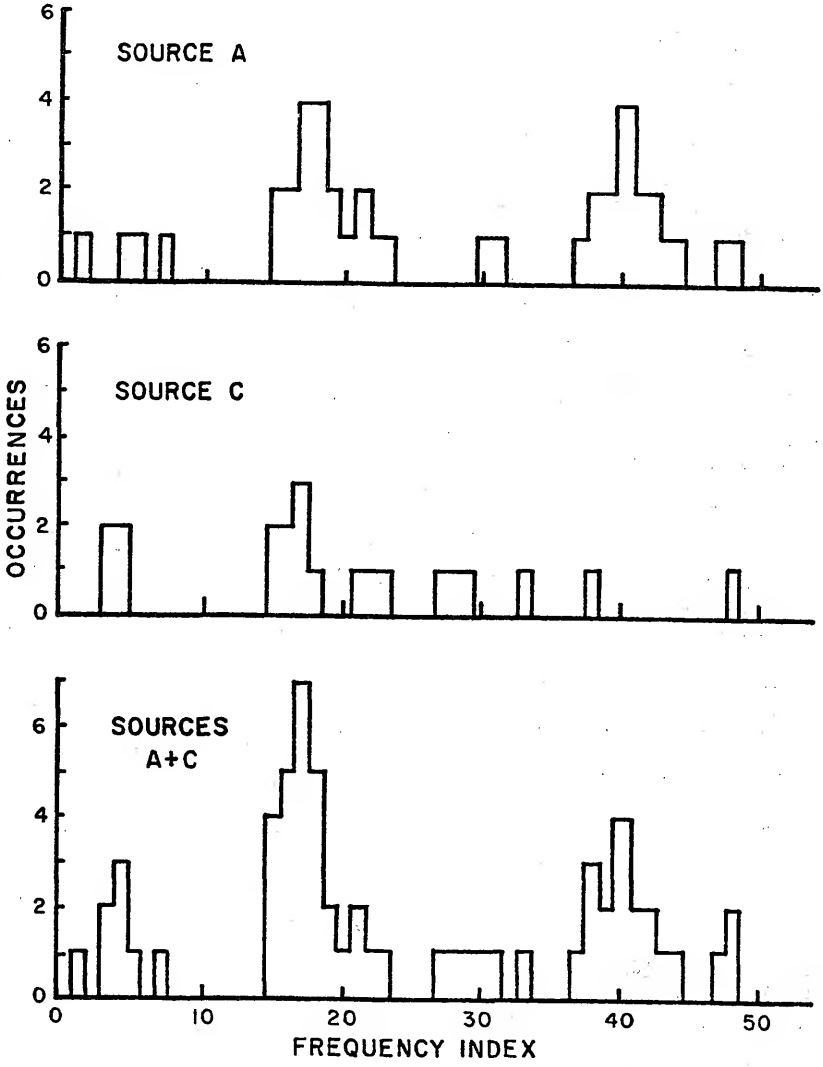

Figure 42. Histograms of 90% confidence spectral features. 1967-68 and 1974 values are merged for each source.

dominant features, one at index 17, one at index 40 and one at index 4. The index 4 maximum corresponds to the 27-day period mentioned in connection with the solar correlation.

The index 17 peak is rather interesting. It is near, but essentially uncoupled, from the second order Io peak (J-I) that straddles indices 15 and 16. Though the entire line profile about 17 does include power at 15 and 16, it is weaker and there is no contribution at 14--the site of another equally strong second order Io peak (2I). Since the Jovian frequencies are well suppressed not only in the composite histogram but in the individual spectrograms which provide the indices 15 and 16 contribution, rule 2 says that if 15 and 16 are Jupiter-Io contaminants (J-I) the source must be unsuppressed Io information. However, the 2I peak is missing as it should be by rule 3 because, more importantly, the fundamental's alias at index 47 is missing. The only information at 47 in the composite histogram was contributed by only 1 of the 7 spectograms which contributed to index 17, and it is probably not the Io fundamental. As a result, we can rule out Io contamination as the source of index 17, or the whole feature from 15 to 20 for that matter.

Another curious aspect of index 17 is that mentioned in relation with the activity spectograms, Figures 30 and 31, where all the Io activity was left in. Specifically, the source B spectrum has a sharp independent peak to the side of the Io indices 14, 15, and 16 maxima but this peak is not found in the corresponding source A Io activity line

profile. This strongly suggests, first that the index 17 line is capable of being quite strong--rivaling some Io peaks--and second, in addition to all other arguments, it is not an Io feature because it goes away in source A.

Almathea and the other Galilean satellites have been examined to see if they can account for the peak. The only possible candidate for a simple satellite-System III process analogous to the Io effect is Ganymede. But the fundamental from Ganymede falls not on index 17 but index 15 and thus it seems to be an unlikely source of the "17 effect." Joint interactions between two and three satellites have been explored through the third order with only one promising candidate, Io-Europa.

Table 12 displays the expected frequencies of the Io-Europa system. It is seen that one of the two lowest order frequencies corresponds to index 17. The remaining second and third order frequencies correspond reasonably well to the secondary features in the vicinities of indices 14, 30, and 47.

The index 40 line is not associated with any Jovian or Io line except for a third order line (2J+I) at index 42. This third order line is not even visible in the A and B activity spectra and is too far removed from index 40 to have any connection with the index 40 peak. In fact, no combination of satellite and Jovian interactions studied in the search outlined above can account for the line. Index 40 corresponds to

Table 12

Frequencies of the Io-Europa System

Source	Frequency (c/d)	Period (d)	Index (1/108 c/d)
I+E	0.155	6.46	17
I-E	0.283	3.53	31
J+I+E	0.263	3.80	29
J+I-E	0.300	3.33	32
J-I+E	0.430	2.32	46
J-I-E	0.133	7.54	14-15

2.70 days. The line is seen only in source A but it is seen in both 1967-68 and 1974. In both cases it was seen at all frequencies though it was not plotted for 1967-68 MHz because those data are suspect and it was not plotted for 1974 to 18 MHz because it just failed to reach the 90% confidence limit. For now, the source of the index 40 line is a mystery.

CHAPTER 6

OCCURRENCE DISTRIBUTIONS

Statistical Approach

For many populations it is either impossible or impractical to measure desired parameters of every member of the population. One of the basic objectives of modern statistics is to enable one to infer from a sample certain characteristics about the population from which the sample is drawn.

In the case of the Jovian decametric radiation, the stroboscopic effect of the three rotating and revolving bodies, the earth, Io, and Jupiter, conceals much of the emission population from the observer. One must be content with the samples which are available. The preceding chapters have dealt basically with the question of periodic or quasi-periodic properties of the radio emission. Periodicity is one form of non-random process and evidences of this property have been offered. The focus in this segment of the work is the attack on the general question of randomness.

The Service Problem

If one assumes that the Jovian emissions stem from some truly random process, then the characteristics of that process

can be modeled in a fashion analogous to many terrestrial situations. For example, the likelihood of random Jovian emission during any given period of time would behave the same as the likelihood of a bank customer approaching a teller for service during any given period of time. In both situations the radio astronomer and the teller are passive observers viewing presumably random events.

If time may be subdivided into small periods so that the probability of an event occurring in that subinterval is small, if the probability of occurrence is constant in time, if occurrences are independent and almost never occur twice in one subinterval, the probability distribution of these events is a Poisson distribution. To the extent the experimental distribution departs from the Poisson one or more of these conditions are not being met.

Thus if Jupiter's emissions are random independent events with a constant probability of occurrence, the distribution of the number of storms detected per unit time (say a few 5° CML zones) should obey a Poisson distribution.

Furthermore, if the requests for service are random and the time of completion is short, the lengths of the service times--the storm lengths in this analogy--obey an exponential distribution (see for instance Hartnet, 1970). Consequently, one expects that the distribution of occurrences and the distribution of storm lengths will yield information about the underlying processes.

Unfortunately, there are some potential problems in pursuing this course. (As an aside, it must be said that this particular effort--distributions-- is the newest and hence the least developed part of this study.) The key feature is the testing of the concept of constant probability (i.e., not time dependent). To do this adequately one must be certain that there are not other time dependent influences on the probability of detection of Jovian radio storms. Of course, there are. Due to interference and degraded ionospheric transparency, the detection of activity toward the end of an apparition is more difficult. Lebo (1964) has considered this and several related effects and has shown that they all have measurable influences. Equipped with this knowledge the next logical question is: Can the influence of these effects be removed? Heuristically it seems that they can, but it appears that the burgeoning science of statistics has yet to deal fully with this problem. A further discussion of this particular situation and its possible solutions will be taken up in the final chapter. For the present, a less sensitive, more robust aspect of this area will be pursued.

Storm Lengths

Due to the various data limiting problems mentioned in the preceding chapter the following presentation is limited to a merge of the source A data for 18, 22, and 27 MHz in 1967-68

and, separately, in 1974. Figures 43 and 44 show the distribution of observation lengths (in zones) and storm lengths (in zones). The observation spectra in both cases are entirely reasonable. They show that the distribution of zones observed is essentially constant from 1 through 18. But, since there are 19 zones in the source, corresponding to about 2.6 hours of observing time, about 30% of the time the observing station "saw" all 19 source zones. As a result there is a strong peak at 19.

Inspection of the observation length and storm length distributions for both 1967-68 and 1974 reveals that 80% of the observations lasted 6 zones or more while 80% of the storm lengths were 6 zones or less. Thus there was a 20% probability that the 20% of the storms which exceeded 6 zones were truncated by short observations. Put another way, the overall probability of observed storms being truncated by the beginning or end of the observation of the source is only 4%. As a consequence, the storm length distributions in Figures 43 and 44 are good estimates of the true distribution of storm lengths at observable flux levels.

If the storms are produced by a random process (that is, one assumes they have a Poisson distribution) and the storm lengths are relatively short and of random length, the storm length should have an exponential distribution. Specifically,

$$f(n) = \lambda e^{-\lambda n}$$

where λ is the reciprocal of the average value of the storm

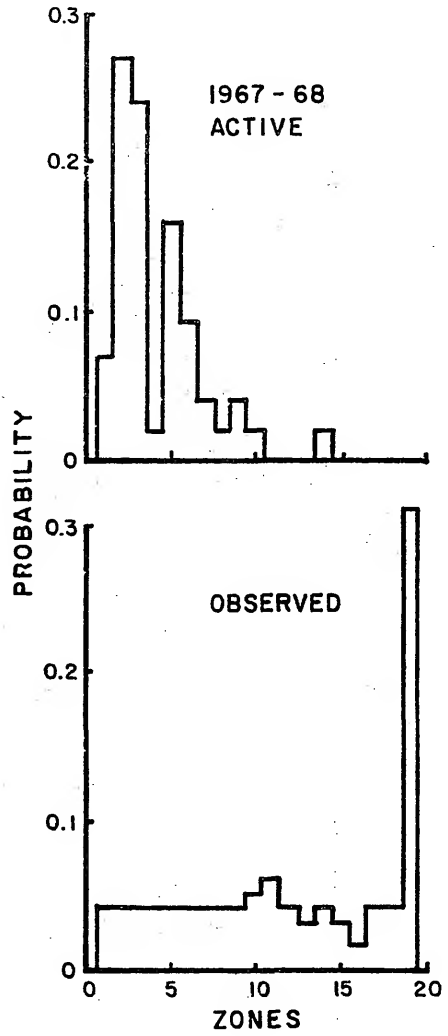

Figure 43. Frequency distributions of source A storm lengths and observation lengths in units of 5° CML zones, 1967-68.

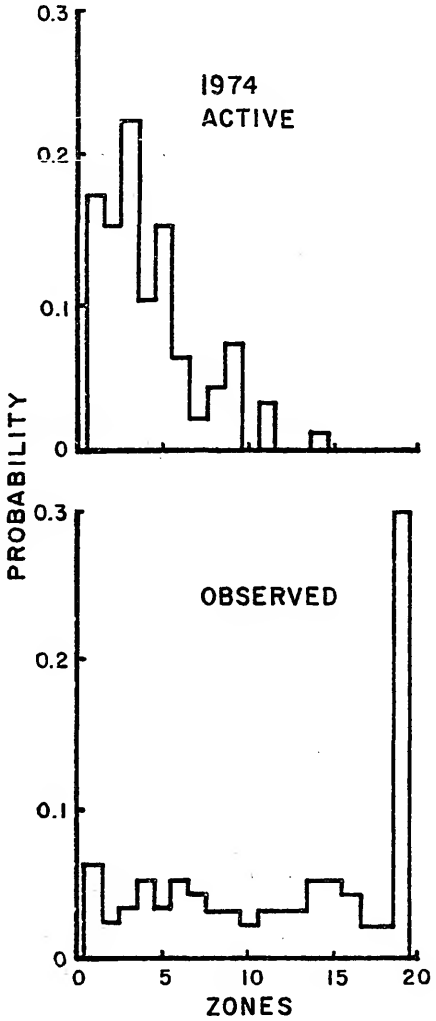

Figure 44. Frequency distributions of source A storm lengths and observation lengths in units of 5° CML zones, 1974.

lengths and n is the zone number. However, in the present problem it has been defined that the shortest possible storm is one zone long. The equation above assumes that the minimum value is zero zones. This is rectified by a simple translation of axes so that one obtains

$$f(n) = \lambda e^{-\lambda(n-1)}$$

while the average value of the storm length must be reduced to $\bar{n}-1$. These values are calculated directly from the experimental distributions and are found to be 2.16 in 1967-68 and 2.07 in 1974. Thus, the values for λ are

0.463 in 1967-68

and

0.483 in 1974.

The theoretical and actual storm length distributions are shown in Figure 45. The actual storm lengths differ from those in Figures 43 and 44 only in that they have been unnormalized to show the actual storm counts for each length. It will be noted that the number of single zone storms falls short of the predicted value in both cases. Generally speaking the actual number of longer storms exceeds the predicted value. If apparition-phase edge effects were significant in this plot, just the opposite would be expected since the storms would be artificially shortened as ionosphere or interference permitted only the strongest part of a storm to be observed.

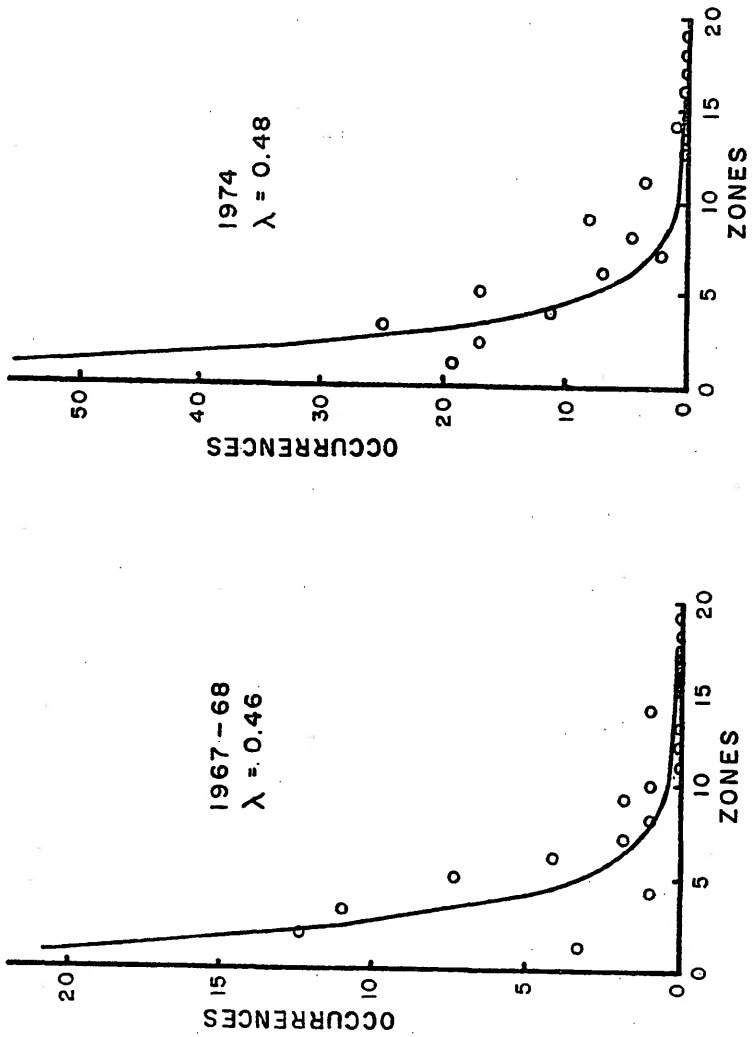

Figure 45. Theoretical random and actual storm length distributions, 1967-68.

Confidence intervals. If one has a table of observed and theoretical values for a frequency distribution, the sampling distribution of the statistics

$$\chi^2 = \sum_{1}^{M}{}_i \frac{(X_i - T_i)^2}{T_i}$$

where X_i are the observed values, T_i are the theoretical values and M is the number of values observed, is a chi-square distribution with M-1 degrees of freedom. This statistic can be used to determine confidence intervals for the "goodness of fit" between the observed and theoretical values. It is worth remarking that it is imperative that the frequency distribution must be in the un-normalized form as in Figure 45 because the confidence interval in the chi-square test is very dependent on the actual number of events observed. Normalization of the frequency distribution as in Figures 43 and 44 obscures this information and leads to a nonsense result in the test.

Application of the chi-square test to the storm length distribution leads to

$$\chi^2_{1967\text{-}68} = 52.34$$

$$\chi^2_{1974} = 110.35.$$

Both values far exceed the 99.5% confidence interval and thus both observed storm length distributions are considered nonrandom.

Chree Analysis

In Chapter 4, Chree analysis was used extensively to compare Jovian events with modeled solar wind events. In the process many superposed epoch diagrams of the Jovian data similar in character to those shown in Figure 46 were generated. A persistent feature seen in most of these plots was the four peaked structure seen there.

The universality of these features has led to an investigation of the probability that these modulations could occur by chance. Each point in the analysis plot represents the mean of a sample drawn from the population of emissions. If one assumed a null hypothesis that the population had a Gaussian distribution, the population of the means of all samples of that population would be a t distribution. Thus, one could use that distribution to check the variation from the long-term sample mean. However, the assumption of a Gaussian distribution can be eliminated by again resorting to the chi-square test.

In applying the chi-square procedure to the Chree analysis there is a problem in that the number of zones observed is not the same for each day in the epoch. However, this will be sidestepped by assuming that all days have the same sample size. The goodness of fit test will then be done on the resulting distribution of activity zones versus days. Again attention will be directed to source A at 18, 22, and 27 MHz during 1967-68 and 1974.

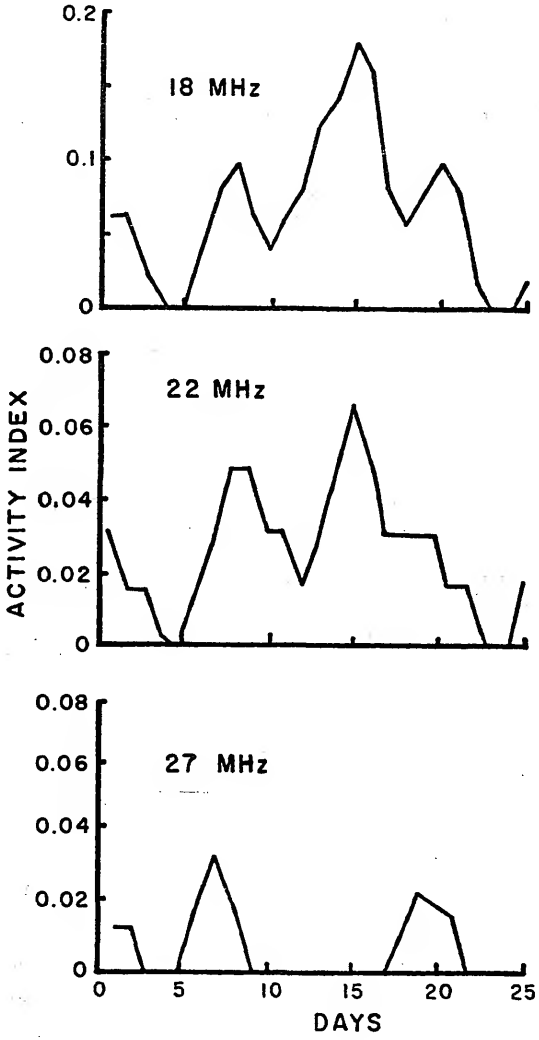

Figure 46. 1967-68 source A activity index Chree analyses.

Under ordinary circumstances the 25-day period of the analysis would result in 24 degrees of freedom. However, in the cross-correlation procedure the Chree analysis tables were Hanning smoothed before correlating. The smoothed tables will be used here as well, thus leaving 12 degrees of freedom.

The results of the chi-square test are summarized in Table 13.

Table 13

Chree Analysis Confidence Intervals

Frequency	χ^2	Confidence (%)
1967-68		
18	44.2	>99.5
22	25.4	>97.5
27	32.7	>99.5
1974		
18	89.7	>99.5
22	55.7	>99.5
27	121.2	>99.5

Since all values of the statistic exceed 97.5% confidence and all but one exceeds 99.5% confidence, it is concluded that the Chree analysis variations are also not the effect of a random process.

CHAPTER 7

OVERVIEW

Summary of Results

Wind Models

Two models for solar wind velocity stream interactions have been developed. These models describe the transformation of the velocity wave into a density wave. The magnetic-field-free model appears to give acceptable results when the peak-to-peak velocity amplitude is not too great and the radial distance is also not too great. A test has been devised to measure the propriety of the model in a given situation. The simple-field model solves the diffusion problem that restricts the field-free model. However, it permits the density wave to build up as a infinitesimally thin sheet.

Both models are adequate for a coarse description of the wave exchange process. Nevertheless, future work might well be directed at a more detailed model of the density wave, including the effects of magnetic and thermal pressure which will limit the compression of the plasma to some physically realistic size.

Jupiter-Solar Correlation

Employing the two solar wind models, the 1967-68 and 1974 apparitions, with stable solar magnetic sector structures,

have been studied. Evidence of a correlation between the non-Io related component of Jovian decametric emission in the 18 to 27 MHz range and the solar wind flux has been offered for both apparitions. Positive correlations exceeding 95% confidence occur in source A at 22, 26, and 27 MHz, and source C at 18, 22, 26, and 27 MHz. The validity of the source A 22, 26, and 27 MHz correlations is clouded by the predominance of single zone storms. Evidence of an anticorrelation between the Io component of source B at 18, 22, and 27 MHz is provided.

The solar wind velocity data which serve as the input to the simple-field wind model used for the 1974 apparition are limited to 81 days near opposition. A re-examination of that apparition when more complete data are available should be undertaken.

The correlation maximum precedes the predicted density wave arrival at Jupiter. This raises the question of whether the density wave itself or shocks, caused by stream collisions moving ahead of the wave, is the exciting agent. Other possibilities include the build-up of the density wave 1 to 3 days ahead of the peak of the velocity wave, and the acceleration of the solar wind with radial distance as predicted by so many models. The possibility of an accidental correlation also remains.

Occurrence spectral analysis shows a period in the decametric emission for 1974 near the 26-day solar rotation period giving further weight to the reality of the correlation. The 1967-68 spectral data are inconclusive.

In connection with the wind acceleration the author believes that the method of reporting solar wind velocities for Mariner 2 and Pioneers X and XI would conceal the acceleration if it exists. It is suggested that both velocity and density or flux data from the Pioneer X and XI projects can be used with a mass weighted average technique to resolve this problem.

The proposition of Vladimirsky and Levitsky (1976) that there is a 4° wide quiet zone centered on the solar equatorial plane can be neither confirmed or denied since Jupiter was well within that zone during both apparitions. Their suggestion that ejecta or shocks from solar proton events produce Jovian emissions is compatible with the results of the present study. The energy density of such events exceeds that of common flare ejecta by several orders of magnitude. Though it is not possible to predict the energy density of the stream generated mass density waves without knowing how compressed they can become, it is believed that the proton events exceed the stream wave's energy density, Thus if the stream generated wave can excite decametric emission surely proton events may do so.

Spectral Analysis

A persistent spectral line at frequency index 17 (6.35d) is seen in sources A and C during both apparitions at most frequencies. This and other, secondary, features can be explained by a joint Io-Europa effect. Miller (1970) has presented and discounted evidence of such an effect by showing activity on a plot of Io versus Europa locations from geocentric

superior conjunction. This matter definitely bears further investigation employing more than the two apparition's worth of data used here.

When one does a spectral analysis of the source B activity data without removing the Io data a pronounced activity spike is found at index 17 during 1974. However, the same treatment of source A, with Io, yields no visible line. This intensifies the argument for a joint effect since the index 17 peak cannot be explained by Io alone.

A second line at index 40 (2.7d) has been discovered in source A during both apparitions. It has thus far defied identification.

Statistics

The lengths of non-Io related storms in source A have been shown to be non-random as have the apparently periodic fluctuations in the solar-Jupiter Chree analysis plots. In source A at 18 MHz these Chree analysis peaks are seen, though shifted in position, even though there seem to be no solar correlations at that frequency. These four peaks correspond to a period of about 6.4d and may be connected with the Io-Europa effect.

Future work in the probability distribution area may be directed at removing the known long-term time dependence from the activity distribution. In principle, this might be done by fitting a low order polynomial, such as a parabola, to the data. The inversion of this function can then be used to

amplify the activity probability near the extremes of the apparition and thus remove the effect.

Conclusions

It appears that below the strata of the terrestrial, Jovian and Ioian effects on the decametric emission there is a set of discernable secondary and tertiary exciters participating in the "underlying" processes. The current examination has revealed evidence of three such exciters, one correlated with solar wind interactions with the Jovian magnetosphere, one identified with an Io-Europa effect, and the third at index 40 whose possible identify is not known. It is hoped that further studies will resolve these effects.

APPENDIX

APPENDIX

Data Reduction Programs

Four basic computer programs form the nucleus of this study. These programs are written in FORTRAN IV and should be compatible with virtually any compiler with few, if any, modifications. The principal functions of these routines are outlined below. The programs are internally documented with numerous comment statements. Source listings, including these comments, follow the outline.

Snoplow. The solar wind interaction models are generated by this program. The input data consist of a table of daily solar wind velocities on some solar radial line (the sun-Jupiter radial in the present study). This table is entered in card form using a 10(I5,I3) format where the I5 represents the five digit Julian date and the I3 represents the corresponding velocity. In this study the table has been in chronological order with no missing dates though the program will handle both scrambed and missing dates (the latter are interpolated). The output is both printed and punched.

Jupzone. This program is the interface between the "intermediate deck" and the two Jupiter data reduction programs, Jupcor3 and Jupsol5. This program contains the

filter which separates and counts zones for a given source into activity and observations for the Io and non-Io related components. Jupzone accepts its input from either tape or cards and generates both printed and punched output.

Jupcor3. Both solar wind and Jovian data are the input to this routine. Jupcor3 performs the autocorrelation and Fourier transform procedure on these data and prints both values and plots.

Jupsol5. Solar wind and Jupiter data are fed to this program which begins by performing the Chree analysis based on a user specified period. The solar wind Chree analysis table is the cross-correlated with each of the Jovian tables. The routine prints values and plots for both the Chree analyses and the cross-correlation functions.

```
FORTRAN IV G LEVEL  21                  MAIN                    DATE = 75314          16/32/52
C
C
C
C       **********************    SNOPLOW    **********************
C
C       -------- A MODEL OF THE SOLAR WIND AND ITS PARAMETERS.
C       MODEL IS ALONG A TIME AXIS WHICH FOLLOWS WIND PROGRESS IN TIME.
C       AS GROUPS OF PARTICLES RELEASED BY THE SUN AT SIX HOUR INTERVALS
C       PROGRESS OF EACH GROUP IS TRACKED FOR FORTY DAYS.
C       INTERACTIONS BETWEEN GROUPS ARE ALLOWED FOR AND TIME OR SPACE
C       DEPENDENT VARIATIONS OF PARAMETERS ARE ACCESSABLE.........
C
C
C       THIS PROGRAM ACCEPTS AS DATA THE SOLAR WIND VELOCITY INTERPOLATED
C       TO CORRESPOND TO THAT AT ONE A.U. EVERY DAY. IT THEN EXTRAPOLATES
C       THE DAILY VELOCITIES BACK TO THE SUN TO OBTAIN THE DATE AT WHICH
C       THE MATERIAL LEFT THE SUN (SUNDAT). IT PRODUCES A TABLE OF SOLAR
C       WIND VELOCITIES VS. JULIAN DATE AT THE SUN, AVERAGING AND
C       INTERPOLATING AS REQUIRED TO ACCOMODATE MULTIPLE ENTRIES FOR A
C       DATE, OR, FOR NO ENTRY FOR A DATE.
C       AT THIS POINT THE PROGRAM USES THE VELOCITY TABLE AS INPUT TO
C       A MODEL OF THE SOLAR WIND AND ITS SELF INTERACTIONS.
C       THE INTENTION BEING TO MODEL THE 'SNOWPLOW EFFECT'. ONCE THE MODEL
C       HAS BEEN CONSTRUCTED VARIOUS PARAMETERS SUCH AS THE FLUX, B FIELD
C       OR THE VELOCITY MAY BE OUTPUTTED.
C
C
0001            DIMENSION SUNST(3,325),JDATA(2,300),WNDPRM(6,160),PRMSX(6,60)
0002            DIMENSION B(30),WIND(5,300)
C
0003            COMMON SUNST,JDATA,WNDPRM,LAST,PRMSX,KCOUNT,B,WIND,ISTART,ISTOP
0004            COMMON AINC
C
C
C       INITIALIZE WIND.
C
C
0005            DO 1 I=1,5
0006            DO 1 J=1,300
0007          1 WIND(I,J)=0
C
C
0008            CRIT=16
0009            CALL INPUT
0010            CALL SUNDAT
0011            CALL SOLWIN (CRIT)
0012            CALL OUTPUT
C
0013            STOP
0014            END
```

```
FORTRAN IV G LEVEL  21                  INPUT                   DATE = 76314          16/52/52
0001                  SUBROUTINE INPUT
                C
                C
                C      READ IN JULIAN DATES VS. SOLAR WIND VELOCITIES AT THE EARTH
                C      (JDATA). THIS TABLE HAS CONSECUETIVE ENTERIES WITH NO HOLES.
                C      THE SOLAR WIND TABLE MAY CONTAIN UP TO 300 CONSECUETIVE ENTRIES.
                C
                C
0002                  DIMENSION SUNST(3,325),JDATA(2,300),WNDPRM(6,160),PRMSX(6,60)
0003                  DIMENSION B(30),WIND(3,300)
                C
0004                  COMMON SUNST,JDATA,WNDPRM,LAST,PRMSX,KCOUNT,B,WIND,ISTART,ISTOP
0005                  COMMON AINC
                C
                C     ISTART: THE JULIAN DATE THE ANALYSIS BEGINS
                C     ISTOP: THE JULIAN DATE THE ANALYSIS STOPS
                C
0006                  READ (5,901) ISTART, ISTOP
0007                  READ (5,903)  AINC
0008                  DO 27 J=1,291,10
0009                  M=J+9
0010                  READ(5,902)((JDATA(K,L),K=1,2),L=J,M)
0011                  IF(JDATA(1,J).EQ.0) GO TO 28
0012                  GO TO 27
0013               28 DO 29 K=M,300
0014                  DO 29 L=1,2
0015               29 JDATA(L,K)=0
0016                  GO TO 30
0017               27 CONTINUE
                C
                C     INITIALIZE 'WIND'.
                C
0018               30 DO 31 I=1,300
0019                  DO 31 J=1,3
0020               31 WIND(J,I)=0.
                C
0021                  RETURN
                C
0022              901 FORMAT(I5,1X,I5)
0023              902 FORMAT (10(I5,I3))
0024              903 FORMAT(F3.1)
0025                  END
```

```
FORTRAN IV G LEVEL  21                  SUNDAT              DATE = 76314      16/52/52
0001                  SUBROUTINE SUNDAT
                C
                C
                C
                C     THIS SUBROUTINE EXTRAPOLATES THE TABLE OF SOLAR WIND VELOCTIES AT
                C     THE EARTH BACK TO THE SUN AND CREATES A NEW TABLE OF DAILY WIND
                C     VELOCITIES AT THE SUN. MULTIPLE ENTRIES ARE REPLACED BY THEIR MEAN
                C     AND VACANT ENTRIES ARE REPLACED BY VALUES INTERPOLATED BETWEEN
                C     NEAREST AVAILABLE ENTRIES.
                C
                C
                C
                C
                C
                C      THE VARIABLE ITOFLT REPRESENTS THE TIME OF FLIGHT BACK TO THE
                C     SUN.  ITS DEFINITION DEPENDS ON THE DISTANCE OF THE EARTH TO THE
                C     SUN.  THE EXPRESSION: ITOFLT=1730./A+0.5  APPLIES AT ONE AU.  THE
                C     NUMERICAL VALUE (1730) MUST BE VARIED PROPORTIONAL TO THE DEPARTURE
                C     FROM 1 AU.  THE EXPRESSION OCCURS TWICE IN THIS ROUTINE.
                C
                C
0002                  DIMENSION SUNST(3,325),JDATA(2,300),WNDPRM(6,160),PRMSX(6,50)
0003                  DIMENSION B(30),WIND(5,300)
                C
0004                  COMMON SUNST,JDATA,WNDPRM,LAST,PRMSX,KCOUNT,B,WIND,ISTART,ISTOP
0005                  COMMON AINC
                C
                C     FIND FIRST SUN DATE
                C
0006                  A=JDATA(2,1)
0007                  ITOFLT=1730./A+0.5
0008                  ISUNDT=JDATA(1,1)-ITOFLT
                C
                C      DATE AND INITIALIZE SUNST
                C
0009                  DO 200 J=1,325
0010                  SUNST(1,J)=ISUNDT+J-1
0011                  SUNST(2,J)=0
0012              200 SUNST(3,J)=0
                C
                C     EXTRAPOLATE TIME AND VELOCITY BACK TO SUN
                C
0013                  DO 201 I=1,300
0014                  IF(JDATA(1,I).EQ.0) GO TO 201
0015                  A=JDATA(2,I)
0016                  ITOFLT=1730./A+0.5
0017                  SUNDT=JDATA(1,I)-ITOFLT
0018                  AVEL=JDATA(2,I)
                C
                C     ENTER VELOCITY WITH CORRESPONDING DATE IN SUNST
                C     IF A VELOCITY ENTRY ALREADY EXISTS- ENTER MEAN VALUE
                C
0019                  DO 207 J=1,325
0020                  IF(SUNDT.EQ.SUNST(1,J)) GO TO 203
0021                  GO TO 207
0022              203 IF(AVEL.GT.SUNST(2,J)) SUNST(2,J)=AVEL
0023                  GO TO 206
0024              205 SUNST(2,J)=AVEL
0025              206 SUNST(3,J)=SUNST(3,J)+1
0026              207 CONTINUE
0027              201 CONTINUE
                C
                C     LOOK FOR BEGINNING OF 'HOLES' IN VELOCITY ENTRIES IN SUNST
                C
0028                  DO 208 I=1,325
0029                  IF(SUNST(2,I).NE.0..AND.SUNST(2,(I+1)).EQ.0.) GO TO 211
0030                  IF(I.EQ.325) LAST=325
0031                  GO TO 208
                C
                C     IF FOUND- LOOK FOR END OF HOLE
                C
0032              211 NA=I+1
0033                  DO 209 J=NA,324
0034                  IF(SUNST(2,J).EQ.0..AND.SUNST(2,(J+1)).NE.0.) GO TO 212
0035                  IF((J+1).EQ.325) GO TO 213
0036                  GO TO 209
                C
                C     ENTER INTERPOLATED VELOCITIES TO FILL HOLES
```

```
FORTRAN IV G LEVEL  21                  SUNDAT                  DATE = 75314          16/52/52
                C
0037              212 LA=J-I+1
0038                  NB=LA-1
0039                  DO 210 L=1,NB
0040                  A=L
0041                  AA=LA
0042              210 SUNST(2,(I+L))=SUNST(2,I)*((AA-A)/AA)+SUNST(2,J+1)*(1/AA)
                C
                C     CONTINUE LOOKING FOR HOLES
                C
0043                  GO TO 208
                C
                C     IF OUT OF DATA- SUNST IS COMPLETE SO RETURN
                C
0044              213 LAST=I
0045                  GO TO 214
0046              209 CONTINUE
0047              208 CONTINUE
0048              214 RETURN
                C
0049                  END
```

```
FORTRAN IV G LEVEL  21                  SOLWIN              DATE = 76314          15/52/52
0001                  SUBROUTINE SOLWIN (CRIT)
                C
                C
                C
                C     THIS SUBROUTINE REPRESENTS THE FUNCTIONAL DETAILS OF THE SOLAR
                C     WIND MODEL. SEVERAL OPTIONS ARE AVAILABLE. THE USER MAY OBTAIN
                C     A (MAGNETIC) FIELD FREE MODEL, A SIMPLE FIELD MODEL WHICH CONSERVES
                C     KINETIC MOMENTUM, BUT ALLOWS MASS TO BUILD UP AS INFINITELY THIN
                C     SHEETS, OR FINALLY, A MODEL WHICH ASSUMES AN INVERSE POWER LAW
                C     FORCE IS EXERTED BY EACH GROUP ON EVERY OTHER GROUP.
                C
                C
                C
0002                  DIMENSION SUNST(3,325),JDATA(2,300),WNDPRM(6,160),PRMSX(6,60)
0003                  DIMENSION B(30),WIND(5,300)
                C
0004                  COMMON SUNST,JDATA,WNDPRM,LAST,PRMSX,KCOUNT,B,WIND,ISTART,ISTOP
0005                  COMMON AINC
                C
                C
                C     WNDPRM WILL REPRESENT THE ARRAY OF 6 HOUR GROUPS OF PARTICLES
                C     WNDPRM(1,N)= DATE
                C     WNDPRM(2,N)= VELOCITY IN KM/S
                C     WNDPRM(3,N)= DISTANCE IN AU
                C     WNDPRM(4,N)= MASS IN ARTIRARY UNITS
                C     WNDPRM(5,N)= SPARE
                C     WNDPRM(6,N)= BUNCH #
                C
                C
                C     INITIALIZE WNOPRM
                C
0006                  DO 100 I=1,160
0007                  DO 100 J=1,6
0008                100 WNDPRM(J,I)=0
                C
                C     PRINT THE SCALE FOR 'PLOT2'.
                C
0009                  WRITE(6,901) AINC
                C
0010                  L=0
0011                  AK=1
                C
                C     '103 LOOP' STEPS GROUPS THROUGH WNDPRM AT 6 HOUR INTERVALS
                C
0012                  NC=4*LAST+160
0013                  DO 103 M=1,NC
                C
                C     '101 LOOP' REPOSITIONS EACH GROUP IN WNDPRM EACH 6 HOURS
                C
0014                  DO 101 I=1,160
0015                  J=101-I
0016                  WNDPRM(1,J)=SUNST(1,1)+(0.25*L)
0017                  IF(J.EQ.1) GO TO 102
0018                  WNDPRM(2,J)=WNDPRM(2,(J-1))
0019                  WNDPRM(3,J)=WNDPRM(3,(J-1))+(WNDPRM(2,(J-1))/6925.83)
0020                  WNDPRM(4,J)=WNDPRM(4,(J-1))
0021                  WNDPRM(5,J)=WNDPRM(5,(J-1))
0022                  WNDPRM(6,J)=WNDPRM(6,J-1)
0023                  GO TO 101
                C
                C     EMIT MOST RECENT GROUP OF PARTICLES FROM THE SUN
                C
0024                102 K=AK
0025                  AK=AK+0.25
0026                  IF(K.GT.LAST) GO TO 110
0027                  L=L+1
0028                  WNDPRM(2,I)=SUNST(2,K)
0029                  WNDPRM(3,I)=0
0030                  WNDPRM(4,I)=1
0031                  WNDPRM(5,I)=1
0032                  WNDPRM(6,I)=L
0033                  GO TO 101
0034                110 WNDPRM(2,I)=0
0035                  WNDPRM(3,I)=0
0036                  WNDPRM(4,I)=0
0037                  WNDPRM(5,I)=0
0038                  WNDPRM(6,I)=0
0039                  L=L+1
```

```
FORTRAN IV G LEVEL  21                  SOL#IN              DATE = 75314          16/52/52
0040          101 CONTINUE
C
C
C                                  ******************************
C       FOR FIELD FREE MODEL INSERT: GO TO 114.
C
C       FOR SIMPLE FIELD MODEL INSERT: GO TO 115.
C       ------------------------------------------------------------------------------
0041          GO TO 115
C       ------------------------------------------------------------------------------
C                                  ******************************
C
C
C
C       THE FOLLOWING ROUTINE CALCULATES THE FORCE EXERTED ON EACH GROUP
C       BY EACH OTHER GROUP AND ADJUSTS THE SUBJECT GROUP'S VELOCITY
C       ACCORDING TO THE NET ACCELERATION PRODUCED
C       THE ASSUMPTION MADE IS THAT THE FORCE IS AN INVERSE POWER LAW
C       FORCE. FURTHER IT IS ASSUMED THAT THE FORCE ACTS ON A UNIT MASS
C       OVER A PERIOD OF SIX HOURS. CONSEQUENTLY THE NET CHANGE IN SPEED
C       IS PROPORTIONAL TO A(X)**(-P).
C       "A" IS THE FORCE CONSTANT
C       "P" IS THE POWER OF THE ASSUMED POWER LAW FORCE
C
C
0042          150 CONTINUE
0043              A=3
0044              P=2
0045              DO 104 I=1,160
0046              IF(#NDPRM(6,I).EQ.0) GO TO 104
0047              IF(I.GT.1) #NDPRM(2,I-1)=#NDPRM(2,I-1)+F
0048              F=0
0049              DO 105 J=1,160
0050              IF(#NDPRM(6,J).EQ.0) GO TO 105
0051              IF(I.EQ.J)GO TO 105
0052              X=(#NDPRM(3,I)-#NDPRM(3,J))
0053              IF(X.EQ.0) GO TO 105
0054              G=A*((ABS X)**(-P))*(ABS X)/X
0055              F=F+G
0056          105 CONTINUE
0057          104 CONTINUE
0058              #NDPRM(2,160)=#NDPRM(2,160)+F
C
C
0059          115 CONTINUE
C
C
C       FOR SIMPLE FIELD MODEL LOOK ONCE A DAY, NOT EVERY SIX HOURS.
C
C
0060              K=#NDPRM(1,1)
0061              C=#NDPRM(1,1)-K
0062              IF(C.NE.0.) GO TO 103
C
C
0063              II=1
0064          116 JI=1
0065              II=II+1
0066              IF(II.GT.160) GO TO 114
0067              Z=1
0068              S=#NDPRM(2,II)
0069              IF(S.EQ.0) GO TO 116
0070          117 IF(#NDPRM(3,JI).LT.#NDPRM(3,II)) GO TO 118
0071              #NDPRM(3,JI)=#NDPRM(3,II)
0072              Z=Z+1
0073              S=S+#NDPRM(2,JI)
0074          118 JI=JI+1
0075              IF(JI.LT.II) GO TO 117
0076              JI=1
0077          119 IF(#NDPRM(3,JI).NE.#NDPRM(3,II)) GO TO 120
0078              #NDPRM(2,JI)=S/Z
0079          120 JI=JI+1
0080              IF(JI.LE.II) GO TO 119
0081              GO TO 116
C
C
0082          114 CONTINUE
```

```
FORTRAN IV G LEVEL  21                SOLWIN              DATE = 75314          16/52/52
                C
                C       AT THIS POINT WNDPRM HAS BEEN REORGANIZED FOR THIS 6 HOUR PERIOD
                C       IT MAY NOW BE EXAMINED FOR WHATEVER PROPERTIES ARE OF INTEREST
                C
0083                    CALL PARM
                C
0084               103  CONTINUE
0085                    RETURN
                C
0086               901  FORMAT(' ',//,26X,'SOLAR WIND PARAMETER "DENSITY" VS. JULIAN DATE'
                   1,///,' JULIAN',19X,'INCREMENT IN SPACE IS',F4.1,' ASTRONOMICAL UNI
                   2TS.',/,'  DATE',6X,29('1...'),'I')
                C
0087                    END
```

```
FORTRAN IV G LEVEL 21                PARM                DATE = 76314      16/32/52
0001                  SUBROUTINE PARM
                C
                C
                C
                C     THIS SUBROUTINE, CALLED BY 'SOLWIN', EXTRACTS FROM THE MODEL WIND
                C     PARAMETERS THOSE WHICH ARE OF INTEREST FOR LATER DISPLAY.
                C     PRESENT OPTIONS ARE:
                C
                C                              1. THE FLUX DENSITIES AT X AU.
                C                                 TWO VALUES MAY BE OBTAINED.
                C                                 THEY ARE AT X=AINC*I AU.
                C                                 THE RESULTS ARE STORED AS
                C                                 WIND(2,ICOUNT)=B(I)  AND
                C                                 WIND(3,ICOUNT)=B(I).
                C
                C                              2. THE PARTICLE DENSITIES
                C                                 LOCATED AND STORED AS ABOVE.
                C
                C                              3. THE VELOCITIES AT RADIAL
                C                                 DISTANCES AS SPECIFIED
                C                                 IN STATEMENTS 150 AND 151.
                C
                C
                C
0002                  DIMENSION SUNST(3,325),JDATA(2,300),WNDPRM(6,160),PRMSX(6,60)
0003                  DIMENSION B(30),WIND(5,300)
0004                  DIMENSION A(6,160)
                C
0005                  COMMON SUNST,JDATA,WNDPRM,LAST,PRMSX,KCOUNT,B,WIND,ISTART,ISTOP
0006                  COMMON AINC
                C
0007                  DATA A, ICOUNT/960*0.,0/
                C
                C
                C     LOOK ONLY ONCE EACH DAY - NOT EVERY SIX HOURS
                C
                C
0008                  K=WNDPRM(1,1)
0009                  C=WNDPRM(1,1)-K
0010                  IF(C.NE.0.) GO TO 105
                C
                C
                C     INITIALIZE B.
                C
                C
0011                  DO 103 I=1,30
0012                103 B(I)=0.
                C
                C
                C                          ******************************
                C     FOR FLUX INSERT: NOTHING.
                C
                C     FOR DENSITY INSERT: GO TO 116.
                C     ------------------------------------------------------------
                C     ------------------------------------------------------------
0013                115 CONTINUE
                C     FIND FLUX PAST POINT X IN STEPS OF AINC IN AU
                C
0014                  DO 100 I=1,30
0015                  AI=I
0016                  X=AI*AINC
                C
                C     CHECK THE FIRST FOUR ELEMENTS OF WNDPRM TO SEE IF THEY HAVE PASSED
                C     THE PLANE OF X.
                C
0017                  DO 106 K=1,4
0018                  IF(WNDPRM(3,K).GE.X) GO TO 107
0019                  GO TO 106
0020                107 B(I)=B(I)+1
0021                106 CONTINUE
                C
                C     NOW CHECK THE REMAINING ELEMENTS OF WNDPRM AND A (THE 'OLD' VALUES
                C     OF WNDPRM) TO SEE IF ANY HAVE PASSED THJUGH THE PLANE OF X.
                C
0022                  DO 101 J=1,156
0023                  IF(A(3,J).LT.X.AND.WNDPRM(3,J+4).GE.X) GO TO 102
0024                  GO TO 101
0025                102 B(I)=B(I)+WNDPRM(4,J+4)
```

```
FORTRAN IV G LEVEL  21                  PARM                    DATE = 70314          10/52/52
0001                  SUBROUTINE PARM
                C
                C
                C
                C     THIS SUBROUTINE, CALLED BY 'SOLWIN', EXTRACTS FROM THE MODEL WIND
                C     PARAMETERS THOSE WHICH ARE OF INTEREST FOR LATER DISPLAY.
                C     PRESENT OPTIONS ARE:
                C
                C                              1. THE FLUX DENSITIES AT X AU.
                C                                 TWO VALUES MAY BE OBTAINED.
                C                                 THEY ARE AT X=AINC*I AU.
                C                                 THE RESULTS ARE STORED AS
                C                                 WIND(2,ICOUNT)=B(I)  AND
                C                                 WIND(3,ICOUNT)=B(I).
                C
                C                              2. THE PARTICLE DENSITIES
                C                                 LOCATED AND STORED AS ABOVE.
                C
                C                              3. THE VELOCITIES AT RADIAL
                C                                 DISTANCES AS SPECIFIED
                C                                 IN STATEMENTS 150 AND 151.
                C
                C
                C
0002                  DIMENSION SUNST(3,325),JDATA(2,300),WNDPRM(6,160),PRMSX(6,60)
0003                  DIMENSION B(30),WIND(5,300)
0004                  DIMENSION A(6,160)
                C
0005                  COMMON SUNST,JDATA,WNDPRM,LAST,PRMSX,KCOUNT,B,WIND,ISTART,ISTOP
0006                  COMMON AINC
                C
0007                  DATA A, ICOUNT/960*0.,0/
                C
                C
                C     LOOK ONLY ONCE EACH DAY - NOT EVERY SIX HOURS
                C
                C
0008                  K=WNDPRM(1,1)
0009                  C=WNDPRM(1,1)-K
0010                  IF(C.NE.0.) GO TO 105
                C
                C
                C     INITIALIZE B.
                C
                C
0011                  DO 103 I=1,30
0012                103 B(I)=0.
                C
                C
                C                             ******************************
                C     FOR FLUX INSERT: NOTHING.
                C
                C     FOR DENSITY INSERT: GO TO 116.
                C     ------------------------------------------------------------
                C     ------------------------------------------------------------
                C                             ******************************
0013                115 CONTINUE
                C     FIND FLUX PAST POINT X IN STEPS OF AINC IN AU
                C
0014                  DO 100 I=1,30
0015                  AI=I
0016                  X=AI*AINC
                C
                C     CHECK THE FIRST FOUR ELEMENTS OF WNDPRM TO SEE IF THEY HAVE PASSED
                C     THE PLANE OF X.
                C
0017                  DO 106 K=1,4
0018                  IF(WNDPRM(3,K).GE.X) GO TO 107
0019                  GO TO 106
0020                107 B(I)=B(I)+1
0021                106 CONTINUE
                C
                C     NOW CHECK THE REMAINING ELEMENTS OF WNDPRM AND A (THE 'OLD' VALUES
                C     OF WNDPRM) TO SEE IF ANY HAVE PASSED THOUGH THE PLANE OF X.
                C
0022                  DO 101 J=1,156
0023                  IF(A(3,J).LT.X.AND.WNDPRM(3,J+4).GE.X) GO TO 102
0024                  GO TO 101
0025                102 B(I)=B(I)+WNDPRM(4,J+4)
```

```
FORTRAN IV G LEVEL  21                  PLOT2                   DATE = 76314          10/52/52
0001                  SUBROUTINE PLOT2
                C
                C
                C     THIS SUBROUTINE IS CALLED BY 'FLUX'. IT PRODUCES A DISPLAY OF
                C     JULIAN DATE VS. SOLAR WIND DENSITY VS. RADIAL DISTACE IN A.U. FROM
                C     THE SUN.
                C
0002                  DIMENSION SUNST(3,325),JDATA(2,300),WNDPRM(6,160),PRMSX(6,60)
0003                  DIMENSION B(30),WIND(5,300)
0004                  DIMENSION IOUT(11),KOUT(90), LOUT(30)
                C
0005                  COMMON SUNST,JDATA,WNDPRM,LAST,PRMSX,KCJUNT,B,WIND,ISTART,ISTOP
0006                  COMMON AINC
                C
0007                  DATA IOUT/' ','1','2','3','4','5','6','7','8','9','0'/
                C
0008                  DO 100 I=1,88,3
0009                  J=(I+2)/3
0010                  IA=(B(J)+.5)/10.
0011                  A=IA
0012                  JA=(B(J)+.5)-10.*A
0013                  KOUT(I)=IOUT(1)
0014                  IF(IA.EQ.0) KOUT(I+1)=IOUT(1)
0015                  IF(IA.EQ.0.AND.JA.EQ.0) KOUT(I+2)=IOUT(1)
0016                  IF(IA.NE.0.AND.JA.EQ.0) KOUT(I+2)=IOUT(11)
0017                  DO 101 K=1,9
0018                  IF(IA.EQ.K) KOUT(I+1)=IOUT(K+1)
0019              101 IF(JA.EQ.K) KOUT(I+2)=IOUT(K+1)
0020              100 CONTINUE
                C
                C     MAP WIND DENSITY.
                C
0021                  WRITE(6,900) WNDPRM(1,1),(KOUT(I),I=1,90)
                C
                C     PUNCH OUT WIND MAP.
                C
0022                  DO 102 I=1,30
0023              102 LOUT(I)=B(I)
0024                  IDATE=WNDPRM(1,1)
0025                  WRITE(7,901) IDATE, (LOUT(I),I=1,30)
                C
0026                  RETURN
                C
0027              900 FORMAT(' ',F6.0,3X,90(A1))
0028              901 FORMAT(I5,3G12)
0029                  END
```

```
FORTRAN IV G LEVEL  21                  OUTPUT              DATE = 79314        16/52/52

0001                  SUBROUTINE OUTPUT
                C
                C
                C     PUNCH OUT 'WIND',
                C
                C
0002                  DIMENSION SUNST(3,325),JDATA(2,300),WNDPRM(6,163),PRMSX(6,60)
0003                  DIMENSION B(30),WIND(5,300)
0004                  DIMENSION IW(2,10)
                C
0005                  COMMON SUNST,JDATA,WNDPRM,LAST,PRMSX,KCOUNT,B,WIND,ISTART,ISTOP
0006                  COMMON AINC
0007                  WRITE(6,902)
                C
0008                  DO 1 N=2,5
0009                  J=0
0010                  K=I
0011                  DO 1 I=1,KCOUNT
0012                  IF(K.EQ.10) J=J+10
0013                  K=I-J
0014                  IW(1,K)=WIND(1,I)
0015                  IW(2,K)=WIND(N,I)
0016                  IF(K.EQ.10) WRITE(7,900)((IW(L,M),L=1,2),M=1,10)
0017                  IF(I.EQ.KCOUNT) WRITE(7,900)((IW(L,M),L=1,2),M=1,K)
0018                1 CONTINUE
                C
                C
0019                  DO 2 I=1,KCOUNT
0020                2 WRITE(6,901) WIND(1,I), WIND(4,I), WIND(5,I)
                C
                C
0021                  RETURN
                C
0022              900 FORMAT(10(I5,I3))
0023              901 FORMAT(' ',3F8.0)
0024              902 FORMAT('1')
                C
0025                  END
```

```
81-JUPZONE -FORT     -SYSPRINT

 FORTRAN IV G LEVEL  21                    MAIN              DATE = 76314          16/02/17

                C
                C
                C       ****************  JUPZONE  ****************
                C
                C
                C       THIS ROUTINE TAKES THE INTERMEDIATE DECK AS INPUT AND PRODUCES
                C       A PUNCHED AND PRINTED OUTPUT.  THE OUTPUT IS THE NUMBER OF ZONES
                C       STORMING AND OBSERVED FOR IO AND NON-IO EACH JULIAN DAY.  UP TO
                C       FOUR DIFFERENT SOURCES MAY BE SPECIFIED BY JZONES.  FOR EACH
                C       VALUE OF INDEX JZONES(1) AND JZONES(2) ARE THE BEGINNING AND
                C       ENDING FIVE DEGREE ZONES OF THE SOUCE CML.  JZONES(3) AND
                C       JZONES(4) ARE THE BEGINNING AND ENDING IO ZONES (ISC).
                C
  0001                  DIMENSION JZONES(4,4), KDATA(5,2000)
  0002                  COMMON INDEX, KDATA, JZONES, IFLUX
                C
  0003                  CALL INPUT
                C
  0004                  DO 899 INDEX=1,4
                C
  0005                  CALL ZONES
  0006                899 CONTINUE
  0007                  STOP
  0008                  END
```

```
FORTRAN IV G LEVEL  21                  INPUT                   DATE = 76314          16/02/17

0001                  SUBROUTINE INPUT
                C
                C
0002                  DIMENSION JZONES(4,4), KDATA(15,2000)
0003                  COMMON INDEX, KDATA, JZONES, IFLUX
                C
                C     READ IN ALL DATA
                C
0004                  READ(5,600)((JZONES(I,J),I=1,4),J=1,4)
0005                  READ(5,602) IMIN,IMAX
                C
                C
0006                  DO 23 J=1,2000
0007                1 READ(8,ERR=21,END=21)(KDATA(I,J),I=1,15),IFLUX
0008                  IF(KDATA(5,J).LT.IMIN) GO TO 1
0009                  IF(KDATA(5,J).GT.IMAX) GO TO 21
000A                  GO TO 23
000B               21 KDATA(1,J)=0
000C                  KDATA(5,J)=0
                C
                C
                C
000D                  DO 10 I=1,500
000E               10 WRITE(6,605) KDATA(5,I),KDATA(12,I),KDATA(13,I),KDATA(14,I),
                     2KDATA(15,I)
000F              605 FORMAT(1X,5I7)
                C
0010                  RETURN
                C
                C     ALL DATA MATRICES ARE NOW LOADED
                C
0011               23 CONTINUE
                C
                C
0012              600 FORMAT(16(1X,I3))
0013              601 FORMAT(1X,I2,1X,3I2,I5,6I2,16X,2I2,12X,2I2,3X,I7)                    S D ZON
0014              602 FORMAT(I5,1X,I5)
0015                  END
```

```
FORTRAN IV G LEVEL  21                    ZONES                DATE = 76314          16/02/17
0001                  SUBROUTINE ZONES
                C
                C
0002                  DIMENSION JZONES(4,9), KDATA(15,2000)
0003                  DIMENSION JSPC(100), NSPC(100), ISPC(100)
0004                  COMMON INDEX, KDATA, JZONES, IFLUX
                C
                C
                C
                C     THIS ROUTINE COUNTS JUPITER ZONES STORMING AND OBSERVED FOR IO AND
                C     NON-IO FOR EACH DAY.  DAYS WHERE NO INTERMEDIATE DECK DATA ARE
                C     AVAIABLE ARE SHOWN AS "NO OBSERVATION" DAYS.  PRINTED AND PUNCHED
                C     OUTPUT ARE PROVIDED.
                C
                C
                C
                C
                C
                C     SOURCE INITIALIZATION SEQUENCE.
                C
0005                  JBSEC1=JZONES(1,INDEX)
0006                  JNSEC1=JZONES(2,INDEX)
0007                  IBZ1=JZONES(3,INDEX)
0008                  INZ1=JZONES(4,INDEX)
0009                  JBSEC2=JBSEC1+72
0010                  JNSEC2=JNSEC1+72
0011                  IBZ2=IBZ1+72
0012                  INZ2=INZ1+72
0013                  NJZS=0
0014                  NJZ=0
0015                  IJZS=0
0016                  IJZ=0
0017                  JUL=0
0018                  JNOB1=0
0019                  ICOUNT=0
0020                  ICARD=1
0021                  IFF=KDATA(1,1)
0022                  ILINES=0
                C
                C
                C     IF THERE ARE NO MORE SOURCES SPECIFIED--EXIT.
                C
0023                  IF(JZONES(1,INDEX).EQ.0.AND.JZONES(2,INDEX).EQ.0) GO TO 999
                C
                C     WRITE FIRST PAGE HEADINGS.
                C
0024                  WRITE(6,605) JBSEC1, JNSEC1, IBZ1, INZ1, IFF
0025                  WRITE(6,603)
                C
                C     PUNCH DATA BLOCK HEADER
                C
0026                  WRITE(7,604)(JZONES(I,INDEX),I=1,4)
                C
                C     END OF SOURCE INITIALIZATION.
                C
                C     BEGIN DAILY COMPUTATIONS.
                C
0027                1 IF=KDATA(1,ICARD)
0028                  IY=KDATA(2,ICARD)
0029                  IM=KDATA(3,ICARD)
0030                  ID=KDATA(4,ICARD)
0031                  JULIAN=KDATA(5,ICARD)
0032                  JBOB=KDATA(6,ICARD)
0033                  JNOB=KDATA(7,ICARD)
0034                  JBAC1=KDATA(8,ICARD)
0035                  JNAC1=KDATA(9,ICARD)
0036                  IBOB=KDATA(10,ICARD)
```

```
FORTRAN IV G LEVEL 21                ZONES                DATE = 76314          16/02/17

0037                  INOB=KDATA(II,ICARD)
0038                  ICARD=ICARD+1
                C
                C
                C     DATA FOR NEXT DAY'S VALUES ARE STORED PENDING OUTPUT OF CURRENT
                C     DAY'S VALUES.
                C
                C
                C     IF THIS IS THE LAST DATA CARD -- RETURN.
                C
                C
0039                  IF(IF.EQ.0.AND.JULIAN.EQ.0) GO TO 409
                C
                C
                C     IF THIS IS THE FIRST DAY FOR THIS SOURCE, THERE IS NOTHING TO
                C     OUTPUT YET -- BEGIN COMPUTATIONS.
                C
                C
0040                  IF(JUL.EQ.0) GO TO 7
                C
                C
                C     IF THIS IS AN ADDITIONAL CARD FOR THE CURRENT DAY -- CONTINUE
                C     COMPUTATION.
                C
                C
0041                  IF(JULIAN.EQ.JUL) GO TO 18
                C
                C
                C     IF CARD OUT OF ORDER, PRINT MESSAGE...
                C
0042                  IF (JULIAN.LT.JUL) GO TO 20
0043                  ICOUNT=ICOUNT+1
0044                  GO TO 19
                C
0045               20 PRINT 903
0046                  PRINT601,IF,IY,IM,ID,JULIAN,JBOB,JNOB,JBAC1,JNAC1,IBOB,INOB
                C
0047               18 IF(JNOB.EQ.JNOB1) GO TO 1
0048                  IF(JBOB.EQ.JNOB1) JBOB=JBOB+1
0049                  GO TO 7
                C
                C
                C     IF FORTY LINES OF OUTPUT PRINTED GO ON TO NEXT PAGE, LABEL AND GO.
                C
                C
0050               19 ILINES=ILINES+1
0051                  IF(ILINES.EQ.41) GO TO 40
0052                  GO TO 22
                C
                C
0053               40 WRITE(6,605)
0054                  WRITE(6,603)
0055                  ILINES=1
                C
                C
                C     PRINT AND PUNCH OUTPUT.......
                C
                C
0056               22 IF(NJZS.GT.0) GO TO 25
0057                  WRITE(6,602) JUL,IJZS,IJZ,NJZS,NJZ
0058                  GO TO 21
                C
                C
0059               25 WRITE(6,602) JUL,IJZS,IJZ,NJZS,NJZ
0060                  WRITE(7,607) JUL,IJZS,IJZ,NJZS,NJZ,IF
                C
                C
                C     IF THERE IS A DAY MISSING FROM THE INTERMEDIATE DECK--SHOW IT AS
                C     A DAY WITH NO OBSERVATIONS.
                C
                C
0061               21 IF(JULIAN.EQ.(JUL+1)) GO TO 23
0062                  JUL=JUL+1
                C
                C
                C     IF FORTY LINES OF OUTPUT PRINTED GO ON TO NEXT PAGE, LABEL AND GO.
                C
                C
```

```
FORTRAN IV G LEVEL  21                    ZONES                DATE = 76314          16/02/17

0063            42 ILINES=ILINES+1
0064               IF(ILINES.EQ.41) GO TO 41
0065               GO TO 43
                C
                C
0066            41 WRITE(6,605)
0067               WRITE(6,603)
0068               ILINES=1
                C
                C
                C     PRINT AND PUNCH MISSING DAY.
                C
                C
0069            43 WRITE(6,606)JUL
0070               WRITE(7,602) JUL, IF
0071               GO TO 21
                C
0072            23 CONTINUE
                C
                C
                C
                C     BEGIN NEXT DAY.
                C
                C
                C
0073               IJZ=0
0074               NJZ=0
0075               IJZS=0
0076               NJZS=0
0077             7 N=1
0078               M=0
0079               IF(JBOB.GT.JNOB) JNOB=JNOB+72
0080               IF(IBOB.GT.INOB) INOB = INOB + 72
0081               IF(JBAC1.GT.JNAC1) JNAC1=JNAC1+72
0082               JBAC2=JBAC1+72
0083               JNAC2=JNAC1+72
0084               JBO=JBOB
0085             3 IF(JBOB.GE.JBSRC1.AND.JBOB.LE.JNSRC1) GO TO 4
0086             5 IF(JBOB.GE.JBSRC2.AND.JBOB.LE.JNSRC2) GO TO 4
0087               JSRC(N)=0
0088               GO TO 6
0089             4 JSRC(N)=JBOB
0090               M=M+1
0091             6 JBOB=JBOB+1
0092               N=N+1
0093               IF(JBOB.LE.JNOB) GO TO 3
0094               JNOB1=JNOB
0095             8 DO 9 J=N,99
0096             9 JSRC(J)=0
                C
                C
                C     IF NO SOURCE ZONES OBSERVED M=0. GO READ ANOTHER DATA CARD
                C
                C
0097               IF(M.EQ.0) GO TO 17
                C
                C
                C     CALCULATE JUP ZONES CORRESPONDING TO IO BOUNDARIES FOR TWO CYCLES
                C
                C
0098               IBO=IBOB
0099               X=2548.8/595.495
0100               JIBZ1=JBO+X*(IBZ1-IBO)
0101               JINZ1=JBO+X*(INZ1-IBO)
0102               JIBZ2=JBO+X*(IBZ2-IBO)
0103               JINZ2=JBO+X*(INZ2-IBO)
                C
                C
                C     GENERATE TWO NEW MATICES,ONE WITH ALL OBSERVED IO RELATED ZONES
                C     THE OTHER WITH NON-IO ZONES
                C
                C
0104               DO 12 J=1,99
0105               IF(JSRC(J).EQ.0) GO TO 11
0106               IF(JSRC(J).GE.JIBZ1.AND.JSRC(J).LE.JINZ1) GO TO 10
0107               IF(JSRC(J).GE.JIBZ2.AND.JSRC(J).LE.JINZ2) GO TO 10
0108            NSRC(J)=JSRC(J)
0109               ISRC(J)=0
```

```
FORTRAN IV G LEVEL  21                  ZONES                   DATE = 76314          16/02/17

0110                    GO TO 12
0111                 10 ISRC(J)=JSRC(J)
0112                    NSRC(J)=0
0113                    GO TO 12
0114                 11 ISRC(J)=0
0115                    NSRC(J)=0
0116                 12 CONTINUE
                C
                C
                C       COUNT STORMING AND NON-STORMING IO AND NON-IO ZONES
                C
                C
0117                    DO 16 J=1,99
0118                    IF(ISRC(J).EQ.0) GO TO 14
0119                    IJZ=IJZ+1
0120                    IF(ISRC(J).GE.JBAC1.AND.ISRC(J).LE.JNAC1) GO TO 13
0121                    IF(ISRC(J).GE.JBAC2.AND.ISRC(J).LE.JNAC2) GO TO 13
0122                    GO TO 14
0123                 13 IJZS=IJZS+1
0124                 14 IF(NSRC(J).EQ.0) GO TO 16
0125                    NJZ=NJZ+1
0126                    IF(NSRC(J).GE.JBAC1.AND.NSRC(J).LE.JNAC1) GO TO 15
0127                    IF(NSRC(J).GE.JBAC2.AND.NSRC(J).LE.JNAC2) GO TO 15
0128                    GO TO 16
0129                 15 NJZS=NJZS+1
0130                 16 CONTINUE
0131                 17 JUL=JULIAN
0132                    GO TO 1
                C
                C
0133               898 CALL EXIT
                C
0134               409 RETURN
                C
                C
0135               601 FORMAT (1X, I2, 1X, 3I2, I5, 6I2)
0136               602 FORMAT ('                ', I5, 3X, 4I10)
0137               603 FORMAT(////,10X,'JULIAN',9X,'IO RELATED ZONES',6X,'NON-IO ZONES',7
                     1X,/,11X,'DATE',9X,'ACTIVE',3X,'TOTAL',4X,'ACTIVE',5X,'TOTAL',//)
0138               604 FORMAT(4(I2,2X))
0139               605 FORMAT('1',////,35X,'JUPZONE',//,10X,'SOURCE LIES FROM ZONE',I3,'
                     1TO',I3,'.',3X,'IO ZONES ARE FROM',I3,' TO',I3,'.',/,10X,'FREQUENCY
                     2',I3,' MHZ.  ZONES ARE FIVE DEGREES OF CML WIDE.')
0140               606 FORMAT(' ',9X,I5,3X,4(9X,'0'))
0141               607 FORMAT('   ',I5,3X,4I10,2X,I2)
0142               608 FORMAT('   ',I5,3X,4(9X,'0'),2X,I2,'    NO DATA FOR THIS DATE.')
0143               609 FORMAT('1',////)
0144               903 FORMAT (//,5X,'DATA CARD OUT OF ORDER FOLLOWS',/)
0145                   END
```

```
FORTRAN IV G LEVEL  21                MAIN              DATE = 76314        16/08/48

                C
                C
                C
                C     >>>>>>>>>>>>>>>>>>>>>>  JUPCOR3  <<<<<<<<<<<<<<<<<<<<<<
                C
                C
                C
                C     THIS ROUTINE CALCULATES AUTOCORRELATION AND POWER SPECTRA OF
                C     JUPITER ACTIVITY AND OBSERVATIONS. IT DOES THE SAME FOR THE SOLAR
                C     WIND MODEL DENSITY.
                C
                C
0001                  DIMENSION AEPOCH(3,300), WIND(2,300), IDATA(5,300), JZONES(4)
0002                  COMMON AEPOCH,IBEG,IEND, WIND, IDATA, JZONES, IFREQ1
                C
                C
0003                  CALL INPUT1
                C
                C
0004                  DO 400 I=1,300
0005                  AEPOCH(1,I)=WIND(1,I)
0006                  AEPOCH(2,I)=WIND(2,I)
0007             400  AEPOCH(3,I)=-1
                C
                C
                C     CALCULATE WIND DENSITY AUTOCORRELATIONS AND SPECTRA.
                C
                C
0008             203  WRITE(6,900)
0009                  CALL COREL
                C
                C
                C     BEGIN CALCULATIONS FOR THE JUPITER DATA.
                C
                C
0010             201  CALL INPUT2
0011             202  DO 401 I=1,300
0012                  AEPOCH(1,I)=IDATA(1,I)
0013                  AEPOCH(2,I)=-1
0014             401  AEPOCH(3,I)=-1
                C
                C
                C     CALCULATE IO ACTIVITY INDICES.
                C
                C
0015                  DO 402 I=1,300
0016                  C=IDATA(1,I)
0017                  A=IDATA(2,I)
0018                  B=IDATA(3,I)
0019                  IF(B.EQ.0)B=-1
0020                  D=A/B
0021                  IF(B.EQ.-1)D=-1
                C
                C
                C     CALCULATE NON-IO ACTIVITY INDICES.
                C
                C
0022                  A=IDATA(4,I)
0023                  B=IDATA(5,I)
0024                  IF(B.EQ.0)B=-1
0025                  E=A/B
0026                  IF(B.EQ.-1)E=-1
                C
                C
                C     LOAD INDICES INTO AEPOCH.
                C
                C
0027                  DO 402 J=1,300
0028                  IF(AEPOCH(1,J).EQ.C) GO TO 403
0029                  GO TO 402
0030             403  AEPOCH(2,J)=D
0031                  AEPOCH(3,J)=E
0032             402  CONTINUE
                C
                C     CALCULATE ACTIVITY AUTOCORRELATIONS AND SPECTRA
                C
0033                  WRITE(6,901)(JZONES(I),I=1,4), IFREQ1
0034                  CALL COREL
```

```
FORTRAN IV G LEVEL  21                    MAIN                    DATE = 76314      .   16/08/48
                C
0035                  DO 200 I=1,300
0036                  DO 200 J=2,3
0037                  L=2*J-1
0038                  A=IDATA(L,I)
0039              200 AEPOCH(J,I)=A
                C
                C
                C     CALCULATE OBSERVATION AUTOCORRELATIONS AND SPECTRA.
                C
0040                  WRITE(6,902)(JZONES(I),I=1,4), IFREQ1
0041                  CALL COREL
                C
0042                  GO TO 201
                C
0043              900 FORMAT('1',///,35X,'JUPCOR3',//,10X,'SOLAR WIND DENSITY AUTOCORREL
                   1ATION AND SPECTRUM.')
0044              901 FORMAT('1',////,35X,'JUPCOR3',//,10X,'SOURCE LIES FROM ZONE',I3,'
                   1TO',I3,'.',3X,'IO ZONES ARE FROM',I3,' TO',I3,'.',/,10X,'FREQUENCY
                   2 IS',I3,'.  ZONES ARE FIVE DEGREES OF CML WIDE.')
0045              902 FORMAT('1',////,35X,'JUPCOR3  -- OBSERVATIONS ONLY',//10X,'SOURCE
                   1LIES FROM ZONE',I3,' TO',I3,'.',3X,'IO ZONES ARE FROM',I3,' TO',I3
                   2,'.',/,10X,'FREQUENCY IS',I3,'.  ZONES ARE FIVE DEGRESS OF CML WI
                   3DE.')
                C
                C
0046                  STOP
0047                  END
```

```
FORTRAN IV G LEVEL  21                    MAIN                    DATE = 75314          16/08/48

0001                  SUBROUTINE INPUT1
                C
                C
                C     THIS ROUTINE READS IN THE SOLAR WIND DATA AND STORES IT IN WIND.
                C
0002
0003                  DIMENSION AEPOCH(3,300), WIND(2,300), IDATA(5,300), JZONES(4)
                C     COMMON AEPOCH,IBEG,IEND, WIND, IDATA, JZONES, IFREQ1
                C
0004                  DO 1 I=1,291,10
0005                  M=I+9
0006                  READ(5,901)((WIND(J,L),J=1,2),L=I,M)
0007                  DO 2 K=I,M
0008                  IF(WIND(1,K).EQ.0) GO TO 3
0009                2 CONTINUE
0010                1 CONTINUE
                C
                C
                C     IF WIND IS OUT OF DATA -- DEFINE IBEG AND IEND.
                C
0011                3 IBEG=WIND(1,1)
0012                  IEND=WIND(1,K-1)
                C
                C
0013                  RETURN
                C
                C
0014              901 FORMAT(10(F5.0,F3.0))
                C
                C
0015                  END
```

```
FORTRAN IV G LEVEL  21                  MAIN                    DATE = 76314          16/08/48

0001                  SUBROUTINE INPUT2
                C
                C
                C     THIS ROUTINE LOADS THE JUPITER DATA BLOCKS.
                C
                C
0002                  DIMENSION AEPOCH(3,300), WIND(2,300), IDATA(5,300), JZONES(4)
0003                  COMMON AEPOCH,IBEG,IEND, WIND, IDATA, JZONES, IFREQ1
                C
                C
                C     LOAD JUPITER DATA BLOCK.
                C
                C
0004                1 READ(5,901) IOPT
0005                2 READ(5,902,END=8)(JZONES(I),I=1,4)
                C
                C
                C     SKIP BLANK OR IOPT CARDS.
                C
                C
0006                  IF(JZONES(2).EQ.0.AND.JZONES(3).EQ.0) GO TO 2
                C
                C
0007                3 I=0
0008                4 I=I+1
0009                  READ(5,903,END=8)(IDATA(J,I),J=1,5),IFREQ
                C
                C
                C     IF IDATA FULL -- RETURN
                C
                C
0010                  IF(I.EQ.300) GO TO 6
                C
                C
                C     IF OUT OF INPUT DATA -- ENTER ZEROES FOR NEXT DAY.
                C
                C
0011                  IF(IDATA(1,I).EQ.0) GO TO 6
                C
                C
0012                  IFREQ1=IFREQ
0013                  GO TO 4
0014                6 DO 7 K=1,5
0015                7 IDATA(I,K)=0
0016                  IBEG=IDATA(1,1)
0017                  IEND=IDATA(1,I-1)
                C
                C
0018                  RETURN
                C
                C
0019                8 CALL EXIT
                C
                C
0020              901 FORMAT(I1)
0021              902 FORMAT(4(I2,2X))
0022              903 FORMAT(2X,I5,3X,4I10,2X,I2)
                C
                C
0023                  END
```

```
FORTRAN IV G LEVEL  21                  MAIN                    DATE = 76314      16/08/48

0001                  SUBROUTINE COREL
                C
                C
                C     THIS ROUTINE CALCULATES THE AUTOCORRELATION COEFFICIENTS.
                C
                C
0002                  DIMENSION AEPOCH(3,300), CORCOF(3,55)
0003                  COMMON AEPOCH,IBEG,IEND
                C
                C
                C     THE MAXIMUM LAG WILL BE 55 DAYS.
                C
                C
0004                  JLIM=0
0005                  ILIM=55
                C
                C
                C     INITIALIZE VALUES.
                C
                C
0006                301 DO 304 I=2,3
0007                  DO 304 K=1,ILIM
0008                  SUM1=0
0009                  SUM2=0
0010                  SQR1=0
0011                  SQR2=0
0012                  CROS=0
0013                  JDIV=0
0014                  JLIM=IEND-IBEG-K+2
                C
                C
                C     CALCULATE THE COEFFICIENTS.
                C
                C
0015                  DO 303 J=1,JLIM
0016                  L=J+K-1
0017                  ALPHA=AEPOCH(I,J)
0018                  BETA=AEPOCH(I,L)
0019                  IF(ALPHA.LT.0.OR.BETA.LT.0) GO TO 303
0020                  JDIV=JDIV+1
0021                  SUM1=SUM1+ALPHA
0022                  SUM2=SUM2+BETA
0023                  SQR1=SQR1+ALPHA**2
0024                  SQR2=SQR2+BETA**2
0025                  CROS=CROS+ALPHA*BETA
                C
                C
0026                303 CONTINUE
                C
                C
                C     AVOID DIVISION BY ZERO.
                C
                C
0027                  IF(JDIV.EQ.0) GO TO 302
                C
                C
0028                  A=CROS-SUM1*SUM2/JDIV
0029                  B=SQRT(SQR1-SUM1**2/JDIV)
0030                  C=SQRT(SQR2-SUM2**2/JDIV)
                C
                C
                C     AVOID DIVISION BY ZERO.
                C
                C
0031                  IF(B.EQ.0.OR.C.EQ.0) GO TO 302
                C
                C
0032                  COEF=A/(B*C)
                C
                C
0033                  GO TO 305
0034                302 COEF=-99
                C
                C
0035                305 CONTINUE
                C
                C
```

```
FORTRAN IV G LEVEL  21                  CORCL                   DATE = 76314        16/38/48
C       LOAD VALUES INTO CORCOF.
C
C
0036            CORCOF(I,K)=K-1
0037          304 CORCOF(I,K)=COEF
C
C
C       BEGIN PLOTTING SEQUENCE.
C
C
0038            L=2
0039            M=3
0040            N=55
0041            IHIST=1
C
0042            CALL PLOT(CORCOF,L,M,ILIM,IHIST)
0043            CALL SPCTRM(CORCOF,L,M,ILIM)
C
0044            L=3
0045            CALL PLOT(CORCOF,L,M,ILIM,IHIST)
0046            CALL SPCTRM(CORCOF,L,M,ILIM)
0047            RETURN
0048            END
```

```
FORTRAN IV G LEVEL  21                MAIN                DATE = 76314          16/05/48

0001                  SUBROUTINE SPCTRM (R,L1,M1,N1)
                C
                C
                C     THIS ROUTINE CALCULATES THE POWER SPECTRUM OF THE FUNCTION WHOSE
                C     AUTOCORRELATION COEFFICIENT IS STORED IN R USING A HANNING WINDOW.
                C
                C
0002                  DIMENSION R(M1,N1)
0003                  DIMENSION G(2,55)
                C
                C
                C     THERE WILL BE 54 INCREMENTS IN FREQUENCY.
                C
                C
0004                  L=2
0005                  M=54
0006                  MA=M+1
                C
                C
                C     INITIALIZE G.
                C
                C
0007                  DO 3 I=1,N1
0008                3 G(2,I)=0
                C
                C
                C     CALCULATE THE SPECTRUM.
                C
                C
0009                  DO 2 K=1,MA
0010                  DO 1 N=2,M
0011                  AM=M
0012                  AN=N-1
0013                  AK=K-1
0014                  B=3.14159*AN/AM
0015                  A=R(L1,N)*(COS(B)+1)*COS(B*AK)
0016                  IF(R(L1,N).EQ.-99.) A=0
0017                1 G(2,K)=G(2,K)+A
                C
                C
                C     WHEN K=1 THE PERIOD IS INFINITE -- FORCE A FINITE OVERFLOW.
                C
                C
0018                  IF(K.EQ.1) GO TO 4
0019                  G(1,K)=108./(AK)
0020                  GO TO 2
0021                4 G(1,K)=100000.
0022                2 G(2,K)=(G(2,K)+R(L1,1))**2
                C
                C
                C     PLOT AS A HISTOGRAM.
                C
                C
0023                  IHIST=1
                C
                C
0024                  CALL PLOT(G,L,L,N1,IHIST)
                C
                C
0025                  RETURN
                C
                C
0026                  END
```

```
FORTRAN IV G LEVEL  21                  MAIN                    DATE = 75314        15/03/48

0001                  SUBROUTINE PLOT (A,L,M,N,IHIST)
                C
                C
0002                  DIMENSION A(M,N),SCALE(11),OUTPUT(101)
0003                  DATA AST,BLNK,BAR/1H*,1H ,1H|/
                C
                C
                C     FIND THE MAXIMUM AND MINIMUM VALUES OF THE DATA IN THE ARRAY
                C
0004               10 AMAX=A(L,1)
0005                  AMIN=0
0006                  DO 1 I=1,N
0007                  IF(A(L,I).GT.AMAX) AMAX=A(L,I)
                C
                C     THE VALUE -99 IS GIVEN TO "NO DATA" POINTS-- THESE ARE IGNORED
                C
0008                  IF(A(L,I).EQ.-99) GO TO 1
0009                  IF(A(L,I).LT.AMIN) AMIN=A(L,I)
0010                1 CONTINUE
                C
                C
                C     SELECT THE PROPER SCALE FOR THE PLOT
                C
0011                  ISCALE=1
0012                  JSCALE=0
0013                  DO 2 I=1,50
0014                  J=-I*I+1
0015                  IF(AMAX.GT.I.AND.AMAX.LE.(I+1)) ISCALE=I+1
0016                  IF(AMIN.LT.J.AND.AMIN.GE.(J-1)) JSCALE=J-1
0017                2 CONTINUE
                C
                C     DECIDE WHICH IS GREATER THE MAXIMUM OR THE ABSOLUTE OF THE MINIMUM
                C     SET THE GREATER EQUAL TO THE SCALE MAXIMUM VALUE...
                C     THEN DECIDE IF THERE ARE NEGATIVE VALES IN THE DATA -- IF SO THE
                C     PLOT WILL GO FROM THE NEGATIVE OF THE MAXIMUM SCALE POINT TO THE
                C     POSITIVE VALUE-- OTHERWISE THE PLOT WILL START AT ZERO
                C
0018                  KSCALE=-1*JSCALE
0019                  IF(ISCALE.LT.KSCALE) ISCALE=KSCALE
0020                  IF(JSCALE.EQ.0) AJ=0
0021                  IF(JSCALE.NE.0) AJ=ISCALE
0022                  DO 3 J=1,11
0023                  I=J-1
0024                  SCALE(J)=I*ISCALE
0025                  SCALE(J)=SCALE(J)/10
0026                3 IF(JSCALE.NE.0) SCALE(J)=SCALE(J)*2-AJ
0027                  WRITE(6,900) (SCALE(J),J=1,11)
                C
                C
                C     PLOT THE POINT
                C
0028                  BMAX=ISCALE
0029                  DO 4 K=1,N
0030                  IF((A(L,K).EQ.0).AND.((A(L,(K-1)).EQ.0).OR.(A(L,(K+1)).EQ.0)))
                     1GO TO 4
0031                  I=(A(L,K)/BMAX)*100+.5
0032                  IF(JSCALE.NE.0) I=((A(L,K)/BMAX)+1)/2*100.+.5
0033                  DO 5 J=1,101
0034                  IF(IHIST.EQ.1) GO TO 8
0035                  GO TO 9
0036                8 IF(I.GE.(J-1)) GO TO 6
0037                  GO TO 7
0038                9 IF(I.EQ.(J-1)) GO TO 6
0039                  GO TO 7
0040                6 OUTPUT(J)=AST
0041                  GO TO 5
0042                7 OUTPUT(J)=BLNK
0043                5 CONTINUE
0044                  IF(JSCALE.NE.0) OUTPUT(51)=BAR
0045                  WRITE(6,901) A(L,K),A(L,K),(OUTPUT(J),J=1,101)
0046                4 CONTINUE
0047                  WRITE(6,902)(SCALE(J),J=1,11)
                C
                C
0048               12 RETURN
                C
                C
```

```
FORTRAN IV G LEVEL  21                  PLOT                    DATE = 75314
0049          900 FORMAT(' ',7X,11(5X,F5.1),/,16X,'1',10('.........I'))
0050          901 FORMAT(1X,F7.3,1X,F5.2,1X,101A1)
0051          902 FORMAT(' ',15X,'1',10('.........I'),/,8X,11(5X,F5.1),/,'1')
              C
              C
0052                END
```

```
FORTRAN IV G LEVEL  21                MAIN                DATE = 76314      16/37/02
C
C
C
C     ******************   JUPSOL V   ****************
C
C
C
C     THIS PROGRAM ACCEPTS AS INPUT DATA THE SOLAR WIND DENSITY, JUPITER
C     IO AND NON-IO OBSERVATION AND ACTIVITY ZONE COUNTS, ALL VERSUS
C     JULIAN DATE.
C
C
C     IT THEN PRODUCES SUPERPOSED EPOCHS FOR SOLAR WIND DENSITY AND
C     THE IO AND NON-IO ACTIVITY INDICES. *** THE NUMBER OF CHANNELS IN
C     THE EPOCH ( IBINS ) MUST BE AN ODD INTEGER. ***
C
C
C     FINALLY, IT CROSS CORRELATES THE WIND AND JUPITER ACTIVITY SUPER-
C     POSED EPOCHS AND PLOTS THE RESULTS.  THE SUPERPOSED EPOCHS ARE
C     THEN SUBJECTED TO THE RANNING SMOOTHING PROCEDURE AND CROSS
C     CORRELATED AND PLOTTED AGAIN.
C
C
C
C
C     >>>>>>>  MAIN  <<<<<<<
C
0001          DIMENSION WIND(2,360), IZONES(4), IDATA(5,1000), AEPOCH(3,31)
0002          DIMENSION BEPOCH(3,63), CORCOF(3,31), IFREQ(4), IEPOCH(5,31)
C
0003          COMMON INDEX, PER,DD, IBINS, WIND, IZONES, IDATA, AEPOCH, BEPOCH
0004          COMMON CORCOF, IOPT, IFREQ, INSMO, ICOUNT, IEPOCH
C
0005          INDEX=1
0006        1 CALL INPUT
0007          CALL EPOCHA
0008          CALL EPOCHB
0009          CALL COREL
0010          CALL OUTPUT
0011          INDEX=INDEX+1
0012          GO TO 1
0013          END
```

```
FORTRAN IV G LEVEL  21                  INPUT                   DATE = 76314      15/37/02
 0001                  SUBROUTINE INPUT
                C
                C
                C
                C     READ INPUT DATA....PERIOD, IBINS, WIND, ZONES AND IDATA
                C
                C     PERIOD, IBINS AND WIND ARE READ IN ONLY ONCE. THAT IS WHEN INDEX=1
                C     PERIOD IS THE PERIOD OF THE SUPERPOSED EPOCH.
                C     IBINS IS THE NUMBER OF BINS (CHANNELS) THE EPOCH IS SORTED OVER.
                C     WIND IS THE SOLAR WIND DENSITY VS. DATE AT JUPITER.
                C     WIND MAY HAVE 300 CONSECUTIVE ENTRIES.
                C     IDATA MAY HAVE 1000 ENTRIES FOR EACH BLOCK OF JUPITER DATA.
                C     IFREQ PERMITS EACH JUPITER BLOCK TO CONTAIN DATA ON UP TO FOUR
                C     FREQUENCIES.
                C
 0002                  CONTINUE
                C
                C           >>>>> DATA DECK STACKING <<<<<
                C
                C     CARD I: PERIOD, IBINS
                C     CARD 2: FIRST CARD OF SOLAR WIND DATA
                C             LAST CARD MUST BE A BLANK CARD
                C     CARD I: IOPT..... EQUALS 1 IF JUPITER DATA IS TO BE PRINTED,
                C                       EQUALS BLANK IF IT IS NOT TO BE PRINTED
                C                       EQUALS 2 IF THIS IS THE END OF THE OVERALL DATA.
                C     CARD J: ZONES..... FOR THE FOLLOWING JUPITER BLOCK.
                C     CARD K: FIRST CARD OF THE JUPITER BLOCK. SHOULD HAVE IFREQ1 ON IT.
                C             LAST CARD OF THE JUPITER BLOCK IS  BLANK.
                C     CARD L: IOPT EQUALS 2 IF THERE ARE NO MORE JUPITER BLOCKS.
                C             EQUALS 1 OR BLANK IF THERE ARE MORE JUPITER BLOCKS. SEE
                C             ABOVE.
                C
                C     AFTER ALL DATA.../*...
                C
                C
                C
 0003                  DIMENSION WIND(2,300), IZONES(4), IDATA(5,1000), AEPOCH(3,31)
 0004                  DIMENSION BEPOCH(3,63), CORCOF(3,31), IFREQ(4)
                C
 0005                  COMMON INDEX, PERIOD, IBINS, WIND, IZONES, IDATA, AEPOCH, BEPOCH
 0006                  COMMON CORCOF, IOPT, IFREQ, INSMO, ICOUNT
                C
                C
                C     FIRST CHECK TO SEE IF PERIOD, IBINS AND WIND ARE ALREADY IN CORE.
                C     IF SO, SKIP DOWN TO 4 AND READ ZONES AND IDATA.
                C
 0007                  IF(INDEX.GT.1) GO TO 4
                C
 0008                  READ(5,900) PERIOD, IBINS
                C
                C     READ IN SOLAR WIND DATES AND DENSITIES.
                C
 0009                  DO 1 I=1,291,10
 0010                  M=I+9
 0011                  READ(5,901) ((WIND(J,L),J=1,2),L=I,M)
 0012                  IF(WIND(1,1).EQ.0.) GO TO 2
 0013                1 CONTINUE
 0014                  GO TO 3
                C
                C     IF WIND IS OUT OF DATA, FILL THE REMAINING SPACES WITH ZEROS.
                C
 0015                2 DO 3 I=M,300
 0016                  DO 3 J=1,2
 0017                  WIND(J,I)=0
 0018                3 CONTINUE
                C
                C     IF IOPT = 1,IDATA WILL NOT BE PRINTED
                C     READ IOPT, IZONES AND IDATA (JUPITER DATA).
                C
 0019                4 READ(5,904) IOPT
```

```
FORTRAN IV G LEVEL  21                    INPUT                    DATE = 76314          16/37/02
C
C       IF OUT OF DATA, PROGRAM EXECUTION IS COMPLETE. SO, CALL EXIT.
C
0020          IF(IOPT.EQ.2) CALL EXIT
0021          READ(5,902) (IZONES(I),I=1,4)
C
C       INITIALIZE IFREQ, AND IA.
C
0022          DO 9 I=1,4
0023        9 IFREQ(I)=0
0024          IA=1
C
C       READ JUPITER DATA.
C
0025          I=0
0026        5 I=I+1
0027          ICOUNT=I
C
0028      800 READ(5,903) ((IDATA(J,I),J=1,5),IFREQI
C
C       IF IDATA IS FULL, RETURN.
C
0029          IF(I.EQ.1000) GO TO 7
C
C       IF OUT OF INPUT DATA, FILL REMAINING SPACES IN IDATA WITH ZEROS.
C
0030          IF((IDATA(1,I).EQ.0) GO TO 6
C
C             .
C       IF IFREQI IS NON-ZERO AND DIFFERENT FROM THE PREVIOUS ENTRY GO TO
C       AND MAKE AN ENTRY TO IFREQ.
C
0031          IF(I.EQ.1) IFREQ(IA)=IFREQI
0032          IF(IFREQI.NE.IFREQ(IA).AND.IFREQI.NE.)) GO TO 8
0033          GO TO 5
0034        8 IA=IA+1
0035          IFREQ(IA)=IFREQI
0036          GO TO 5
C
0037        6 ICOUNT=I-1
0038          DO 7 J=I,1000
0039          DO 7 K=1,5
0040          IDATA(K,J)=0
0041        7 CONTINUE
C
0042          RETURN
C
0043      900 FORMAT(F4.2,I2)
0044      901 FORMAT(10(E5.0,,3.0))
0045      902 FORMAT(4(I2,2X))
0046      903 FORMAT(2X,I5,5X,4(7X,I3),2X,I2)
0047      904 FORMAT (I1)
C
0048          END
```

```
FORTRAN IV G LEVEL 21                    EPOCHA                    DATE = 76314          15/37/02
0001                  SUBROUTINE EPOCHA
                C
                C
                C     THIS SUBROUTINE TAKES THE JUPITER ZONE COUNT AND, FIRST, GENERATES
                C     THE SUPERPOSED EPOCH WITH 'IBINS' CHANNELS WITH AN EPOCH PERIOD
                C     OF 'PERIOD' USING THE SEPARATE ACTIVITY COUNTS AND OBSERVATION
                C     COUNTS FOR IO AND NON-IO. THIS IS STORED IN THE ARRAY 'IEPOCH'.
                C
                C     SECONDLY, IT CALCULATES THE ACTIVITY INDEX FOR EACH DAY (CHANNEL)
                C     OF THE EPOCH AND STORES THIS INFORMATION IN THE ARRAY 'AEPOCH'.
                C
                C     IF THERE IS NO OBSERVATION FOR ANY DAY (CHANNEL) IN THE EPOCH
                C     THE VALUE '-99' IS STORED IN THAT LOCATION IN AEPOCH AS A FLAG.
                C
                C
0002                  DIMENSION WIND(2,300), IZONES(4), IDATA(5,1000), AEPOCH(3,31)
0003                  DIMENSION BEPOCH(3,63), CORCOF(3,31), IFREQ(4), IEPOCH(3,31)
                C
0004                  COMMON INDEX, PERIOD, IBINS, WIND, IZONES, IDATA, AEPOCH, BEPOCH
0005                  COMMON CORCOF, IOPT, IFREQ, INSMO, ICOUNT, IEPOCH
                C
                C
                C     INITIALIZE THE INTERMEDIATE ARRAY 'IEPOCH'. LOAD EPOCH DAY
                C     (CHANNEL #) INTO THE FIRST ROW AND ZEROES INTO THE SECOND AND
                C     THIRD ROWS.
                C
0006                  DO 400 J=1,31
0007                  IEPOCH(1,J)=J
0008                  DO 400 I=2,5
0009              400 IEPOCH(I,J)=0
                C
                C     COMPUTE THE EPOCH DAY (CHANNEL) EACH REAL DAY CORRESPONDS TO.
                C
0010              401 DO 403 I=1,ICOUNT
0011                  JULIAN= IDATA(1,I)
0012                  DAY=JULIAN/PERIOD
0013                  IDAY=DAY
0014                  DAY=DAY-IDAY
0015                  DAY=DAY*IBINS
0016                  IDAY=DAY+1
                C
                C     SUM THE ACTIVITY AND OBSERVATION ZONES FOR IO AND NON-IO FOR EACH
                C     EPOCH DAY (CHANNEL).
                C
0017                  DO 403 J=2,5
0018              403 IEPOCH(J,IDAY)=IEPOCH(J,IDAY)+IDATA(J,I)
0019              402 DO 404 I=1,IBINS
0020                  AEPOCH(1,I)=IEPOCH(1,I)
0021                  DO 404 J=2,4,2
0022                  L=2+(J-2)/2
0023                  K=J+1
                C
                C     IF IEPOCH CONTAINS NO ENTRY FOR A GIVEN DAY SET ITS VALUE TO '-99'
                C
0024                  IF(IEPOCH(K,I).EQ.0) GO TO 411
0025                  GO TO 412
0026              411 IEPOCH(K,I)=1
0027                  IEPOCH(J,I)=-99
                C
                C     COMPUTE THE IO AND NON-IO ACTIVITY INDICES FOR EACH EPOCH DAY
                C     AND STORE THEM IN THE ARRAY 'AEPOCH' (SECOND AND THIRD ROWS).
                C
0028              412 A=IEPOCH(J,I)
0029                  BB=IEPOCH(K,I)
0030              404 AEPOCH(L,I)=A/BB
                C
                C     IF THE ABOVE IS '404 AEPOCH(L,I)=A/BB' THE ACTIVITY INDICES ARE
                C     BEING COMPUTED. IF IT IS '404 AEPOCH(L,I)=BB' THE OBSERVATION
                C     ZONES ARE BEING TALLYED.
                C
                C
                C     FILL ALL UNUSED SPACES IN AEPOCH WITH ZEROES.
                C
0031                  JBINS=IBINS+1
0032                  DO 410 J=JBINS,31
0033                  DO 410 I=1,3
0034              410 AEPOCH(I,J)=0
                C
```

```
FORTRAN IV G LEVEL  21                  EPOCHA              DATE = 76314.        16/37/02
                C       AEPOCH NOW CONTAINS : THE EPOCH DAY, IO ACTIVITY INDICES, NJN-IO
                C       ACTIVITY INDICES.
                C
0035                    RETURN
0036                    END
```

```
FORTRAN IV G LEVEL  21                EPOCHB              DATE = 76314          16/37/02
0001                  SUBROUTINE EPOCHS
                C
                C
                C     THIS SUBROUTINE TAKES THE SOLAR WIND DENSITIES AND GENERATES A
                C     SUPERPOSED EPOCH WITH 'IBINS' CHANNELS AND AN EPOCH PERIOD
                C     OF 'PERIOD'. ***** NOTE: THE NUMBER OF DAYS IN THE EPOCH (CHANNELS
                C     ). THAT IS, 'IBINS', MUST BE AN ODD POSITIVE INTEGER. 'PERIOD',
                C     HOWEVER MAY BE ANY POSITIVE NUMBER.*****
                C     THE DENSITY FOR EACH DAY (CHANNEL) IS NORMALIZED BY THE TOTAL
                C     NUMBER OF ACTUAL DAYS CONTRIBUTING TO EACH EPOCH DAY (CHANNEL).
                C
                C     THIS INFORMATION IS STORED, IN TWO CYCLES, IN THE ARRAY 'BEPOCH'.
                C
                C
0002                  DIMENSION WIND(2,3000), IZONES(4), IDATA(3,1000), AEPOCH(3,31)
0003                  DIMENSION BEPOCH(3,63), CORCOF(3,31), IFREQ(4)
                C
0004                  COMMON INDEX, PERIOD, IBINS, WIND, IZONES, IDATA, AEPOCH, BEPOCH
0005                  COMMON CORCOF, IOPT, IFREQ, INSMO, ICOUNT
                C
                C     BEPOCH IS FIRST USED TO STORE THE EPOCH DAY (CHANNEL #), THE SUM
                C     OF THE FLUX DENSITIES FOR THAT DAY AND THE NUMBER OF REAL DAYS
                C     FOLDED ONTO THAT CHANNEL. THUS IT IS A THREE ROW ARRAY.
                C
                C     INITIALIZE BEPOCH BY LOADING THE EPOCH DAY INTO ROW ONE AND ZEROES
                C     INTO ROWS TWO AND THREE.
                C
0006                708 N=300
0007                    JBINS=2*IBINS
0008                    DO 700 J=1,63
0009                    BEPOCH(1,J)=0
0010                    BEPOCH(2,J)=0
0011                    BEPOCH(3,J)=0
0012                    IF(J.LE.IBINS) GO TO 704
0013                    K=J-IBINS
0014                    IF(J.GT.JBINS) K=0
0015                    GO TO 700
0016                704 K=J
0017                700 BEPOCH(1,J)=K
                C
                C     COMPUTE THE EPOCH DAY (CHANNEL) EACH REAL DAY CORRESPONDS TO.
                C
0018                701 DO 703 I=1,N
                C
                C     IF 'WIND' OUT OF DATA GO TO 703.
                C
0019                    IF(WIND(1,I).EQ.0) GO TO 703
                C
                C     CALCULATE THE EPOCH DAY FOR THE FIRST CYCLE(IDAY) AND FOR THE
                C     SECOND CYCLE (JDAY).
                C
0020                    JULIAN=WIND(1,I)
0021                    DAY=JULIAN/PERIOD
0022                    IDAY=DAY
0023                    DAY=DAY-IDAY
0024                    DAY=DAY*IBINS
0025                    IDAY=DAY+1
0026                    JDAY=.DAY+IBINS
                C
                C     COUNT THE NUMBER OF REAL DAYS FOLDED ON EACH EPOCH DAY OF BOTH
                C     CYCLES.
                C
0027                    BEPOCH(3,JDAY)=BEPOCH(3,JDAY)+1
0028                    BEPOCH(3,IDAY)=BEPOCH(3,JDAY)
                C
                C     SUM THE FLUX IN EACH EPOCH DAY FOR BOTH CYCLES.
                C
0029                    BEPOCH(2,JDAY)=BEPOCH(2,JDAY)+WIND(2,I)
0030                702 BEPOCH(2,IDAY)=BEPOCH(2,IDAY)+WIND(2,I)
0031                703 CONTINUE
                C
                C     IF NO ENTRY HAS BEEN MADE FOR A GIVEN EPOCH DAY SET BEPOCH(3,I)
                C     TO 1 TO AVOID DIVISION BY ZERO.
                C
0032                    DO 709 I=1,JBINS
                C
                C     NORMALIZE THE FLUX BY THE NUMBER OF REAL DAYS IN EACH CHANNEL AND
                C     STORE THESE VALUES IN BEPOCH(2,I).
```

```
FORTRAN IV G LEVEL  21                    EPOCH            DATE = 75314          16/37/02
              C
0033                IF(BEPOCH(3,I).EQ.0) BEPOCH(3,I)=1
0034          709   BEPOCH(2,I)=BEPOCH(2,I)/BEPOCH(3,I)
              C
              C     BEPOCH(I,J) NOW CONTAINS SUPERPOSED DATES AND SOLAR WIND FLUXS
              C
0035                RETURN
0036                END
```

```
FORTRAN IV G LEVEL  21                    COREL                DATE = 76314          16/37/02
0001                  SUBROUTINE COREL
                C
                C
                C     THIS CALCULATES THE CORRELATION COEF BETWEEN AEPOCH AND BEOPCH.
                C
0002                  DIMENSION WIND(2,300), IZONES(4), IDATA(5,1000), AEPOCH(3,31)
0003                  DIMENSION BEPOCH(3,63), CORCOF(3,31), IFREQ(4)
                C
0004                  COMMON INDEX, PERIOD, IBINS, WIND, IZONES, IDATA, AEPOCH, BEPOCH
0005                  COMMON CORCOF, IOPT, IFREQ, INSMO, ICOUNT
                C
0006                300 JLIM=IBINS
0007                  ILIM=JLIM
0008                301 DO 304 I=2,3
0009                  DO 304 K=1,ILIM
                C
                C     INITIALIZE THE VARIOUS SUMMATIONS TO ZERO.
                C
0010                  SUM1=0
0011                  SUM2=0
0012                  SQR1=0
0013                  SQR2=0
0014                  CROS=0
0015                  JDIV=0
                C
                C     CALCULATE THE VARIOUS SUMMATIONS FOR A SHIFT OF (K-1) DAYS.
                C
0016                  DO 303 J=1,JLIM
0017                  L=J+K-1
0018                  ALPHA=AEPOCH(I,J)
0019                  BETA=BEPOCH(2,L)
                C
                C     IF EITHER AEPOCH OR BEPOCH HAS NO DATA ENTRY FOR A GIVEN ELEMENT
                C     DO NOT INCLUDE THIS PAIR IN THE CALCULATION OF THE COEFFICIENT.
                C
0020                  IF(ALPHA.LT.0.OR.BETA.LT.0) GO TO 303
0021                  JDIV=JDIV+1
0022                  SUM1=SUM1+ALPHA
0023                  SUM2=SUM2+BETA
0024                  SQR1=SQR1+ALPHA**2
0025                  SQR2=SQR2+BETA**2
0026                  CROS=CROS+ALPHA*BETA
0027                303 CONTINUE
                C
                C     AVOID DIVISION BY ZERO.
                C
0028                  IF(JDIV.EQ.0) GO TO 302
                C
                C     CALCULATE THE VALUE OF THE CORRELATION COEFFIENT.
                C
0029                  A=CROS-SUM1*SUM2/JDIV
0030                  D=SQRT(SQR1-SUM1**2/JDIV)
0031                  C=SQRT(SQR2-SUM2**2/JDIV)
                C
                C     AVOID DIVISION BY ZERO.
                C
0032                  IF(D.EQ.0.OR.C.EQ.0) GO TO 302
0033                  COEF=A/(D*C)
0034                  GO TO 309
0035                302 COEF=-99
                C
                C
                C     EVENTS WHICH OCCUR WITH A HIGHER DAY NUMBER IN THE WIND EPOCH THAN
                C     IN THE JUPITER EPOCH OCCUR BEFORE ENCOUNTER AND ARE REGARDED AS
                C     HAVING NEGATIVE SHIFTS IN THE CROSS CORRELATION. CONVERSELY, EVENTS
                C     WHICH OCCUR WITH HIGHER JUPITER DAY NUMBERS HAPPEN AFTER ENCOUNTER
                C     AND ARE REGARDED TO HAVE POSITIVE SHIFTS.
                C
                C
                C
                C     ARRANGE THE DATA IN THE ARRAY CORCOF SO THAT THE ZERO SHIFT
                C     VALUE IS IN THE CENTER OF THE ARRAY, WITH THE MAXIMUN NEGATIVE
                C     SHIFT AT THE BEGINNING GOING DOWN TO ZERO AT THE CENTER AND UP TO
                C     MAXIMUM POSITIVTE SHIFT AT THE END.
                C
0036                309 A=ILEM
                C
```

```
FORTRAN IV G LEVEL  21                  COREL                DATE = 75314          16/37/32
                C       THE VARIABLE 'IA' IS THE VALUE OF THE INDEX OF THE CENTER OF THE
                C       ARRAY CORCOF.
                C
0037                    IA=A/2.+.5
                C
                C       THE VARIALBE 'IB' HAS THE VALUE OF THE SHIFT ABOUT THE CENTER OF
                C       THE ARRAY CORCOF.
                C
0038                    KA=-(K-1)
0039                    IB=IA+KA
0040                    IF(K.GT.IA) GO TO 305
0041                    GO TO 306
0042              305   KA=ILIM+KA
0043                    IB=ILIM+IB
0044              306   CONTINUE
0045                    CORCOF(1,IB)=KA
0046              304   CORCOF(1,IB)=COEF
                C
                C       FILL UNUSED SPACES IN CORCOF WITH ZEROES.
                C
0047                    ILIM=ILIM+1
0048                    DO 307 I=ILIM,31
0049                    DO 307 J=1,3
0050              307   CORCOF(J,I)=0
                C
                C       CORCOF NOW CONTAINS: THE SHIFT AND THE CORRELATION COEFFICIENT.
                C
0051                    RETURN
                C
0052                    END
```

```
FORTRAN IV G LEVEL  21                  PLOT                    DATE = 76314      16/37/02
0001                  SUBROUTINE PLOT (A,L,M,N,IHIST)
                C
                C
                C
                C
0002                  DIMENSION WIND(2,360), IZONES(4), IDATA(5,1000), AEPOCH(3,31)
0003                  DIMENSION BEPOCH(3,63), CORCOF(3,31), IFREQ(4)
0004                  DIMENSION A(M,N), SCALE(11), OUTPUT(101)
                C
0005                  COMMON INDEX, PERIOD, NBINS, WIND, IZONES, IDATA, AEPOCH, BEPOCH
0006                  COMMON CORCOF, IOPT, IFREQ, INSMO
                C
0007                  DATA AST,BLNK,BAR/1H*,1H ,1H|/
                C
                C
                C     FIND THE MAXIMUM AND MINIMUM VALUES OF THE DATA IN THE ARRAY
                C
0008                  ICOUNT=0
0009               10 AMAX=A(L,1)
0010                  AMIN=0
0011                  DO 1 I=1,N
0012                  IF(A(L,I).GT.AMAX) AMAX=A(L,I)
                C
                C     THE VALUE -99 WAS GIVEN TO "NO DATA" POINTS-- THESE ARE IGNORED
                C
0013                  IF(A(L,I).EQ.-99) GO TO 1
0014                  IF(A(L,I).LT.AMIN) AMIN=A(L,I)
0015                1 CONTINUE
                C
                C
                C     SELECT THE PROPER SCALE FOR THE PLOT
                C
0016                  ISCALE=1
0017                  JSCALE=0
0018                  IF(AMAX.GT.100.OR.AMIN.LT.-99) GO TO 13
0019                  LA=1
0020                  MA=100
0021                  NA=1
0022                  GO TO 14
0023               13 LA=100
0024                  MA=1000
0025                  NA=100
0026               14 DO 2 I=LA,MA,NA
0027                  J=-1*I+1
0028                  IF(AMAX.GT.I.AND.AMAX.LE.(I+NA)) ISCALE=I+NA
0029                  IF(AMIN.LT.J.AND.AMIN.GE.(J-NA)) JSCALE=J-NA
0030                2 CONTINUE
                C
                C     DECIDE WHICH IS GREATER THE MAXIMUM OR THE ABSOLUTE OF THE MINIMUM
                C     SET THE GREATER EQUAL TO THE SCALE MAXIMUM VALUE...
                C     THEN DECIDE IF THERE ARE NEGATIVE VALUES IN THE DATA -- IF SO THE
                C     PLOT WILL GO FROM THE NEGATIVE OF THE MAXIMUM SCALE POINT TO THE
                C     POSITIVE VALUE-- OTHERWISE THE PLOT WILL START AT ZERO
                C
0031                  KSCALE=-1*JSCALE
0032                  IF(ISCALE.LT.KSCALE) ISCALE=KSCALE
0033                  IF(JSCALE.EQ.0) AJ=0
0034                  IF(JSCALE.NE.0) AJ=ISCALE
0035                  DO 3 J=1,11
0036                  I=J-1
0037                  SCALE(J)=I*ISCALE
                C
                C     SET SCALE VALUES FOR ALL POSITIVE DATA
                C
0038                  SCALE(J)=SCALE(J)/10
                C
                C     SET SCALE VALUES FOR POSITIVE AND NEGATIVE DATA
                C
0039                3 IF(JSCALE.NE.0) SCALE(J)=SCALE(J)*2-AJ
0040                  WRITE(6,900) (SCALE(J),J=1,11)
                C
                C
                C     PLOT THE POINT
                C
0041                  BMAX=ISCALE
0042                  DO 4 K=1,N
                C
                C     IF OUT OF DATA GO TO 4
```

```
FORTRAN IV G LEVEL  21                  PLOT                    DATE = 76314      15/37/02
                      C
0043                        IF((A(I,K).EQ.0).AND.((A(I,(K-1)).EQ.0).OR.(A(I,(K+1)).EQ.0)))
                           1GO TO 4
                      C
                      C     SCALE THE DATA FROM 0 TO 100 IF ALL POSITIVE
                      C
0044                        I=(A(L,K)/BMAX)*100+.5
                      C
                      C     SCALE THE DATA FROM -50 TO +50 IF POSITIVE AND NEGATIVE
                      C
0045                        IF(JSCALE.NE.0) I=((A(L,K)/BMAX)+1)/2*100.+.5
                      C
                      C     THE ARRAY 'OUTPUT' WILL BE FILLED WITH ASTERIXES, BLANKS, OR, BARS
                      C     AND REPRESENTS ONE LINE OF PRINT FOR THE PLOT.
                      C
0046                        DO 5 J=1,101
                      C
                      C     IF A HISTOGRAM DISPLAY IS DESIRED, 'IHIST' = 1.
                      C
0047                        IF(IHIST.EQ.1) GO TO 8
0048                        GO TO 9
0049                      8 IF(I.GE.(J-1)) GO TO 6
0050                        GO TO 7
0051                      9 IF(I.EQ.(J-1)) GO TO 6
0052                        GO TO 7
0053                      6 OUTPUT(J)=AST
0054                        GO TO 5
0055                      7 OUTPUT(J)=BLNK
0056                      5 CONTINUE
                      C       :
                      C     IF THE PLOT IS TO HAVE A ZERO CENTER, THE CENTER ELEMENT OF OUTPUT
                      C     WILL BE A BAR. *** NOTE: THE CENTER BAR WILL OVERRIDE AN ASTERIX
                      C     IF THE CORRESPONDING DATA VALUE IS ZERO. ***
                      C
0057                        IF(JSCALE.NE.0) OUTPUT(51)=BAR
                      C
                      C     PRINT THE LINE OF ASTERIXES, BARS AND BLANKS.
                      C
0058                        WRITE(6,901) A(L,K),A(1,K),(OUTPUT(J),J=1,101)
0059                      4 CONTINUE
                      C
                      C     PRINT THE CLOSING SCALES AND HEADINGS.
                      C
0060                        WRITE(6,902)(SCALE(J),J=1,11)
0061                        ICOUNT=ICOUNT+1
                      C
                      C     IF SMOOTHING IS TO BE INHIBITED, 'INSMO' = 1.
                      C
0062                        IF(INSMO.EQ.1) GO TO 11
                      C
                      C     IF THIS IS THE FIRST TIME THIS TABLE HAS BEEN PLOTTED, THEN SMOOTH
                      C
0063                        IF(ICOUNT.EQ.1) CALL SMOOTH(A,L,M,N,ICOUNT)
                      C
                      C     IF THE SMOOTHING HAS OCCURED GO BACK AND PRINT OUT THE PLOT.
                      C
0064                        IF(ICOUNT.EQ.1) GO TO 10
                      C
                      C     IF RETURNING AFTER SMOOTHING, ADVANCE PAGE ON PRINTER.
                      C
0065                     12 WRITE(6,903)
0066                     11 RETURN
0067                    900 FORMAT(1X,7X,11(5X,F5.1),/,16X,'I',10('.........I'))
0068                    901 FORMAT(1X,F7.3,3X,F4.0,1X,101A1)
0069                    902 FORMAT(16X,'I',10('.........I'),/,8X,11(5X,F5.1))
0070                    903 FORMAT('1')
0071                        END
```

```
FORTRAN IV G LEVEL  21                  SMOOTH              DATE = 76314        10/37/02
0001                  SUBROUTINE SMOOTH (A,L,M,N,ICOUNT)
                C
                C
                C     THIS SUBROUTINE IS CALLED BY 'PLOT'. IT PERFORMS A HANNING SMOOTH-
                C     ING ON WHATEVER ARRAY 'PLOT' HAS JUST PLOTTED ON THE PRINTER.
                C
                C
0002                  DIMENSION A(M,N)
                C
0003                  JBINS=N
0004                  DO 10 I=1,N
0005               10 IF(A(1,I).GT.0.AND.A(1,(I+1)).EQ.0) JBINS=I
0006                  AS=A(L,JBINS)
0007                  BS=A(L,1)
0008                  DO 11 I=1,JBINS
0009                  J=I+1
0010                  IF(I.EQ.JBINS) J=1
0011                  CS=A(L,J)
0012                  AD=2
0013                  BD=2
0014                  CD=2
0015                  BDD=0
0016                  IF(AS.LT.0) AD=1
0017                  IF(CS.LT.0) CD=1
0018                  IF((AD+CD).EQ.2) BDD=-1
0019                  D=(AD*CD)
0020                  IF(BS.LT.0) D=D/2
0021                  IF(BS.LT.0) BD=1
0022                  A(L,I)=(BD-1)*BS/(2+BDD)+(AD-1)*AS+(CD-1)*CS)/D
0023                  IF((BD+BDD).EQ.0) A(L,I)=-1
0024                  AS=BS
0025               11 BS=CS
                C
                C     IF TWO PLOTS THIS SIZE WONT FIT ON ONE PAGE, ADVANCE TO NEXT PAGE.
                C
0026                  IF(N.LT.41) GO TO 14
0027                  WRITE(6,901)
0028                  GO TO 12
0029               14 WRITE(6,902)
0030               12 RETURN
                C
0031              901 FORMAT('1',' THREE DAY WEIGHTED SMOOTHING')
0032              902 FORMAT('0',//,' THREE DAY WEIGHTED SMOOTHING')
                C
0033                  END
```

```
FORTRAN IV G LEVEL  21                  OUTPUT                  DATE = 76314          16/37/02
0001                  SUBROUTINE OUTPUT
                C
                C
                C     OUTPUT ROUTINES FOLLOW
                C
                C
0002                  DIMENSION WIND(2,300), IZONES(4), IDATA(5,1000), AEPOCH(3,31)
0003                  DIMENSION BEPOCH(3,63), CORCOF(3,31), IFREQ(4), IEPOCH(5,31)
                C
0004                  COMMON INDEX, PERIOD, IBINS, WINO, IZONES, IDATA, AEPOCH, BEPOCH
0005                  COMMON CORCOF, IOPT, IFREQ, INSMO, ICOUNT, IEPOCH
                C
                C
                C     PRINT ZONE AND FREQUENCY HEADINGS.
                C
0006                  WRITE(6,605) (IZONES(I),I=1,4), (IFREQ(J),J=1,4)
                C
                C     INITIALIZE IPLOT AND INSMO.
                C
0007                  IPLOT=0
0008                  INSMO=0
                C
                C     IF 'IOPT'=1, PRINT OUT THE JUPITER DATA
                C
0009                  IF(IOPT.NE.1) GO TO 803
                C
0010                800 WRITE(6,603)
0011                    DO 801 J=1,ICOUNT
0012                    IF(IDATA(1,J).EQ.0) GO TO 801
0013                    WRITE(6,602)(IDATA(I,J),I=1,5)
0014                801 CONTINUE
0015                    WRITE(6,901)
0016                    DO 806 I=1,31
0017                    IF(I.GT.IBINS) GO TO 809
0018                806 WRITE(6,602) (IEPOCH(J,I),J=1,5)
0019                809 CONTINUE
                C
                C     IN THE FOLLOWING SEQUENCE 'PLOT' IS CALLED TO PLOT AEPOCH, BEPOCH
                C     AND CORCOF, THEN 'PLOT' CALLS 'SMOOTH' WHICH PERFORMS AN HANNING
                C     SMOOTHING ON AEPOCH AND BEPOCH. THE ORIGINAL VALUES ARE REPLACED
                C     IN THE ARRAYS BY THE NEW VALUES. 'PLOT' THEN PLOTS THE SMOOTHED
                C     AEPOCH AND BEPOCH. FINALLY 'CUREL' IS CALLED AGAIN TO CORRELATE
                C     THE NEW AEPOCH AND BEPOCH. THEN CORCOF IS PLOTTED FOR THE SMOOTHED
                C     DATA.
                C
0020                    WRITE(6,905)
0021                    GO TO 802
                C
                C     IF THE JUPITER DATA IS NOT PRINTED OUT THEN BEGIN THE PLOTS ON
                C     THE SAME PAGE.
                C
0022                803 WRITE(6,904)
0023                802 L=2
0024                    M=3
0025                    N=31
0026                    IHIST=1
0027                    CALL PLOT(AEPOCH,L,M,N,IHIST)
0028                    WRITE(6,907)
0029                    L=3
0030                    CALL PLOT(AEPOCH,L,M,N,IHIST)
0031                805 WRITE(6,909)
0032                    L=2
0033                    M=3
0034                    N=63
0035                    IHIST=1
0036                    CALL PLOT(BEPOCH,L,M,N,IHIST)
0037                807 WRITE(6,911)
0038                    INSMO=1
0039                    L=2
0040                    M=3
0041                    IHIST=0
0042                    CALL PLOT(CORCOF,L,M,IBINS,IHIST)
0043                    WRITE(6,913)
0044                    L=3
0045                    CALL PLOT(CORCOF,L,M,IBINS,IHIST)
0046                    IPLOT=IPLOT+1
                C
                C     IPLOT = 1 SAYS THAT THIS IS THE FIRST TIME THE PROGRAM POINTER
```

```
FORTRAN IV G LEVEL  21                      OUTPUT                  DATE = 76314          16/37/02
C       HAS PASSED THROUGH 'OUTPUT' FOR THIS JUPITER DATA. SO CORRELATE
C       THE MANNING SMOOTHED DATA.
C
0047          IF(IPLOT.NE.1) GO TO 804
0048          CALL COREL
0049          WRITE(6,910)
0050          GO TO 807
0051      804 RETURN
0052      602 FORMAT (' ', I5, 3X, 4I10)
0053      603 FORMAT('////,2X,'JULIAN',8X,'IO RELATED ZONES',6X,'NON IO ZONES',7X
            1,/,3X,'DATE',9X,'ACTIVE',5X,'TOTAL',4X,'ACTIVE',5X,'TOTAL',//)
0054      605 FORMAT('1',27X,'JUPSOL V',///,2X,'SOURCE LIES FROM ZONE',I3,' TO',
            113,'.',3X,'IO ZONES ARE FROM',I3,' TO',I3,'.',/,2X,'FREQUENCY(MHZ)
            2',4(I3,'. '))
0055      901 FORMAT(' ',//,16X,'EPOCH DAY TOTALS')
0056      904 FORMAT('0',1X,'IO RELATED JUPITER ACTIVITY INDICES - SUPERPOSED')
0057      905 FORMAT('1',1X,'IO RELATED JUPITER ACTIVITY INDICES - SUPERPOSED')
0058      907 FORMAT(' ',1X,'NON-IO JUPITER ACTIVITY INDICES - SUPERPOSED')
0059      909 FORMAT('0',1X,'SOLAR WIND FLUX AT JUPITER - SUPERPOSED')
0060      910 FORMAT('1','THREE DAY WEIGHTED SMOOTHING')
0061      911 FORMAT('0',1X,"IO JUP ACTIVITY / SOL WIND FLUX CORRELATION COEF')
0062      913 FORMAT(' ',//,1X, 'NON-IO JUP ACTIVITY/SOL WIND FLUX CORREL COEF')
0063          END
```

BIBLIOGRAPHY

BIBLIOGRAPHY

Adams, W. M., Sturrock, P. A. 1975, Ap. J., 202, 259.

Bame, S. J., Asbridge, J. R., Feldman, W. C., Gosling J. T. 1976, Ap. J., 207, 977.

Barnes, A. 1974, Ap. J., 188, 645.

Barrow, C. H. 1972, Planet Space Sci., 20, 2051.

Bartels, J. 1932, Terrest. Magnetism Atmospheric Elec., 37, 1.

Beard, D. B. 1965, J. Geophys. Res., 70, 4181.

Biermann, L. 1951, Z. Ap., 29, 274.

Bigg, E. K. 1964, Nature, 203, 1008.

Bigg, E. K. 1966, Planet Space Sci., 14, 741.

Bigg, E. K. 1969, Astrophys. Letters, 3, 77.

Blackman, R. B., Tukey, J. W. 1958, The Measurement of Power Spectra, Dover Publications, New York.

Bracewell, R. 1965, The Fourier Transform and Its Applications, McGraw-Hill, New York.

Burke, B. F., Franklin, K. L. 1955, J. Geophys. Res., 60, 213.

Burlaga, L. F., Ogilvie, K. W., Fairfield, D. H., Montgomery, M. D., Bame, S. J. 1971, Ap. J., 164, 137.

Carr, T. D. 1958, American Astronomical Society, Gainesville, Florida (unpublished).

Carr, T. D. 1972, Phys. Earth Planet. Interiors, 6, 21.

Carr, T. D., Smith, A. G., Bollhagen, H. 1960, Phys. Rev. Letters, 5, 418.

Carr, T. D., Smith, A. G., Bollhagen, H., Six, N. F., Jr., and Chatterton, N. E. 1961, Ap. J., 134, 105.

Carr, T. D., Smith, A. G., Pepple, R., Barrow, C. H. 1958, Ap. J., 127, 274.

Chamberlain, J. W. 1960, Ap. J., 131, 47.

Chapman, S. 1954, Ap. J., 120, 151.

Chapman, S. 1963, Geophysics: The Earth's Environment, Dewitt, C., et al. Eds., Gordon & Breach, New York.

Chree, C. 1912, Philosophical Transaction of the Royal Society of London, Series A, 212, 75.

Collard, H. R., Wolfe, J. H. 1974, The Solar Wind III, University of California, Los Angeles.

Conseil, L., Leblanc, Y., Antonini, G., Quemada, D. 1971, Astrophys. Letters, 8, 133.

Cuperman, S., Metzler, N. 1975, Ap. J., 196, 205.

Davis, L., Jr. 1972, Solar Wind, NASA, Washington, D. C.

Desch, M. D. 1976 (Ph.D. Thesis, University of Florida).

Dessler, A. J., Fejer, J. A. 1963, Planet Space Sci., 11, 505.

Donivan, F. F., Carr, T. D. 1969, A. P. J., Letters, 157, L65.

Douglas, J. N. 1964, IEEE Trans. M.1. Electron., MIL-8, 173.

Douglas, J. N., Boyzan, F. A. 1970, Astrophys. Letters, 4, 227.

Dulk, G. A. 1965a (Ph.D. Thesis, University of Colorado).

Dulk, G. A. 1965b, Science, 148, 1585.

Duncan, R. A. 1965, Planet. Space Sci., 13, 997.

Duncan, R. A. 1966, Planet. Space Sci., 14, 1291.

Duncan, R. A. 1967, Planet. Space Sci., 15, 1687.

Duncan, R. A. 1971, Planet. Space Sci., 19, 391.

Ellis, G. R. A. 1973, Nature, 241, 387.

Goldreich, P., Lynden-Bell, D. 1969, Ap. J., 156, 59.

Gosling, J. T., Bame, S. J. 1972, J. Geophys. Res., 77, 12.

Gosling, J. T., Hansen, R. T., Bame, S. J. 1971, J. Geophys. Res., 76, 1811.

Gulkis, S., Carr, T. D. 1966, Science, 154, 257.

Hartle, R. E., Sturrock, P. A. 1968, Ap. J., 151, 1155.

Hartnet, D. L. 1970, Introduction to Statistical Methods, Addison-Wesley, Reading, Massachusetts.

Holmes, J. R. 1966, Technical Note R-206, Brown Engineering, Huntsville.

Hundhausen, A. J. 1970, Rev. Geophys, and Space Phys., 8, 729.

Hundhausen, A. J., Bame, S. J., Montgomery, M. D., Jr. 1971, J. Geophys. Res., 76, 5145.

Intriligator, D. S. 1974, Ap. J., 188, L23.

Jones, R. H. 1962, Ann. Math. Statist., 33, 455.

Kaiser, M. L., Alexander, J. K. 1972, Astrophys. Letters, 12, 215.

Kaiser, M. L., Alexander, J. K. 1973, Astrophys. Letters, 14, 55.

Kennedy, J. R., Pomphrey, R. B., Lebo, G. R. 1973, Bul. Amer. Phys. Soc., 18, 264 (abstract).

Kovalenko, V. A. 1971, Soviet Astronomy-AJ, 15, 478.

Kraus, J. D. 1958, Proc. I.R.E., 46, 266.

Krausche, D. S. 1975 (Ph.D. Thesis, University of Florida).

Krausche, D. S., Lebo, G. R., Flagg, R. S., Kennedy, J. R. 1973, Bull. Am. Phys. Soc., 18, 264 (abstract).

Krieger, A. S., Timothy, A. F., Roelof, E. C. 1973, Solar Phys., 29, 505.

Leacock, R. J. 1971 (Ph.D. Thesis, University of Florida).

Lebo, G. R. 1964 (Ph.D. Thesis, University of Florida).

Miller, H. R. 1970 (Ph.D. Thesis, University of Florida).

Miller, H. R., Smith, A. G., Leacock, R. J. 1972, Icarus, 17, 73.

Nerney, S. F., Suess, S. T. 1975, Ap. J., 196, 837.

Ness, N. F. 1968, Ann. Rev. Astron. Astrophy., 6, 79.

Neugebauer, M., Snyder, C. W. 1966, J. Geophys. Res., 71, 4469.

Newkirk, G., Jr. 1971, Proc. 1970 NATO Advanced Study Inst. on Physics of the Solar Corona, Reider - Dordrecht.

Newkirk, G., Jr. 1972, Solar Wind, NASA, Washington, D. C.

Noble, L. M., Scarf, F. L. 1963, Ap. J., 138, 1169.

Papadopoulos, K. 1973, Ap. J., 179, 931.

Parker, E. N. 1958, Ap. J., 128, 664.

Razdan, H., Colburn, D. S., Sonett, C. P. 1965, Planet. Space Sci., 13, 1111.

Register, H. I. 1968 (Ph.D. Thesis, University of Florida).

Sastry, C. V. 1968, Planet. Space Sci., 16, 1147.

Shain, C. A. 1956, Australian J. Phys., 19, 167.

Siscoe, G. L., Finley, L. T. 1970, J. Geophys. Res., 75, 1817.

Six, N. F., Jr. 1962 (Ph.D. Thesis, University of Florida).

Smith, A. G., Lebo, G. R., Six, N. F., Carr, T. D., Bollhagen, H., May, J., Levy, J. 1965, Ap. J., 141, 457.

Smith, E. J., Davis, L., Jr., Jones, D. E., Colburn, D. S., Coleman, P. J., Jr., Dyal, P., Sonnett, C. P. and Frandsen, A.M.A. 1974, Science, 183, 305.

Smith, R. A. 1975, Jupiter, the Giant Planet, University of Arizona Press, in press.

Snyder, C. W., Neugebauer, M., Rao, U. R. 1963, J. Geophys. Res., 68, 6361.

Svalgaard, L. 1976, Stanford University Inst. Plasma Res. Report No. 629.

Svalgaard, L. 1976, Stanford University Inst. Plasma Res. Report No. 648.

Urch, I. H. 1969, Solar Phys., 10, 219.

Vasyliunas, V. M. 1975, Ap. J., 202, L159.

Vladimirsky, B. M., Levistky, L. S. 1976, Nature, 260, 27.

Warwick, J. W. 1960, Science, 132, 1250.

Weber, E. J., Davis, L. J. Jr. 1967, Ap. J., 148, 217.

Whang, Y. C. 1971, Ap. J., 169, 369.

Whang, Y. C. 1972, Ap. J., 178, 221.

Whang Y. C., Chang, C. C. 1965, J. Geophys. Res., 70, 4175.

Wilcox, J. M. 1970, J. Geophys. Res., 75, 6366.

Wilcox, J. M. 1971, Private Communication.

Wilcox, J. M., Colburn, D. S. 1969, J. Geophys. Res., 74, 2388.

Wilcox, J. M., Colburn, D. S. 1970, J. Geophys. Res. 75, 6366.

Wilcox, J. M., Ness, N. F. 1965, J. Geophys. Res., 70, 5793.

Wolff, C. L., Brandt, J. C., Southwick, G. R. 1971, Ap. J., 165, 181.

Yeh, T. 1970, Planet. Space Sci., 18, 199.

BIOGRAPHICAL SKETCH

JAMES R. KENNEDY was born the oldest of four children on July 17, 1941, in Fresno, California. He studied physics at St. Mary's College, University of California at Berkeley, and California State University at Fresno; the degree of Bachelor of Science was conferred on September, 1967. The Masters degree with Distinction was conferred on him June, 1969 at California State University at Fresno, California. He moved to Florida in 1969 to begin work on a Ph.D. degree in Physics. During this time he taught at Santa Fe Community College and is currently employed as Director of Operations at the Pacemaker Diagnostic Clinic.

I certify that I have read this study and that in my opinion it conforms to acceptable standards of scholarly presentation and is fully adequate, in scope and quality, as a dissertation for degree of Doctor of Philosophy.

Alex G. Smith

A.G. Smith, Chairman
Professor of Physics and Astronomy

I certify that I have read this study and that in my opinion it conforms to acceptable standards of scholarly presentation and is fully adequate, in scope and quality, as a dissertation for degree of Doctor of Philosophy.

G.R. Lebo

G.R. Lebo, Co-Chairman
Assistant Professor of Astronomy

I certify that I have read this study and that in my opinion it conforms to acceptable standards of scholarly presentation and is fully adequate, in scope and quality, as a dissertation for degree of Doctor of Philosophy.

J.D. Carr

T.D. Carr
Professor of Physics and Astronomy

I certify that I have read this study and that in my opinion it conforms to acceptable standards of scholarly presentation and is fully adequate, in scope and quality, as a dissertation for degree of Doctor of Philosophy.

S.T. Gottesman
Assistant Professor of Astronomy

I certify that I have read this study and that in my opinion it conforms to acceptable standards of scholarly presentation and is fully adequate, in scope and quality, as a dissertation for degree of Doctor of Philosophy.

F.B. Wood
Professor of Astronomy

This dissertation was submitted to the Graduate Faculty of the Department of Physics and Astronomy in the College of Arts and Sciences and to the Graduate Council, and was accepted as partial fulfillment of the requirements for the degree of Doctor of Philosophy.

December 1976

Harry H. Sisler, Dean
Graduate School